# A tensorial thermodynamic framework to account for the $\gamma$ ' rafting in Nickel-based single crystal superalloys

Rodrigue Desmorat, Adriana Mattiello, Jonathan Cormier

# A tensorial thermodynamic framework to account for the $\gamma'$ rafting in Nickel-based single crystal superalloys

R. Desmorat[a], A. Mattiello[a,c], J. Cormier[b]

[a] *LMT-Cachan (ENS Cachan, CNRS, Université Paris Saclay), 94235 Cachan, France*
[b] *Institut Pprime, UPR CNRS 3346, Physics and Mechanics of Materials Departement, ISAE-ENSMA, 1 Clément Ader, BP 40109, 86961 Futuroscope-Chasseneuil, France*
[c] *Safran Helicopter Engine, Avenue Joseph Szydlowski, 64510 Bordes*

**Abstract**

A new model is developed in order to account for the effect of microstructural degradation (i.e. precipitate-directional-coarsening) on the viscoplastic behavior of single crystal superalloys under high temperature exposure. Microstructural changes are modeled by a tensorial description of $\gamma$ channel width evolution formulated in the natural anisotropy basis of the material. The tensorial description of microstructural evolution is combined with the Kelvin modes based viscoplasticity laws thanks to the coupling with the Orowan stress performed within a thermodynamics framework. Isotropic and directional coarsening of the $\gamma'$ hardening phase are modeled as well as its dissolution with temperature changes. Results are presented for isothermal creep of CMSX-4 alloy at 1050°C along $< 001 >$ and $< 111 >$ crystal directions but the formulation allows to account for anisothermal loadings, isotropization of the creep response at high temperature and misaligned loadings. This newly developed tensorial framework for rafting can also apply to single crystal superalloys having a positive misfit.

*Keywords:* Ni-based single crystal superalloys, Microstructure evolution, Creep, Anisotropy

## Introduction

Nickel-based single crystal superalloys are widely used for the design of components in the hottest sections of gas turbines (aero-engines, industrial gas turbines for power generation and turboshaft engines for helicopters) owing to their superior creep and fatigue properties at temperatures above 700°C. High pressure turbine blades and vanes and even first stages of low pressure turbine blades of the most advanced gas turbines are cast using such alloys. Their microstructure consists of a high volume fraction $f_{\gamma'}$ of $\gamma'$-strengthening precipitates coherently merged in a $\gamma$ matrix. Under regular operating conditions, thermomechanical cycles at high temperature (> 950°C) promote the directional coarsening (DC) of the $\gamma'$-precipitates. Such a microstructural evolution is commonly known as the "rafting" mechanism (Caron and Khan , 1983, Draper et al , 1989, Pollock and Argon , 1994, Reed et al , 1999, Tien and Copley , 1971, Tien and Gamble , 1972).This microstructure evolution depends on the mechanical state at the precipitate/matrix scale which is dependent on both the $\gamma/\gamma'$ coherency stresses and macroscopic applied loading. Most of commercial Ni-based single crystal superalloys using for gas turbine applications have a negative $\gamma/\gamma'$ lattice misfit $\delta_u$ at high temperatures (Diologent et al , 2003, Dirand et al , 2003, Epishin et al , 2000, Heckl et al , 2011, Mughrabi , 2014, Reed , 2006, Zhang et al , 2005). For these alloys, it is well established that N-type coalescence is obtained (i.e: Normal to the mechanical loading) if a macroscopic tensile stress is applied, whereas P-type coalescence is obtained in compressive loading (i.e: Parallel to the mechanical stress direction) as illustrated in Fig. 1.

This $\gamma'$ morphological evolution has been observed several times in various high temperature components such as turbine blades after service operations (Biermann et al , 1996, Draper et al , 1989, Epishin et al , 2008, 2010, Mughrabi , 2009) and the characterization of the consequences of this microstructure coarsening on the mechanical properties is of the utmost importance to achieve a reliable design of such components. Still, the rafting of the $\gamma'$-phase in Ni-based single crystal superalloys remains a controversial issue since there is no common agreement on the beneficial or detrimental effects this structure evolution has on mechanical properties. It has already been proved in literature that this lamellar microstructure induces a decrease in high temperature properties compared to cuboidal structures (Fedelich et al , 2012a). In addition, N-type directional coarsening was demonstrated to be deleterious to strain-controlled low cycle fatigue (LCF) and out-of-phase thermo-mechanical fatigue (TMF) properties compared to cuboidal precipitates or P-type DC (Arrel et al , 2004, Epishin et al , 2005, Kirka et al, 2015, Mauget et al , 2016) since it leads to a higher plastic flow, especially in the low temperature part of a TMF cycle. Furthermore, P-type DC is more creep resistant than N-type or even cuboidal $\gamma'$-morphologies, for at least the first percentages of creep deformation, since this microstructure provides efficient barrier to the glide/climb dislocation processes (Li et al , 2007, Mughrabi and Tetzlaff , 2000). The only case where N-type coalescence may improve

*Email address:* desmorat@lmt.ens-cachan.fr (R. Desmorat)

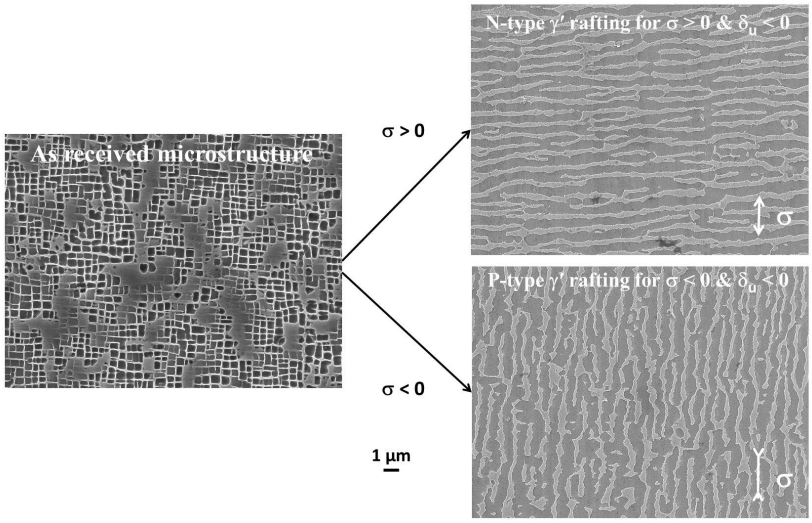


Figure 1: Typical evolution of the $\gamma'$ morphology during high temperature uniaxial tension or compression creep for Ni-based single crystalline superalloys having a negative $\gamma'/\gamma'$ lattice mismatch $\delta_u$

the mechanical properties is creep under high temperatures (> 1000°C) and low stress (Mughrabi and Tetzlaff , 2000). Without any heat treatment before the material is creep-strained, this inevitable morphology evolution is believed to improve isothermal creep properties at high temperatures (i.e: a decrease in the creep strain rate) by providing efficient obstacles to the dislocation motion which mainly consists of glide/climb processes over 1000°C (Mughrabi and Tetzlaff , 2000, Reed et al , 1999, 2007a). However, recent studies under such high temperature/low stress conditions suggest that the N-type rafting mechanism is deleterious to the non-isothermal creep properties of MC2, CMSX-4 and MCNG alloys (Cormier et al , 2007, Cormier and Cailletaud , 2010b, Giraud et al , 2012, le Graverend et al , 2014a,b) while a P-type rafting leads to a decrease of the non-isothermal creep strain rate without affecting the creep life compared to a cuboidal microstructure (Giraud et al , 2012). It is also worth mentioning that a coarsened $\gamma'$ microstructure at the beginning of mechanical tests also leads to a decrease in isothermal or non-isothermal creep properties (Shi et al , 2012, Steuer et al , 2014), as well as thermo-mechanical fatigue ones (Kirka et al, 2015). Since such kind of microstructural evolution (i.e. $\gamma'$ coarsening or rafting) cannot be avoided at temperatures above 850°C, several studies have been conducted to determine the rafting kinetics of the $\gamma'$-phase (Zhou et al , 2007, Svobda and Lukas , 1996, Svoboda and Lukas , 1997), considering uniaxial loadings leading to an homogeneous stress field or under different applied stresses to be able to model the $\gamma'$ rafting process has a function of time, temperature and applied stress (Epishin et al , 2008, 2009, Fedelich et al , 2009, 2012a,b). Based on such experimental characterizations, various models have been proposed to be able to account for the consequences of the $\gamma/\gamma'$ microstructure degradation on the isothermal creep, tensile and LCF properties (Fan et al , 2015, Fedelich et al , 2012a,b, le Graverend et al , 2014a, Leidermark et al , 2010, Svoboda and Lukas , 1998, Svoboda and Lukas , 2000, Tinga et al , 2009). However, most of these approaches were devoted to account for the mechanical behavior evolution along the $< 001 >$ crystallographic orientation with little attention on the $\gamma'$ rafting kinetics along other crystallographic orientations whose process is quite different than along the $< 001 >$ direction (Gaubert et al , 2015, Tian et al , 2012, Tien and Copley , 1971), leading to different consequences on the mechanical behavior. Moreover, very few of them made an attempt to consider fast non-isothermal loadings (i.e. thermo-mechanical loading paths closer to real in service conditions of aero-engines or turboshaft engines for helicopters) inducing both the $\gamma/\gamma'$ microstructure degradation under the form of (directional) coarsening and the dissolution/re-precipitation of hyperfine $\gamma'$ particles after a very high temperature exposure. According to our very best knowledge, the only model tackling this issue is the one proposed recently by le Graverend et al (2014a).

Within this context, the aim of the present paper is to develop a tensorial description of the $\gamma'$ microstructure evolution during high temperature exposure within thermodynamics framework. The aim of this approach is to consider both isothermal and non-isothermal loading paths inducing homothetic coarsening and/or directional coarsening of the $\gamma'$ phase, whatever the crystallographic loading direction. After presenting the assumptions of the models and main microstructure processes taken into account, the equations of the proposed model will be presented as well as experimental data necessary for its identification. An important point (and modeling choice) is the scale at which plasticity and rafting variables are introduced. In the present work one proposes to use a Kelvin modes based initial plasticity framework (Arramon et al , 2000, Bertram and Olschewski , 1996, Biegler and Mehrabadi , 1995, Cowin et al , 1991, Desmorat and Marull , 2011, François , 1995, Mahnken , 2002), the link with single crystal plasticity framework being given as Appendix F. Finally, the performances of the visco-plasticity coupled with tensorial rafting model will be presented and compared to several experimental data specifically generated for this study.

## 1. Background and motivations

In the model we will develop hereafter in the present article, both the isotropic coarsening and the directional coarsening will be considered. The isotropic coarsening of $\gamma'$ particles is a diffusion controlled process following the Lifshitz-Slyozov and Wagner (LSW) theory occurring during thermal exposure in the absence of mechanical applied stress (Lifshitz and Slyozov , 1961, Wagner , 1961). In such a situation, $\gamma'$ particles are first growing keeping a square morphology and then, a loss of such a cuboidal morphology is obtained due to a progressive relaxation of the $\gamma/\gamma'$ interfacial coherency stress during aging (Leidermark et al , 2010, Link et al , 2011). Even if the cuboidal morphology is progressively lost, in the following of the paper, it will be assumed that the growth of $\gamma'$ particles follows the LSW theory:

$$\lambda^3 - \lambda_0^3 = Ct \tag{1}$$

where $\lambda = \lambda(t)$ and $\lambda_0 = \lambda(t = 0)$ are the microstructure periodicity (see Fig. 3) after a given exposure $t$ at high temperature and in the initial state respectively and $C$ is the growth kinetics at a given temperature which is assumed to be of Arrhenius type.

Regarding the $\gamma'$ rafting, extensive literature has been dedicated to the determination of the orientation of $\gamma'$ rafts with respect to mechanical stress orientation and/or misfit value (Ichitsubo et al , 2003, Louchet and Hazotte , 1997, MacKay and Ebert , 1985). Under elastic conditions, the thermodynamic driving force for $\gamma'$ rafting is a function of three main parameters: (i) the applied stress, (ii) the lattice mismatch $\delta_u$ between the $\gamma$ matrix and the $\gamma'$ particles, and (iii) the difference between their elastic constants (Nabarro , 1996). However, during time dependent inelastic straining of Ni-based single crystal superalloys, which is our main focus in this paper, it has been shown that the main driving force for the development of $\gamma'$ rafting is the relaxation of the coherency stresses due to the development of $\gamma/\gamma'$ interfacial dislocations (Fährmann et al , 1996, Matan et al , 1999, Véron et al , 1996). Such interfacial dislocations generally come from high temperature creep deformation of the matrix. Indeed, one of the nicest experiment proof has been provided by Matan et al (1999). They have indeed shown that if a given high temperature creep strain threshold ($\varepsilon^p_{\text{th}} \sim 0.1\%$ at 950°C) is overcome, $\gamma'$ rafting can then proceed without any external applied stress while if the creep strain introduced is lower than this threshold, the $\gamma'$ microstructure remains cuboidal. Up to now, none of the above mentioned model accounting for the consequences of the $\gamma'$ degradation on the mechanical properties has taken into account such a threshold in their formulation, probably since this threshold is quite low and can be neglected from a technological point of view. This will be one of our objective. Moreover, one of our aims is to take into account the different morphological evolutions occurring during creep, either in tension or in compression and along all crystallographic loading direction. For this, the degree of rafting will be described by the evolution of the $\gamma$ channel thickness, as illustrated in Fig. 2 for a tension/compression creep loading along the [001] direction. As an example, when a tensile creep loading is applied along the [001] direction (denoted direction 1), two types of matrix channels are closing ($w_2$ and $w_3$ in Fig. 2) and the last one, normal to the applied load is widening ($w_1$ increases)(Chen and Immarigeon , 1998, Kamaraj , 2003), as already shown Fig. 1. However, when a compressive creep load is applied, former channels perpendicular to the applied load are closing (i.e. $w_1$ is decreasing) and the two other families of $\gamma$ channels are widening (Mughrabi and Tetzlaff , 2000, Ott and Mughrabi , 1999), leading to the development of $\gamma'$ rods aligned along the [001] directions or plates along two directions, as illustrated in Fig. 2. One of our aim with the model we will present in the subsequent sections of this paper will be to reproduce the change in $\gamma'$ rafting direction when first a compressive creep load is applied and then a tensile load, or vice versa. Indeed, as shown by Xingfu et al (2009), as well as by Mughrabi and Tetzlaff (2000), Ott and Mughrabi (1999) and more recently by Giraud et al (2012), if first a compressive creep load is applied along a [001] direction and then a tensile creep load, a P-type rafting will first develop and then, during the stress reversal, a breakdown of the former P-type rafting will occur and progressively lead to the formation of a N-type rafting. Before developing the N-type rafting after the stress reversal, the $\gamma'$ morphology will transiently be almost isotropic (all the $\gamma$ channels $w_i$ having the same width), but without developing once again a cuboidal morphology. We will also take into account the process of $\gamma'$ rafting when a tensile or creep stress is applied along another crystallographic orientation. As examples, when a tensile creep load is applied along a [011] orientation (Tian et al , 2012, Tien and Copley , 1971, Ghighi , 2013, Ghighi et al , 2013, Sass et al , 1996), $\gamma'$ particles are elongating along two $< 100 >$ directions (i.e. only one channel width wi will tend toward 0) while during a tension creep test along a perfect $< 111 >$ orientation (Golubovskii et al , 1987), almost no directional coarsening is observed. Having a tensorial framework is definitely required to be able to capture such evolutions in $\gamma'$ directional coarsening through the widening/closing of the $\gamma$ channels.

Finally, we will not consider at this stage the differences in $\gamma'$ rafting kinetics at the dendritic scale. It has indeed been shown several times that the $\gamma'$ rafting first starts in the primary dendrite arms, and then continue in the interdendritic spacings, due to a high $\gamma/\gamma'$ lattice mismatch in the dendrites (Milhet et al , 2012, Mughrabi , 2009, Reed et al , 2007a). In our opinion, such a difference in $\gamma'$ rafting kinetics can only be captured having a robust modelling framework applied to a finite element simulation accounting for the chemical segregations at the dendritic scale of Ni-based single crystal superalloys. Moreover, we will not consider the $\gamma/\gamma'$ toplogical inversion occurring at the end of creep tests performed at rather low temperature (below 1000°C) and leading to a creep acceleration (Caron et al , 2008, Epishin et al , 2000, 2001, Fredholm and Strudel , 1987, Reed et al , 1999). This means that our modeling approach will remain valid up to reasonable creep strains, typically below 5 percents of creep elongation. In addition, under low creep strain magnitude, the directional coarsening of the $\gamma'$ phase always follow the $< 100 >$ crystallographic direction, even if lattice rotation may occur (le Graverend et al , 2014b).

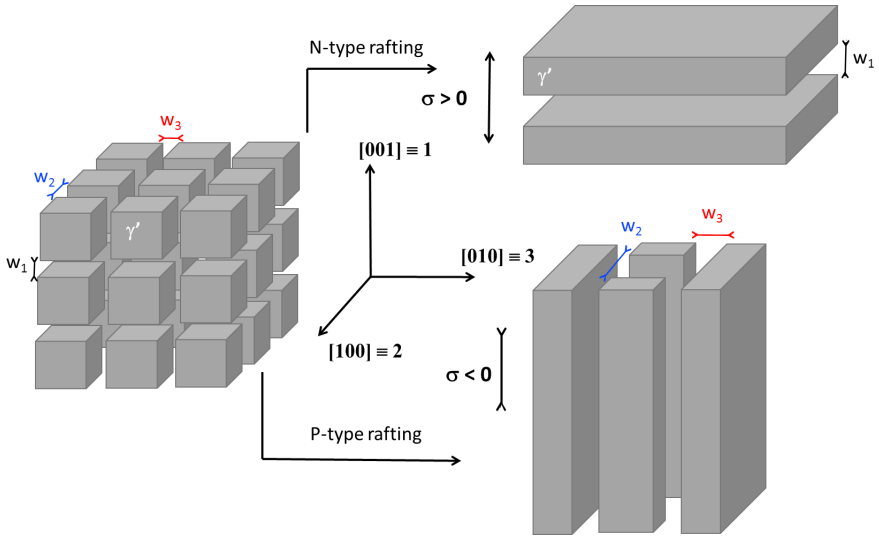


Figure 2: Schematic of the $\gamma'$ microstructure evolution during high temperature creep and definition of the stereological parameter used in present work.

Hence, the use of the channel width values $w_i$ as defined in Fig. 2 will remain valid.

## 2. Kelvin modes based (visco-)plasticity of cubic materials

Single crystal material behavior is often modeled by means of so-called crystal plasticity framework: the permanent strain $\boldsymbol{\epsilon}^p$ of the Representative Volume Element (RVE) of continuum mechanics is then the sum of the individual shearing contributions of the (active) slip planes, gathered by families (Asaro and Rice , 1977, Asaro , 1983, Hill and Rice , 1972, Peirce et al , 1983, Rice , 1975). Schmid law based criterion functions are most often used at the slip planes scale (Schmid and Boas , 1935).

For present Ni-based single crystal superalloys, this approach defines an additional scale smaller of course than the RVE scale, but also smaller than the cuboidal microstructure (rafting) scale described in previous section. The mechanical interactions are quite complex with the evolving microstructure and with Orowan stress relaxation (see Section 4.2). We therefore prefer in the present modeling approach not to introduce such an additional scale and to write plasticity in a phenomenological manner directly at RVE scale using so-called Kelvin mode based macroscopic plasticity.

### *2.1. Kelvin decomposition in elasticity and for plasticity coupling*

Kelvin spectral formulation of elasticity (Kelvin , 1856, 1878) (see Appendix A) concerned initially linear anisotropic elasticity but now also materials with asymmetric elasticity in tension and in compression (Desmorat and Duvaut , 2003), multiaxial strength criteria (Arramon et al , 2000, Desmorat and Marull , 2011), creep (Bertram and Olschewski , 1996, Mahnken , 2002) and Continuum Damage Mechanics (Biegler and Mehrabadi , 1995, Desmorat , 2000, 2009, Desmorat and Marull , 2011, François , 1995). As pointed out by Cowin et al (1991), it is possible to use such a formulation as a tool to derive yield criteria and plasticity theories for initially anisotropic materials, as it naturally extends the concept of deviatoric and hydrostatic stresses to anisotropy.

### *2.2. Yield criterion defined in terms of Kelvin stresses*

A criterion function $f(\boldsymbol{\sigma})$ defines the elasticity domain by $f < 0$ and is often used as an evolution potential to derive, by normality, the plasticity evolution laws. In case of isotropy $f$ is usually expressed in terms of stress invariants. The anisotropic case is more difficult (Barlat et al , 2005, Lemaitre and Chaboche , 1991, Lemaitre et al , 2009, Hill , 1950, 1979). A possibility is to use Kelvin stresses $\boldsymbol{\sigma}^k$ (defined in Appendix A) and to write the criterion function as $f(\boldsymbol{\sigma}) = f(\boldsymbol{\sigma}^{k=1}, ..., \boldsymbol{\sigma}^{k=N})$. Such a formulation is objective (thanks to the objective definition of Kelvin stresses). Global convexity is gained by ensuring the convexity with respect to each Kelvin stress.

*In the isotropic case,* there are only two Kelvin stresses, associated with the Kelvin moduli $3K = E/(1-2\nu)$ and $2G = E/(1+\nu)$ (with $E$ and $\nu$ the Young modulus and the Poisson ratio). They are respectively the hydrostatic stress tensor $\boldsymbol{\sigma}^{\mathrm{H}}$ and the deviatoric stress tensor $\boldsymbol{\sigma}'$

$$\boldsymbol{\sigma}^{\mathrm{H}} = \sigma_H \mathbf{1} = \frac{1}{3}\operatorname{tr}\boldsymbol{\sigma}\,\mathbf{1} \qquad \boldsymbol{\sigma}' = \boldsymbol{\sigma} - \frac{1}{3}\operatorname{tr}\boldsymbol{\sigma}\,\mathbf{1} \tag{2}$$

with $\mathbf{1}$ the second order unit tensor.

*In case of cubic material symmetry,* encountered for instance in FCC single crystals alloys, the elasticity tensor has three Kelvin moduli (eigenvalues) $\Lambda^{k=1} = 3K = E/(1-2\nu)$, $\Lambda^{k=2} = E/(1+\nu)$, $\Lambda^{k=3} = 2G \neq E/(1+\nu)$ and

three Kelvin stresses $\boldsymbol{\sigma}^k = \mathbb{P}^k : \boldsymbol{\sigma}$, the Kevin projectors $\mathbb{P}^k$ being defined in the Appendix (Eq. A.5),
*i) the hydrostatic stress*, associated with the Kelvin modulus $3K = E/(1-2\nu)$,

$$\boldsymbol{\sigma}^{k=1} = \mathbb{P}^{\mathrm{H}} : \boldsymbol{\sigma} = \boldsymbol{\sigma}^{\mathrm{H}} = \frac{1}{3}\,\mathrm{tr}\,\boldsymbol{\sigma}\,\mathbf{1} \tag{3}$$

*ii) the diagonal part of deviatoric stress tensor* $\boldsymbol{\sigma}'$ in (cubic) Natural Anisotropy Basis, associated with the Kelvin modulus $E/(1+\nu)$,

$$\boldsymbol{\sigma}^{k=2} = \mathbb{P}^{\mathrm{d}} : \boldsymbol{\sigma} = \boldsymbol{\sigma}^{\mathrm{d}} \tag{4}$$

*iii) the out of diagonal part of deviatoric tensor* $\boldsymbol{\sigma}'$ still in Natural Anisotropy Basis associated with the Kelvin modulus $2G$,

$$\boldsymbol{\sigma}^{k=3} = \mathbb{P}^{\overline{\mathrm{d}}} : \boldsymbol{\sigma} = \boldsymbol{\sigma}^{\overline{\mathrm{d}}} \tag{5}$$

$\boldsymbol{\sigma}^{\mathrm{d}} = (\boldsymbol{\sigma}^{\mathrm{d}})'$ and $\boldsymbol{\sigma}^{\overline{\mathrm{d}}} = (\boldsymbol{\sigma}^{\overline{\mathrm{d}}})'$ are deviatoric and one has the stress (Kelvin) partition

$$\boldsymbol{\sigma}' = \boldsymbol{\sigma}^{\mathrm{d}} + \boldsymbol{\sigma}^{\overline{\mathrm{d}}} \quad \text{and} \quad \boldsymbol{\sigma} = \boldsymbol{\sigma}^{\mathrm{d}} + \boldsymbol{\sigma}^{\overline{\mathrm{d}}} + \boldsymbol{\sigma}^{\mathrm{H}} \tag{6}$$

in an objective manner in case of cubic material symmetry. An application of this modeling framework to creep of SRR99 Nickel-based single crystal supralloy has been proposed by Bertram and Olschewski (1996).

Following notations are used next for the particular von Mises norms

$$\sigma^{\mathrm{d}}_{eq} = \sqrt{\frac{3}{2}\boldsymbol{\sigma}^{\mathrm{d}} : \boldsymbol{\sigma}^{\mathrm{d}}} \qquad \sigma^{\overline{\mathrm{d}}}_{eq} = \sqrt{\frac{3}{2}\boldsymbol{\sigma}^{\overline{\mathrm{d}}} : \boldsymbol{\sigma}^{\overline{\mathrm{d}}}} \tag{7}$$

### *2.3. Macroscopic Kelvin mode based cubic plasticity*

For cubic material symmetry, the yield criterion is function of the 3 Kelvin modes/stresses (3)-(5): $\boldsymbol{\sigma}^{\mathrm{d}}$ (the diagonal deviatoric part of stress tensor in Natural Anisotropy Basis), $\boldsymbol{\sigma}^{\overline{\mathrm{d}}}$ (the out of diagonal deviatoric part of stress tensor in Natural Anisotropy Basis) and hydrostatic stress $\sigma^{\mathrm{H}} = \sigma_H\,\mathbf{1} = \frac{1}{3}\,\mathrm{tr}\,\boldsymbol{\sigma}$. Incompressible plasticity is assumed so that generic yield criterion is

$$f = f(\boldsymbol{\sigma}^{\mathrm{d}}, \boldsymbol{\sigma}^{\overline{\mathrm{d}}}) \qquad f < 0 \;\rightarrow\; \text{elasticity} \tag{8}$$

Examples of such yield criteria for CMSX-4 and AM1 superalloys are given in Desmorat and Marull (2011) (see also section 2.3). Note just that in order to recover a non homogeneous field in torsion, out of diagonal Kelvin mode $\boldsymbol{\sigma}^{\overline{\mathrm{d}}}$ has to act by means of cubic non quadratic norm $\|\boldsymbol{\sigma}^{\overline{\mathrm{d}}}\|_a = (|\sigma_{12}|^a + |\sigma_{13}|^a + |\sigma_{23}|^a)^{1/a}$ for out of diagonal stress tensor (components in Natural Anisotropy Basis), with $a \neq 2$.

Normality combined with Kelvin projectors (A.5) gives plastic strain rate (Kelvin) partition

$$\dot{\boldsymbol{\epsilon}}^p = \dot{\lambda}\frac{\partial f}{\partial \boldsymbol{\sigma}} = \dot{\boldsymbol{\epsilon}}^{p\mathrm{d}} + \dot{\boldsymbol{\epsilon}}^{p\overline{\mathrm{d}}} \qquad \begin{cases} \dot{\boldsymbol{\epsilon}}^{p\mathrm{d}} = \mathbb{P}^{\mathrm{d}} : \dot{\boldsymbol{\epsilon}}^p = \mathbf{n}^{\mathrm{d}}\,\dot{p}^{\mathrm{d}} \\ \dot{\boldsymbol{\epsilon}}^{p\overline{\mathrm{d}}} = \mathbb{P}^{\overline{\mathrm{d}}} : \dot{\boldsymbol{\epsilon}}^p = \mathbf{n}^{\overline{\mathrm{d}}}\,\dot{p}^{\overline{\mathrm{d}}} \end{cases} \tag{9}$$

with $\dot{\lambda}$ the plastic multiplier. Three accumulated plastic strains are defined in an objective manner for cubic materials

$$p = \int \sqrt{\frac{2}{3}\dot{\boldsymbol{\epsilon}}^p : \dot{\boldsymbol{\epsilon}}^p}\,\mathrm{d}t \qquad p^{\mathrm{d}} = \int \sqrt{\frac{2}{3}\dot{\boldsymbol{\epsilon}}^{p\mathrm{d}} : \dot{\boldsymbol{\epsilon}}^{p\mathrm{d}}}\,\mathrm{d}t \qquad p^{\overline{\mathrm{d}}} = \int \sqrt{\frac{2}{3}\dot{\boldsymbol{\epsilon}}^{p\overline{\mathrm{d}}} : \dot{\boldsymbol{\epsilon}}^{p\overline{\mathrm{d}}}}\,\mathrm{d}t \tag{10}$$

$p$ is standard accumulated plastic strain. It is shown in Desmorat and Marull (2011) that accumulated plastic strain $p^{\mathrm{d}}$ is representative of octahedral slip systems plasticity and that $p^{\overline{\mathrm{d}}}$ is representative of cubic slip systems plasticity (see section Appendix F). One has:

- $p^{\mathrm{d}} = p$, $p^{\overline{\mathrm{d}}} = 0$ for tension/compression in direction $< 001 >$,
- $p^{\mathrm{d}} = 0$, $p^{\overline{\mathrm{d}}} = p$ for tension/compression in direction $< 111 >$.

Using (quadratic) von Mises norms $\sigma^{\mathrm{d}}_{eq}$, $\sigma^{\overline{\mathrm{d}}}_{eq}$ and accumulated plastic strains $p^{\mathrm{d}}$, $p^{\overline{\mathrm{d}}}$, Hill cubic criterion function and associated equivalent stress and accumulated plastic strain are simply

$$f = \sigma_{\mathrm{Hill}} - \sigma_y \qquad \sigma_{\mathrm{Hill}} = \sqrt{(\sigma^{\mathrm{d}}_{eq})^2 + h^2(\sigma^{\overline{\mathrm{d}}}_{eq})^2} \qquad p^{\mathrm{Hill}} = \int \sqrt{(\dot{p}^{\mathrm{d}})^2 + h^{-2}(\dot{p}^{\overline{\mathrm{d}}})^2}\,\mathrm{d}t \tag{11}$$

with $\sigma_y = \sigma_{y001}$ the yield stress in $< 001 >$ direction and $h$ Hill material parameter for cubic plasticity. Plastic power is then $\boldsymbol{\sigma} : \dot{\boldsymbol{\epsilon}}^p = \dot{\lambda}\frac{\partial f}{\partial \boldsymbol{\sigma}} = \sigma_{\mathrm{Hill}}\dot{p}^{\mathrm{Hill}}$ with $\dot{\lambda} = \dot{p}^{\mathrm{Hill}}$(Hill , 1950).

Non quadratic cubic yield criterion functions have been identified in Desmorat and Marull (2011) for CMSX-2 superalloy,

$$f = \left(\frac{\sigma_{eq}^{\mathrm{d}}}{\sigma_y}\right)^n + \left(\frac{\|\boldsymbol{\sigma}^{\overline{\mathrm{d}}}\|_a}{\bar{\tau}_y}\right)^m - 1 \tag{12}$$

using for "diagonal" deviatoric stress tensor (quadratic) von Mises norm $\sigma_{eq}^{\mathrm{d}}$ and for "out of diagonal" stress tensor non quadratic norm $\|.\|_a = (|\sigma_{12}|^a + |\sigma_{13}|^a + |\sigma_{23}|^a)^{1/a}$ (components in cubic Natural Anisotropy Basis): this choice allows to recover a non homogeneous stress field in torsion (see Nouailhas and Cailletaud (1995) for experimental evidences), as shown in Appendix B. Material parameter $\sigma_y = \sigma_{y001}$ is the yield stress in direction $< 001 >$. The yield stress for tension in direction $< 111 >$ is $\overline{\sigma}_y = \sigma_{y111} = 3^{-\frac{1}{a}}\bar{\tau}_y$.

When the value $a = 2$ is considered for non quadratic norm $\|.\|_a$, one gets $(3^{-\frac{1}{a}}\|\boldsymbol{\sigma}^{\overline{\mathrm{d}}}\|_a)_{a=2} = \sigma_{eq}^{\overline{\mathrm{d}}}$ then equal to von Mises norm of "out of diagonal" $\boldsymbol{\sigma}^{\overline{\mathrm{d}}}$. Note that to take $a = 2$ simplifies the writing –for instance of the normality law– and as long as pure shear is not encountered this will be the choice made.

### *2.4. Two criterion function macroscopic modeling*

In order to obtain a close link with Schmid based single crystal plasticity (Asaro , 1983, Hill and Rice , 1972, Rice , 1975), multi-criterion by nature, an alternative two criterion framework can be used, defined at RVE macroscopic scale (Bertram and Olschewski , 1996, Cowin et al , 1991, Mahnken , 2002). We introduce

- a first criterion function $f_1 = f_1(\boldsymbol{\sigma}^{\mathrm{d}}, \boldsymbol{\sigma}^{\overline{\mathrm{d}}})$, mainly function of "diagonal" deviatoric stress $\boldsymbol{\sigma}^{\mathrm{d}}$ representative of octahedral slip plasticity, also function of "out of diagonal" $\boldsymbol{\sigma}^{\overline{\mathrm{d}}}$ (this choice will be justified in section Appendix F),
- a second criterion function $f_2 = f_2(\boldsymbol{\sigma}^{\overline{\mathrm{d}}})$ only function of "out of diagonal" $\boldsymbol{\sigma}^{\overline{\mathrm{d}}}$, representative of cubic slip plasticity.

For multiaxial loading cases, including tension-torsion testing, consider Hill criterion for $f_1$ (introducing parameter $h$ within definitions Eq. (11)),

$$f_1 = \sigma_{\mathrm{Hill}} - \sigma_y \qquad f_2 = 3^{-\frac{1}{a}}\|\boldsymbol{\sigma}^{\overline{\mathrm{d}}}\|_a - \overline{\sigma}_y \qquad \text{(hardening omitted)} \tag{13}$$

For the sake of simplicity set $h = 0$ and $a = 2$, retrieving then von Mises criterion (7) for non deviatoric stress tensor $\boldsymbol{\sigma}^{\overline{\mathrm{d}}}$,

$$f_1 = \sigma_{eq}^{\mathrm{d}} - \sigma_y \qquad f_2 = \sigma_{eq}^{\overline{\mathrm{d}}} - \overline{\sigma}_y \qquad \text{(hardening omitted)} \tag{14}$$

Normality law becomes

$$\dot{\boldsymbol{\epsilon}}^p = \dot{\boldsymbol{\epsilon}}_1^p + \dot{\boldsymbol{\epsilon}}_2^{p\overline{\mathrm{d}}} \qquad \begin{cases} \dot{\boldsymbol{\epsilon}}_1^p = \dot{\lambda}_1 \frac{\partial f_1}{\partial \boldsymbol{\sigma}} = \dot{p}_1^{\mathrm{d}}\mathbf{n}^{\mathrm{d}} + \dot{p}_1^{\overline{\mathrm{d}}}\mathbf{n}^{\overline{\mathrm{d}}} \\ \dot{\boldsymbol{\epsilon}}_2^{p\overline{\mathrm{d}}} = \dot{\lambda}_2 \frac{\partial f_2}{\partial \boldsymbol{\sigma}} = \dot{p}_2^{\overline{\mathrm{d}}}\mathbf{n}^{\overline{\mathrm{d}}} \end{cases} \tag{15}$$

with the two independent (visco-)plastic multipliers equal to $\dot{\lambda}_1 = \dot{p}_1^{\mathrm{Hill}} = \sqrt{(\dot{p}_1^{\mathrm{d}})^2 + \frac{1}{h^2}(\dot{p}_2^{\overline{\mathrm{d}}})^2}$, $\dot{\lambda}_2 = \dot{p}_2^{\overline{\mathrm{d}}}$.

As in case of Schmid single crystal visco-plasticity (Méric et al , 1991), two different viscous stresses are introduced so that visco-plasticity evolution corresponds to :

$$\dot{p}_1^{\mathrm{Hill}} = \left\langle \frac{f_1}{K_N} \right\rangle_+^N \qquad \dot{p}_2^{\overline{\mathrm{d}}} = \left\langle \frac{f_2}{\overline{K}_N} \right\rangle_+^{\overline{N}} \tag{16}$$

with $K_N$, $N$, $\overline{K}_N$, $\overline{N}$ Norton material parameters in cubic visco-plasticity.

For an uniaxial loading along $< 001 >$ Norton law is recovered, with $\sigma_y$ is the yield stress $\sigma_{y001}$ in direction $< 001 >$,

$$|\dot{\varepsilon}^p| = \left\langle \frac{|\sigma| - \sigma_y}{K_N} \right\rangle_+^N \qquad \text{(direction } < 001 >\text{, hardening omitted)} \tag{17}$$

For an uniaxial loading along $< 111 >$ a double viscosity model is obtained (corresponding isotropic framework given in de Bussac (1993)), as well as for Schmid single crystal visco-plasticity modeling when slip planes with different Schmid factors are activated,

$$|\dot{\varepsilon}^p| = h\left\langle \frac{h|\sigma| - \sigma_y}{K_N} \right\rangle_+^N + \left\langle \frac{|\sigma| - \overline{\sigma}_y}{\overline{K}_N} \right\rangle_+^{\overline{N}} \qquad \text{(direction } < 111 >\text{, hardening omitted)} \tag{18}$$

$\overline{\sigma}_y$ is the yield stress $\sigma_{y111}$ in direction $< 111 >$ when it is lower than $\sigma_y/h$.

*2.5. Saturating visco-plasticity law*

The validity domain of Norton law is often limited in terms of strain rate. Most often it applies properly in creep regime but less in tension at $\dot{\varepsilon} \geq 10^{-3}\text{s}^{-1}$ and in dynamics cases of impacts for which a saturation of the viscous stress occurs. This can be simply modeled by means of power-exponential viscosity law, formulated Eq. (19). For criterion function $f_1$ it reads

$$\dot{p}_1^{\text{Hill}} = \left\langle -\frac{\sigma_{v\infty}}{K_N} \ln\left(1 - \frac{f_1}{\sigma_{v\infty}}\right)\right\rangle_+^N \qquad \text{or} \qquad \sigma_v = \sigma_{v\infty}\left(1 - \exp\left(-\frac{K_N}{\sigma_{v\infty}}(\dot{p}_1^{\text{Hill}})^{1/N}\right)\right) \tag{19}$$

Eq. (19) gives well a saturating viscous stress $\sigma_v \to \sigma_{v\infty}$ at high strain rate (such as $f_1 = \sigma_v$ in visco-plasticity). $K_N$, $N$ are previous Norton parameters (identified for $< 001 >$ at low strain rate), saturation value $\sigma_{v\infty}$ is a material parameter, temperature dependent. At low strain rate one recovers $\dot{p}_1^{\text{Hill}} \approx \left\langle \frac{f_1}{K_N}\right\rangle_+^N$, $\sigma_v \approx K_N(\dot{p}_1^{\text{Hill}})^{1/N}$.

## 3. Tensorial variables for rafting

The microstructure evolution under a tensile load along [001] –the crystallographic orientation taken as frame direction 1– is illustrated schematically in Fig. 3. The initial microstructure is assumed perfectly cubic. Geometric lengths $w_i$ and $\ell_i$ with $i = 1, 2, 3$ are respectively the widths of the three matrix channels in direction $i$ and the size of the $\gamma'$ precipitates. The direction [001] $\equiv$ 1 is usually assumed to coincide with the centrifugally stressed axis of blades. Thus, $w_1$ is the width of the channel normal to the loading axis. Similarly, $\ell_1$ is the size of the precipitates along the loading direction. Quantities $w_2$ and $w_3$, as well as $\ell_2$ and $\ell_3$, are the channel widths and the precipitates sizes mesured along transverse directions [100] $\equiv$ 2 and [010] $\equiv$ 3, $\lambda = \lambda_1$ is the vertical periodicity of the microstructure.

Loading the material along the [001] crystallographic direction, the rafting proceeds towards the widening of the $w_1$ channels and the horizontal coalescence of the precipitates. Thus, the $w_2$ and $w_3$ channel widths tend to become thinner (Fig. 3-2) until they vanish (Fig. 3-3). At the same time, the vertical size of precipitates decreases while the horizontal one increases. While the directional coalescence proceeds, the coarsening proceeds too. Thus, the final microstructure presents only non-zero vertical channel width $w_1$ and wider horizontal channels as well as an increased vertical periodicity.

The main question concerns the nature of thermodynamics variables for rafting. Do we need to choose a vetorial or a tensorial description of the microstructure evolution? For instance, it is easier to consider the $w_i$ and $\ell_i$ as principal values of second order tensors $\mathbf{w}$ and $\boldsymbol{\ell}$ (of general components $w_{ij}$, $\ell_{ij}$) rather than vectors, in order to introduce the Natural Anisotropic Basis –cubic, denoted next NAB– of the single crystal within the mechanical modeling (see section 3.3).

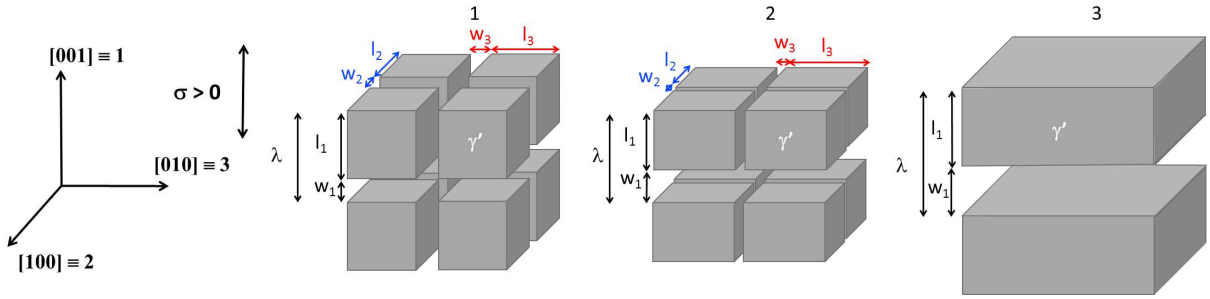


Figure 3: Microstructural evolution: 1) initial microstructure ($w_1 = w_2 = w_3 = w_{001}^0$), 2) intermediate microstructure ($w_1 > w_2 = w_3$), 3) rafted and coarsened microstructure ($w_1 > w_{001}^0$, $w_2 = w_3 = 0$).

*3.1. Fedelich and coworkers variables for rafting*

Let us first summarize some key points present in Fedelich et al (2009, 2012a) concerning the status of the chosen variables for the mechanical description of rafting.

At thermodynamics equilibrium, *i.e.* at low enough thermomechanical loading rate, the $\gamma'$ precipitates volume fraction $f_{\gamma'}$ can be considered as a function of absolute temperature $T$ only, with no delay (see Harada et al (1990), Roebruck et al (2001), Royer et al (1998), Eq. (20) plotted in Fig. 4 for $f_{\gamma'}^0 = 0.7$ and two values of exponent $n$),

$$f_{\gamma'} = f_{\gamma' \text{eq}}(T) = f_{\gamma'}^0\left[1 - \langle T^\star\rangle_+^n\right] \qquad T^\star = \frac{T - T_E}{T_S - T_E} \tag{20}$$

with $f_{\gamma' \text{eq}}(T)$ the equilibrium volume fraction function.

The increase of the periodicity length $\lambda$ – measured in [001] tensile direction – has been found independent of the stress level for all temperatures. In isothermal cases, it is represented by a diffusion type function of temperature

$T$ and time $t$ ($\lambda^0_{001}$: initial periodicity, $Q_\lambda$: activation energy, $\tau_\lambda$: characteristic time, $k_B$: Boltzmann constant, exponent $a_\lambda \approx 3$),

$$\lambda_{[001]} = \lambda(t,T) = \lambda^0_{001}\left[1 + \exp\left(-\frac{Q_\lambda}{k_B T}\right)\frac{t}{\tau_\lambda}\right]^{1/a_\lambda} \tag{21}$$

Eq. (21) generalizes Eq. (1). In such a modeling, the volume fraction $f_{\gamma'} = f_{\gamma' \mathrm{eq}}(T)$ is not considered as a thermodynamics variable, neither is explicitly the periodicity length $\lambda$. One can nevertheless remark that $\lambda$ satisfies the differential equation

$$\dot\lambda = \frac{\left(\lambda^0_{001}\right)^{a_\lambda}}{a_\lambda\,\tau_\lambda}\,\lambda^{1-a_\lambda}\exp\left(-\frac{Q_\lambda}{k_B T}\right) \tag{22}$$

which can be interpreted as an evolution law of thermodynamics of irreversible processes, periodicity length $\lambda$ taken then the status of a state (internal) variable (Lemaitre and Chaboche , 1991).

Rafting for tensile (creep) loading in principal orientation $< 001 >$ is mainly studied in literature and a dimensionless variable $\xi$, this time considered as a thermodynamics state variable, is defined in order to characterize the type of rafting/coarsening change in microstructure (Fedelich et al , 2006),

$$\xi = \frac{w - w_{\mathrm{cube}}}{w_{\mathrm{raft}} - w_{\mathrm{cube}}} \qquad \begin{cases} w_{\mathrm{cube}} = \lambda(t,T)\left(1 - f^{1/3}_{\gamma' \mathrm{eq}}(T)\right) \\ w_{\mathrm{raft}} = \lambda(t,T)\,\left(1 - f_{\gamma' \mathrm{eq}}(T)\right) \end{cases} \tag{23}$$

In Fedelich and co-workers works, the index of rafting $\xi$ is considered as the single thermodynamics variable accounting for rafting in the constitutive modeling. The combined effects of $\gamma'$ precipitates volume fraction (through temperature) and of periodicity length (through time and temperature) are taken into account within single definition (23) for $\xi$ (within $w_{\mathrm{cube}}$ and $w_{\mathrm{raft}}$).

### *3.2. Tinga et al variables for $\gamma'$ rafting (Tinga et al , 2009)*

For the geometrical-mechanical description of $\gamma'$ rafting Tinga *et al* use as internal variables the 3 dimensions $\ell_1, \ell_2, \ell_3$ of large $\gamma'$ precipitates, of initial values $\ell_i(t=0) = \ell_0$, for instance in an evolution law of the form

$$\dot\ell_i = -\frac{\ell_i}{\tau_\ell}\,\frac{3}{2}\,\frac{\sigma'_{ii}}{\sigma_{eq} + \sigma_\varepsilon}\exp\left(-\frac{Q_\ell - \sigma_{eq} U}{k_B T}\right) \qquad \text{(no sum over } i\text{)} \tag{24}$$

with $\sigma_{eq}$ von Mises equivalent stress, $\sigma'_{ii} = \sigma^{\mathrm{d}}_{ii}$ the diagonal components of deviatoric stress tensor $\boldsymbol{\sigma}'$ in the cube Natural Anisotropy Basis. Material parameters are rafting characteristic time $\tau_\ell$, numerical parameter $\sigma_\varepsilon$ (small, it avoids division by zero), activation energy $Q_\ell$, function $U = U(T)$. In Eq. (24) the multiplication by length $\ell_i$ enforces automatically a constant volume of $\gamma'$ precipitates $V_{\gamma'} = \ell_1\ell_2\ell_3 = \ell_0^3$ , feature observed in experiments (Chen and Immarigeon , 1998, Ma et al , 2008).

A time/temperature diffusion like evolution is considered (Eq. (21) with $a_\lambda = 3$), with the assumption $\lambda_1 = \lambda_2 = \lambda_3 = \lambda(t,T)$ of an isotropic periodicity change, with the same remark as in previous section 3.1 on the thermodynamics status of variable $\lambda$. The volume fraction of precipitates is also not an additional variable, it is $f_{\gamma'} = \ell_1\ell_2\ell_3/\lambda^3$. Finally, the widths $w_i$ of the 3 orthogonal $\gamma$ channels are determined from the unit cell geometry, $w_i = \lambda - \ell_i$. They are not additional internal variables neither.

### *3.3. Tensorial variables for rafting*

#### *3.3.1. Tensorial $\boldsymbol{\ell}$ and $\mathbf{e}$*

One can first consider that the large precipitates dimensions $\ell_i$ are the components of a vector $l = (\ell_1, \ell_2, \ell_3)^T$. This point of view is not pertinent in misoriented loading (i.e. out of the [001] crystallographic orientation) cases for which the rotation of the crystal (therefore of the Natural Anisotropy Basis) may occur (Ardakani et al , 1998, Ghighi , 2013, MacKay and Maier , 1982, MacLachlan et al , 2001, Staroselsky et al , 2010, Stinville et al , 2015). This additional information is present within a second order tensor considered then as one of the pertinent internal variable for rafting: principal values of tensor of $\boldsymbol{\ell}$ – which can be diagonalized if chosen symmetric – are the large $\gamma'$ precipitates sizes $\ell_i$ in a possibly rotated basis.

Evolution law (24) for rafting can be rewritten in a tensorial form

$$\dot{\mathbf{e}} = -\frac{1}{\tau_\ell}\,\frac{3}{2}\,\frac{\boldsymbol{\sigma}^{\mathrm{d}}}{\sigma_{eq} + \sigma_\varepsilon}\exp\left(-\frac{Q_\ell - \sigma_{eq} U}{k_B T}\right) \qquad \boldsymbol{\ell} = \ell_0 \exp(\mathbf{e}) \tag{25}$$

where $\boldsymbol{\sigma}^{\mathrm{d}} = \mathbb{P}^{\mathrm{d}} : \boldsymbol{\sigma}$ (Eq. (4), with $\mathbb{P}^{\mathrm{d}}$ a Kelvin projector (A.5)) is diagonal deviatoric part of stress tensor $\boldsymbol{\sigma}$ in Natural Anisotropy Basis, possibly rotating when loading. The definition of symmetric second order tensor $\mathbf{e} = \ln(\boldsymbol{\ell}/\ell_0)$ allows to recover constant volume of $\gamma'$ precipitates (from $\mathrm{tr}\,\boldsymbol{\sigma}^{\mathrm{d}} = 0$, $\mathrm{tr}\,\mathbf{e} = 0$) as

$$V_{\gamma'} = \det \ell = \ell_0^3 \det\left(\exp(\mathbf{e})\right) = \ell_0^3\, e^{\mathrm{tr}\,\mathbf{e}} = \ell_0^3 \tag{26}$$

*3.3.2. Tensorial description of the matrix and microstructure*

The complementary quantities allowing for the geometric description of the evolving microstructure are the $\gamma$ channels widths $w_i$ and the periodicities $\lambda_i$ in the 3 natural anisotropy directions 1 ≡ [001], 2 ≡ [100], 3 ≡ [010]. This means that two additional tensorial variables for the description of $\gamma'$ rafting are $\gamma$ the channel width tensor $\mathbf{w}$ and the periodicity tensor $\boldsymbol{\lambda}$ (assumed isotropic, $\boldsymbol{\lambda} = \lambda\ \mathbf{1}$, in Tinga et al (2009)). Both $\mathbf{w}$ and $\boldsymbol{\lambda}$ are assumed symmetric second order tensors. When the principal basis remains the initial Natural Anisotropy Basis:

$$\mathbf{w} = \left[\begin{array}{ccc} w_1 & 0 & 0 \\ 0 & w_2 & 0 \\ 0 & 0 & w_3 \end{array}\right]_{NAB} \qquad \boldsymbol{\lambda} = \left[\begin{array}{ccc} \lambda_1 & 0 & 0 \\ 0 & \lambda_2 & 0 \\ 0 & 0 & \lambda_3 \end{array}\right]_{NAB} \tag{27}$$

The three tensors $\boldsymbol{\ell}$, $\mathbf{w}$ and $\boldsymbol{\lambda}$ are not independent:

$$\boldsymbol{\ell} + \mathbf{w} = \boldsymbol{\lambda} \tag{28}$$

The $\gamma'$ precipitates volume fraction is then not an independent variable either, it is :

$$f_{\gamma'} = \frac{\ell_1\ell_2\ell_3}{\lambda_1\lambda_2\lambda_3} = \frac{(\lambda_1 - w_1)(\lambda_2 - w_2)(\lambda_1 - w_2)}{\lambda_1\lambda_2\lambda_3} \tag{29}$$

definition which can be generalized to complex rafting cases as intrinsic expression

$$f_{\gamma'} = \frac{\det \boldsymbol{\ell}}{\det \boldsymbol{\lambda}} = \frac{\det (\boldsymbol{\lambda} - \mathbf{w})}{\det \boldsymbol{\lambda}} \tag{30}$$

even when second order tensors $\boldsymbol{\lambda}$ and $\mathbf{w}$ do not remain coaxial.

*3.4. 3D index of $\gamma'$ rafting $x_{raft}$*

An index of $\gamma'$rafting ($\xi$, Eq. (23)) has been introduced in Fedelich et al (2006); it is mainly based on an uniaxial description of $\gamma'$ rafting, for which only one of the three $\gamma$ channel widths is considered (the one in the loading direction $w_1 = w_{[001]} = w_{001}$). Such an index of rafting is built so that $\xi = 0$ for coarsening ($\gamma'$ precipitates remains cubes at $\ell_1 = \ell_2 = \ell_3$, $w_1 = w_2 = w_3$) and $\xi = 1$ for completed rafting in tension (at zero width channel $w_2 = w_3 = 0$). It introduces the two references states $w_{\text{raft}}$ and $w_{\text{cube}}$ at the given volume fraction $f_{\gamma'}$ and periodicity $\lambda$ (in fact the periodicity in direction [100]).

For compression and for misoriented or multiaxial loading cases a pure geometric definition is needed. Using the fact that deviatoric part $\mathbf{w}' = 0$ in coarsening process, we propose to define such a geometric index of rafting as

$$x_{\text{raft}} = \frac{w_{eq}}{\operatorname{tr} \mathbf{w}} \qquad w_{eq} = \sqrt{\frac{3}{2}}\|\mathbf{w}'\| = \sqrt{\frac{3}{2}\mathbf{w}' : \mathbf{w}'} \tag{31}$$

*i.e.* an index built from tensorial $\gamma$ channel width variable only $\mathbf{w}$, of deviatoric part $\mathbf{w}' = \mathbf{w} - \frac{1}{3}\operatorname{tr}\mathbf{w}\,\mathbf{1}$.

One has the following properties for $x_{\text{raft}}$:

- $x_{\text{raft}}$ is dimensionless,
- $x_{\text{raft}} = 0$ for coarsening ($w_{eq} = 0$),
- $x_{\text{raft}} = 1$ for rafting in uniaxial tension along [100] at diagonal $\mathbf{w} = \text{diag}[w_1, 0, 0]$,
- $x_{\text{raft}} = \frac{1}{2}$ for rafting in uniaxial compression along [100] at diagonal $\mathbf{w} = \text{diag}[0, w_2, w_3 = w_2]$.

Let us point out that the value $x_{\text{raft}} = 0$ uniquely correspond to coarsening (spherical tensor $\mathbf{w} = w\,\mathbf{1}$), the value $x_{\text{raft}} = 1$ uniquely corresponds to complete rafting (rafting tensor $\mathbf{w}$ with two eigenvalues equal to zero).

The link with index $\xi$ is given in Appendix D.

**Remark.** *Definition (31) is inspired from the definition of stress triaxiality* $\text{Triax} = \frac{1}{3}\operatorname{tr}\boldsymbol{\sigma}/\sigma_{eq}$ *in the field of ductile rupture and continuum damage mechanics (Lemaitre et al , 2009, Rice and Tracey , 1969).*

*3.5. On the choice of internal variables to represent microstructure degradation*

The question of the choice of the best set of thermodynamics internal variables arises, *a*) for the geometric description of $\gamma'$-rafting, *b*) for the mechanical consequences of rafting. In case *a*) the consideration of two tensorial variables among the three $\boldsymbol{\ell}$, $\mathbf{w}$, $\boldsymbol{\lambda}$, seems an adequate choice (but the question of the tensors coaxiality arises then). In case *b*) different choices are pertinent, including scalars variables – for instance index of rafting $\xi$ (Fan et al , 2015, Fedelich et al , 2006, Tinga et al , 2009), isotropic periodicity $\lambda$ or precipitates volume fraction $f_{\gamma'}$ Cormier and Cailletaud (2010a), Ghighi et al (2013), Giraud et al (2013), le Graverend et al (2014a). One has simply to be careful to the independency of the variables retained.

The first choice made next (section 4.5.1) will be to use tensorial variable $\mathbf{w}$ and scalar variable $f_{\gamma'}$ as state thermodynamics variables for the mechanical description of microstructural changes. Such a preliminary choice is based on the following remarks:

- the $\gamma$ channel width is the quantity that directly acts in Orowan stress, that affects at first order the mechanical response (hardening) of the RVE, the larger the channel width the lower the apparent yield stress; the three direction widths $w_i$ can be measured with less difficulties than anisotropic precipitates shapes $\ell_i$ or anisotropic periodicity lengths $\lambda_i$ in case of advanced rafting,
- if both the sizes of $\gamma'$ precipitates $\boldsymbol{\ell}$ and the periodicities $\boldsymbol{\lambda}$ are omitted, one cannot determine (by means of Eq. (29)-(30)) the $\gamma'$ precipitates volume fraction; the effect of $f_{\gamma'}$ has then :
  - either to be neglected (possible choice at thermodynamics equilibrium as it can be considered at zeroth order as a function of temperature only),
  - or to be set as the second variable for the mechanical description of microstuctural changes (our choice for possibly high thermomechanical loading rates),
- the $\gamma'$ precipitates volume fraction $f_{\gamma'}$ is a scalar, in comparison with tensorial nature of $\boldsymbol{\ell}$ and $\boldsymbol{\lambda}$ (tensors difficult to measure, more costly choice for structural Finite Element applications), it is standardly measured,
- the evolution kinetic of $\gamma$ channel width $w_{001}$ is at first order mainly related to volume fraction $f_{\gamma'}$ with the same quantitative dependency measured for both coarsening and rafting processes. It has indeed already been shown for MC2 alloy, under both isothermal and non-isothermal creep conditions that the $\gamma$ channel width only (mainly) depends on the $\gamma'$ volume fraction for a sufficiently high temperature, typically above 1000°C (Cormier and Cailletaud , 2010a).

Such a first choice is fully consistent with the initial formulation of the Polystar model (Cormier and Cailletaud , 2010a). A second choice will be proposed in section 4.5.2. It is here recalled that the index of rafting $x_{\text{raft}}$ is not an additional variable.

## 4. Thermodynamics of rafting

For nickel-based single crystal superalloys at high temperature, the decrease in mechanical properties associated with the $\gamma'$ rafting mainly results from the widening of $\gamma$ channels where the plastic deformation concentrates (Pollock and Argon , 1994). Indeed, during creep at high temperature and low stress, typically in between 1000 and 1200 °C, depending on the alloy chemistry, the end of the pimary creep stage corresponds to $\gamma'$ completion. The decreasing creep strain rate during this primary creep stage directly results from an easier dislocation mobility in the $\gamma$ channels which can be evaluated by the Orowan Stress, defined as :

$$\sigma_{\text{ORO}} \propto \frac{GB}{w_{001}} \tag{32}$$

with $B$ the Burgers vector magnitude (= 0.254 nm), and $w_{001}$ the $\gamma$ channel width along a < 001 > direction (*i.e* in a (100) or a (010) plane).

Since dislocations under high temperature conditions are mainly gliding in the matrix on octahedral slip systems, a correction factor $\theta$ is considered for Orowan stress at (octahedral) slip systems scale,

$$\tau_{\text{ORO}} = \theta \frac{GB}{w_{001}} \tag{33}$$

with for instance $\theta = \sqrt{2/3}$ obtained when calculating the Orowan stress using $\gamma$ channels width along the [001] direction (Benyoucef et al , 1993). The value of $\theta$ was assumed to be 0.5 in Fedelich et al (2009) and 0.85 in Tinga et al (2009), *i.e* a value close to the $\sqrt{2/3}$ considered in Cormier and Cailletaud (2010a).

### *4.1. Fedelich and coworkers model (Fedelich et al , 2009, 2012a)*

Thermodynamics potential $\rho\psi$ –with $\rho$ the density, $\psi$ specific free energy– is considered as a function of stress tensor $\boldsymbol{\sigma}$, of temperature $T$, of plastic strain tensor $\boldsymbol{\epsilon}$, of isotropic hardening (defined at the slip systems scale), of octahedral $\boldsymbol{\alpha}^o$ and cubic $\boldsymbol{\alpha}^c$ kinematic hardening tensors (homogeneous to strains) and of $\gamma'$ rafting scalar variable $\xi$. If thermal expansion and heat capacity contributions are omitted:

$$\rho\psi = \frac{1}{2}(\boldsymbol{\epsilon} - \boldsymbol{\epsilon}^p) : \mathbb{E} : (\boldsymbol{\epsilon} - \boldsymbol{\epsilon}^p) + \rho\psi_p^{\text{isotropic}} + \rho\psi_p^{\text{kinematic}} + \rho\psi_u \tag{34}$$

Hooke tensor $\mathbb{E}$ has cubic symmetry, the coupling of elasticity with rafting being neglected.

Stored energy density (contribution of the dislocation stresses) is classically quadratic in internal variables $\boldsymbol{\alpha}^o$ and $\boldsymbol{\alpha}^c$. Kinematic hardening contribution is coupled to rafting as

$$\rho\psi_p^{\text{kinematic}} = \frac{1}{2}c^o(1 - \kappa_\alpha\xi)\,\boldsymbol{\alpha}^o : \boldsymbol{\alpha}^o + \frac{1}{2}c^c\boldsymbol{\alpha}^c : \boldsymbol{\alpha}^c \qquad \begin{cases} \mathbf{X}^o = \rho\frac{\partial\psi}{\partial\boldsymbol{\alpha}^o} = c^o(1 - \kappa_\alpha\xi)\,\boldsymbol{\alpha}^o \\ \mathbf{X}^c = \rho\frac{\partial\psi}{\partial\boldsymbol{\alpha}^c} = c^c\,\boldsymbol{\alpha}^c \end{cases} \tag{35}$$

introducing hardening moduli $c^o$, $c^c$ and rafting coupling parameter $\kappa_\alpha$, the superscripts $^o$ and $^c$ respectively standing for octahedral and cubic slip systems.

Misfit energy $\rho\psi_u$ represents the contribution of the $\gamma/\gamma'$ internal coherency stresses (Fedelich , 2002), here relaxing when rafting occurs. It is expressed as (Fedelich et al , 2006)

$$\rho\psi_u = \frac{1}{2}(\kappa_u - \kappa_\xi \xi)\delta_u^2 \tag{36}$$

where $\delta_u$ denotes the unconstrained lattice misfit, with $\kappa_u$ and $\kappa_\xi$ two material parameters. Index $\xi$ is defined by Eq. (23), using Eq. (20) for $f_{\gamma'} = f_{\gamma' \mathrm{eq}}(T)$ and Eq. (21) for $\lambda(t,T)$. The driving force for rafting is then

$$X = -\rho\frac{\partial\psi}{\partial\xi} = \frac{1}{2}\kappa_\alpha c^o\, \boldsymbol{\alpha}^o : \boldsymbol{\alpha}^o + \frac{1}{2}\kappa_\xi \delta_u^2 \tag{37}$$

In the model, the pseudo-cubic slip systems are assumed not affected by the microstructure degradation. Thus, they do not contribute to the rafting thermodynamics force $X$, nor to $\gamma'$ rafting evolution.

Plastic strain rate is gained from single crystal plasticity framework (Asaro , 1983, Cailletaud , 1991, Méric et al , 1991, Peirce et al , 1983),

$$\dot{\boldsymbol{\epsilon}}^p = \dot{\boldsymbol{\epsilon}}^{po} + \dot{\boldsymbol{\epsilon}}^{pc} = \frac{1}{2}\sum_{g=1}^{12}\left(\mathrm{n}_\mathrm{g}^\mathrm{o}\otimes\mathrm{m}_\mathrm{g}^\mathrm{o} + \mathrm{m}_\mathrm{g}^\mathrm{o}\otimes\mathrm{n}_\mathrm{g}^\mathrm{o}\right)\dot{\gamma}_g^o + \frac{1}{2}\sum_{g=1}^{6}\left(\mathrm{n}_\mathrm{g}^\mathrm{c}\otimes\mathrm{m}_\mathrm{g}^\mathrm{c} + \mathrm{m}_\mathrm{g}^\mathrm{c}\otimes\mathrm{n}_\mathrm{g}^\mathrm{c}\right)\dot{\gamma}_g^c \tag{38}$$

The unit vectors $\mathrm{m}_\mathrm{g}^\mathrm{o}$, $\mathrm{m}_\mathrm{g}^\mathrm{c}$ denote the slip directions and $\mathrm{n}_\mathrm{g}^\mathrm{o}$, $\mathrm{n}_\mathrm{g}^\mathrm{c}$ the normal to the slip planes of the slip system $g$, octahedral, and either cubic (Méric et al , 1991) or pseudo-cubic (Fedelich , 2002); $\dot{\gamma}_g$ is the corresponding slip rate. The resolved shear stresses on both families of slip systems are $\tau^o = \mathrm{m}^\mathrm{o}\cdot\boldsymbol{\sigma}\cdot\mathrm{n}^\mathrm{o}$, $\tau^c = \mathrm{m}^\mathrm{c}\cdot\boldsymbol{\sigma}\cdot\mathrm{n}^\mathrm{c}$. The back-stresses at the level of the slip systems are then $x_g^o = \mathrm{m}^\mathrm{o}\cdot\mathbf{X}^\mathrm{o}\cdot\mathrm{n}^\mathrm{o}$, $x_g^c = \mathrm{m}^\mathrm{c}\cdot\mathbf{X}^\mathrm{c}\cdot\mathrm{n}^\mathrm{c}$.

Finally, the evolution law for index of rafting $\xi$ is

$$\dot{\xi} = R_0(1-\xi)\,X^r \tag{39}$$

with $R_0$ and $r$ as material parameters.

Rafting reduces the hardening for the octahedral slip systems only, in a twofold manner,

- it reduces Orowan stress $\tau_\mathrm{ORO} \propto GB/w$, introduced as an isotropic hardening in viscosity law, by increasing the $\gamma$ channel width $w$ according to Eq. (20)-(21) and (23), $B$ being the magnitude of Burgers vector,
- it directly reduces the octahedral kinematic hardening $\mathbf{X}^o$ (Eq. (35)).

The microstructural degradation affects the viscosity law, with, depending on a model parameter, a yield threshold $\tau_\mathrm{th}$ either sharp at $\tau_\mathrm{th} = |\tau_g^o - x_g^o|_\mathrm{th} \approx \tau_\mathrm{ORO}$ or allowing for visco-plasticity at $\tau_\mathrm{th} = |\tau_g^o - x_g^o|_\mathrm{th} < \tau_\mathrm{ORO}$. Following Johnson and Cook (1983), Lemaitre (1971), a multiplicative coupling with isotropic hardening is considered but at the slip systems scale; it is not detailed here, nor are the nonlinear kinematic hardening rules $\dot{\boldsymbol{\alpha}}^o = ...$, $\dot{\boldsymbol{\alpha}}^c = ...$, with nonlinear (sinh type) dynamic and static recovery terms.

### *4.2. Dislocation bypassing energy density*

We propose to derive a thermodynamics framework for rafting directly at the RVE scale, without the use at this stage of the single crystal plasticity framework. We nevertheless need to make the conceptual difference between plasticity due to the octahedral slip systems, which are classically affected by Orowan stress, and plasticity due to the pseudo-cubic slip systems, less affected by Orowan stress. In order to do so at RVE scale, we use Kelvin modes based definitions of section 2 and introduce two accumulated plastic strains representative of $< 001 >$ slip systems ($p^\mathrm{d}$) and of $< 111 >$ slip systems ($p^{\overline{\mathrm{d}}}$) (Desmorat and Marull , 2011). Both accumulated plastic strains $p^\mathrm{d}$ and $p^{\overline{\mathrm{d}}}$ are mean values over the RVE. Corresponding "deviatoric diagonal" $\boldsymbol{\epsilon}^{p\mathrm{d}}$ and "deviatoric out of diagonal" $\boldsymbol{\epsilon}^{p\overline{\mathrm{d}}}$ Kelvin modes based plastic strains are close to octahedral $\boldsymbol{\epsilon}^{po}$ and cubic $\boldsymbol{\epsilon}^{pc}$ plastic strains of single crystal plastic framework (see section Appendix F). Assuming Orowan stress behaves as isotropic hardening and using a mixture law, the corresponding plastic work reads, with $\rho$ the density,

$$\rho\psi_\mathrm{ORO} = f_\gamma\sigma_\mathrm{ORO}p^\mathrm{d} = (1-f_{\gamma'})\,\sigma_\mathrm{ORO}p^\mathrm{d} \propto (1-f_{\gamma'})\frac{GB}{w_{001}}p^\mathrm{d} \tag{40}$$

generalized into dislocation bypassing energy density,

$$\rho\psi_\mathrm{ORO} = \kappa_\mathrm{ORO}g(f_{\gamma'})\,G\frac{w_{001}^0}{\|\mathbf{w}\|}(p^\mathrm{d} + \varpi p^{\overline{\mathrm{d}}}) \qquad \frac{\mathrm{d}g}{\mathrm{d}f_{\gamma'}} < 0 \tag{41}$$

where mean anisotropic Orowan effect over the RVE is simply introduced through quadratic norm $\|\mathbf{w}\| = (\mathrm{tr}\ \mathbf{w}^2)^{1/2}$ of $\gamma$ width channel tensor $\mathbf{w}$, phenomenological function $g(f_{\gamma'})$ of $\gamma'$ precipitates volume fraction, of parameter $\kappa_\mathrm{ORO}$.

By means of material constant $\varpi$, one has introduced in Eq. (41) a macroscopic second order contribution of the accumulated plastic strain $p^{\overline{\mathrm{d}}}$ representative of $< 111 >$ material response (Eq. (10)). The value $\varpi \approx 0.8$–$1$ will be obtained in section 7.4. Quantity $w^0_{001} \approx 50$ nm is the initial (room temperature) mean value of the $\gamma$ channels width, the corresponding initial value for $\gamma'$ precipitates volume fraction is $f^0_{\gamma'}$. Material parameter $\kappa_{\mathrm{ORO}} = \kappa_{\mathrm{ORO}}(T)$ is temperature dependent.

The function $g(f_{\gamma'})$ is a decreasing function of the precipitates volume fraction and it is normed such as $g(f^0_{\gamma'}) = 1$. Two possible expressions are given here, first one corresponding to (linear) mixture law, second one the power law used (and measured) in the Polystar model (Cormier and Cailletaud , 2010a),

$$g(f_{\gamma'}) = \frac{1 - f_{\gamma'}}{1 - f^0_{\gamma'}} \quad \text{or} \quad g(f_{\gamma'}) = \left(\frac{f^0_{\gamma'}}{f_{\gamma'}}\right)^{m_{\gamma'}} \tag{42}$$

with the properties $g(f^0_{\gamma'}) = 1$ and $\frac{\mathrm{d}g}{\mathrm{d}f_{\gamma'}} < 0$

An important remark is that as the precipitate volume fraction changes, the rafting and the coarsening all act in energy density (41) as single (tensorial) dimensionless mechanical rafting variable

$$\boldsymbol{\omega} = \frac{\mathbf{w}}{g(f_{\gamma'})w^0_{001}} \quad \text{or} \quad \omega_{ij} = \frac{w_{ij}}{g(f_{\gamma'})w^0_{001}}. \tag{43}$$

Thus, in the same spirit than for rafting (scalar) variable $\xi$ in Fedelich and coworkers constitutive models, one proposes next to give to dimensionless (tensorial) variable $\boldsymbol{\omega}$ the status of single thermodynamics state variable for microstructure degradation, possibly anisotropic. In this way the dislocation bypassing energy density at RVE scale can be rewritten as

$$\rho\psi_{\mathrm{ORO}} = \kappa_{\mathrm{ORO}} \frac{G}{\|\boldsymbol{\omega}\|}(p^{\mathrm{d}} + \varpi p^{\overline{\mathrm{d}}}) \tag{44}$$

with the physical $\gamma$ channels widths later determined as

$$\mathbf{w} = g(f_{\gamma'})\, w^0_{001}\boldsymbol{\omega} \qquad \text{or} \quad w_{ij} = g(f_{\gamma'})\, w^0_{001}\omega_{ij} \tag{45}$$

which is nothing else than a tensorial extension (with second order tensors $\mathbf{w}$, $\boldsymbol{\omega}$ of component $w_{ij}$, $\omega_{ij}$) of initial (scalar) Polystar equation for tension along [001] (Cormier and Cailletaud , 2010a),

$$w_{[001]} = g(f_{\gamma'})\, w^0_{001}\,(\omega_{\mathrm{mech}} + \omega_{\mathrm{LSW}}) = g(f_{\gamma'})\, w^0_{001}\omega^{\mathrm{Polystar}} \tag{46}$$

constitutive equation shown to apply to thermo-mechanical loading at $\dot{T} \neq 0$, $\dot{f}_{\gamma'} \neq 0$. Dimensionless scalar variable $\omega^{\mathrm{Polystar}} = \omega_{\mathrm{mech}} + \omega_{\mathrm{LSW}}$ is the sum of a mechanical rafting/coarsening contribution $\omega_{\mathrm{mech}}$, stress and/or plastic strain dependent, and of the diffusion term $\omega_{\mathrm{LSW}}$ consistent with Eq. (1).

### *4.3. Coupling elasticity-rafting*

Pineau (1976) by using a micro-mechanics approach and more recently Tinga et al (2009) by using unit cell Finite Element computations have shown that the strain energy during a creep test decreases as yielding and rafting proceed (see also (Fan et al , 2015)). As there is a lack of experimental evidences on the rafting-elasticity coupling, one can simply assume that elasticity remains cubic and sets

$$\rho\psi_e = \frac{1}{2}(\boldsymbol{\epsilon} - \boldsymbol{\epsilon}^p) : \mathbb{E}\,(1 - \kappa_E\omega_{eq}) : (\boldsymbol{\epsilon} - \boldsymbol{\epsilon}^p) = \frac{1}{2}\boldsymbol{\epsilon}^e : \mathbb{E}\,(1 - \kappa_E\omega_{eq}) : \boldsymbol{\epsilon}^e \tag{47}$$

where $\boldsymbol{\epsilon}^e$ is elastic strain tensor and where one has introduced the elasticity-rafting coupling paremeter $\kappa_E$. No effect is considered when coarsening ($\omega_{eq} = \sqrt{\frac{3}{2}}\|\boldsymbol{\omega}'\|$ is the norm of deviatoric part $\boldsymbol{\omega}' = \boldsymbol{\omega} - \frac{1}{3}\,\mathrm{tr}\,\boldsymbol{\omega}\,\mathbf{1}$), if needed replace $\omega_{eq}$ by $\|\boldsymbol{\omega}\|$. The thermodynamics framework derived next will consider such a coupling (in order to recover the energetic contribution to rafting driving force derived in Fan et al (2015)) but the final model proposed in section 6 will neglect it ($\kappa_E\omega_{eq} << 1$, Eq. (74)).

Thermo-mechanical terms are omitted in Eq. (47). Considering the unconstrained misfit[1] $\delta_u$, as a difference in reference temperature for $\gamma$ and for $\gamma'$ phases allows to define a thermo-elastic misfit contribution $-3f_{\gamma'}K_{\gamma'}\delta_u\,\mathrm{tr}\,\boldsymbol{\epsilon} = 3f_{\gamma'}\frac{K_{\gamma'}}{K}|\delta_u|\,\mathrm{tr}\,\boldsymbol{\sigma}$ (see Appendix C), proportional to both the absolute value of the misfit $|\delta_u|$ and to the stress (as in Fedelich (2002), Nabarro et al (1995)). Following Fedelich et al (2006, 2009) for high temperature visco-plastic processes, such a contribution will also be neglected, this time compared to next misfit energy $\rho\psi_u$.

[1] negative for considered CMSX-4 superalloy

*4.4. Misfit energy density $\rho\psi_u$*

The misfit energy density $\rho\psi_u = \frac{1}{2}(\kappa_u - \kappa_\xi\,\xi)\delta_u^2$ (Fedelich et al , 2006), Eq. (36) and definition (23)), with the –here negative– unconstrained mistfit, has the following properties: $\rho\psi_u$ remains constant during coarsening (as then $\xi = 0$), it decreases when rafting takes place (as then $\xi \to 1$). It is worth remarking that the dependency of material parameters $\kappa_u$ and $\kappa_\xi$ with respect to $f_{\gamma'}$ has not been exhibited in pioneering works. In most models (Fan et al , 2015, Fedelich et al , 2006, 2009, 2012a, Tinga et al , 2009) , thermodynamics equilibrium is assumed with biunivoque (instantaneous) relationship between $f_{\gamma'}$ and temperature $T$ so that the dependencies with respect to $f_{\gamma'}$ is hidden into temperature dependency $\kappa_u = \kappa_u(T)$, $\kappa_\xi = \kappa_\xi(T)$.

A first possibility for tensorial rafting framework is to rewrite $\rho\psi_u$ as a function of the 3D dimensionless index of rafting $x_{\text{raft}}$ defined in Eq. (31) (also such as $x_{\text{raft}} = 0$ when coarsening and $x_{\text{raft}} \to 1$ when rafting). Thermodynamics will not allow us to do so (impossibility to prove in any case the positivity of the intrinsic dissipation).

Instead we propose to simply use the remark that one has a zero deviatoric part $\mathbf{w}' = \boldsymbol{\omega}' = 0$ when coarsening and write misfit energy density as

$$\rho\psi_u = \frac{1}{2}\left(\kappa_u - \kappa_\omega\,\omega_{eq}\right)\delta_u^2 \qquad \omega_{eq} = \sqrt{\frac{3}{2}}\|\boldsymbol{\omega}'\| \tag{48}$$

with $\kappa_u$ and $\kappa_\omega$ as temperature dependent material parameters. Misfit energy is expressed as a function of deviatoric part $\boldsymbol{\omega}'$ of mechanical rafting variable and of temperature; therefore it remains constant during a pure isotropic coarsening process and it decreases during the gamma-prime rafting process, as wanted. Compared to Fedelich's expression it is now dependent on the intensity of rafting (the $\gamma$-channels widths). Note that at thermodynamics equilibrium, one has $f'_\gamma = f_{\gamma' \text{eq}}(T)$ so that Eq. (48) becomes equivalent to alternative formulation $\rho\psi_u = \frac{1}{2}\left(\kappa_u - \kappa_\text{w} w_{eq}\right)\delta_u^2$ with an adequate definition of temperature dependency of parameters $\kappa_u = \kappa_u(T)$, $\kappa_\omega = \kappa_\omega(T)$, $\kappa_\text{w} = \kappa_\text{w}(T)$. Remark that present parameter $\kappa_\omega$ has the same dimension but differs in value from $\kappa_\xi$ parameter introduced by Fedelich and coworkers.

*4.5. Thermodynamics potential*

The thermodynamics potential, here Helmholtz free energy density $\rho\psi$, is function of the total strain $\boldsymbol{\epsilon}$, of the temperature $T$ and of internal variables $\boldsymbol{\mathcal{V}}_K$. The thermodynamics forces are (Lemaitre and Chaboche , 1991)

$$\boldsymbol{\sigma} = \rho\frac{\partial\psi}{\partial\boldsymbol{\epsilon}} \qquad s = -\frac{\partial\psi}{\partial T} \qquad \boldsymbol{\mathcal{A}}_K = \rho\frac{\partial\psi}{\partial\boldsymbol{\mathcal{V}}_K} \tag{49}$$

with $s$ the specific entropy and $\boldsymbol{\mathcal{A}}_K$ the associated variables to internal variables $\boldsymbol{\mathcal{V}}_K$.

The intrinsic dissipation is then ("$\bullet$" meaning multiplication for scalar variables, scalar product ":" for tensorial variables)

$$\mathcal{D} = -\sum_K \boldsymbol{\mathcal{A}}_K \bullet \dot{\boldsymbol{\mathcal{V}}}_K \tag{50}$$

and is positive when the second principle of thermodynamics is satisfied.

*4.5.1. $\mathbf{w}$ and $f_{\gamma'}$ as state variables*

The question is then the proper definition of the internal variables for the considered material and applications. Let us follow *a priori* choice made in section 3.5, and first consider as internal variables

- macroscopic plastic strain $\boldsymbol{\epsilon}^p$ (associated with $-\boldsymbol{\sigma}$) instead of the plastic slips over each slip system; note that crystal plasticity constitutive equations will be derived in section Appendix F,
- macroscopic isotropic hardening variables $p^\text{d}$ (associated force: isotropic hardening $R$) for octahedral-like slip systems and $p^{\overline{\text{d}}}$ (associated force: isotropic hardening $\overline{R}$) for cubic-like slip systems,
- tensorial rafting variable $\mathbf{w}$ (associated force: $\mathbf{W}$),
- $\gamma'$ precipitates volume fraction $f_{\gamma'}$ (associated force: $-F_{\gamma'}$),

The state laws are

$$\boldsymbol{\sigma} = \rho\frac{\partial\psi}{\partial\boldsymbol{\epsilon}} = -\rho\frac{\partial\psi}{\partial\boldsymbol{\epsilon}^p} \qquad R = \rho\frac{\partial\psi}{\partial p^\text{d}} \qquad \overline{R} = \rho\frac{\partial\psi}{\partial p^{\overline{\text{d}}}} \qquad \mathbf{W} = -\rho\frac{\partial\psi}{\partial\mathbf{w}} \qquad F_{\gamma'} = -\rho\frac{\partial\psi}{\partial f_{\gamma'}} \tag{51}$$

The intrinsic dissipation is therefore the sum of a plastic contribution (Desmorat and Marull , 2011, Lemaitre and Chaboche , 1991) and of a rafting contribution (which includes $\gamma'$ precipitates evolution):

$$\mathcal{D} = \mathcal{D}_\text{plast} + \mathcal{D}_\text{raft} \qquad \begin{cases} \mathcal{D}_\text{plast} = \boldsymbol{\sigma} : \dot{\boldsymbol{\epsilon}}^p - R\dot{p}^\text{d} - \overline{R}\dot{p}^{\overline{\text{d}}} \\ \mathcal{D}_\text{raft} = \mathbf{W} : \dot{\mathbf{w}} + F_{\gamma'}\,\dot{f}_{\gamma'} \end{cases} \tag{52}$$

The dissipation $\mathcal{D}_{\text{plast}}$ is always positive if criterion functions $f_1 = \sigma^{\text{d}}_{eq} - R - \sigma_y$, $f_2 = \sigma^{\overline{\text{d}}}_{eq} - \overline{R} - \overline{\sigma}_y$ – including Orowan contributions – are considered altogether with standard visco-plasticity loading/unloading conditions (16), as one has then

$$\mathcal{D}_{\text{plast}} = (\sigma^{\text{d}}_{eq} - R)\dot{p}^{\text{d}} + (\sigma^{\overline{\text{d}}}_{eq} - \overline{R})\dot{p}^{\overline{\text{d}}} \geq 0 \tag{53}$$

as $\boldsymbol{\sigma}' = \boldsymbol{\sigma}^{\text{d}} + \boldsymbol{\sigma}^{\overline{\text{d}}}$, and from Eq. (15), $\boldsymbol{\sigma}^{\text{d}} : \mathbf{n}^{\text{d}} = \sigma^{\text{d}}_{eq}\dot{p}^{\text{d}}$ and $\boldsymbol{\sigma}^{\overline{\text{d}}} : \mathbf{n}^{\overline{\text{d}}} = \sigma^{\overline{\text{d}}}_{eq}\dot{p}^{\overline{\text{d}}}$. Presented modeling corresponds to the case of a vanishing Hill parameter $h$. The case $h \neq 0$, *i.e.* of a Hill criterion function $f_1 = \sigma_{\text{Hill}} - R - \sigma_y$, is simply obtained by replacing $\sigma^{\text{d}}_{eq}$ by $\sigma_{\text{Hill}}$ and $(p^{\text{d}}, p^{\overline{\text{d}}})$ by $(p^{\text{Hill}}_1, p^{\overline{\text{d}}}_2)$ (see section 2.4).

Concerning the dissipation due to microstructure degradation $\mathcal{D}_{\text{raft}}$, the thermodynamics does not give specific limitations (one only has to enforce $\mathcal{D} \geq 0$).

But note that at thermodynamics non equilibrium, the $\gamma'$ precipitates volume fraction –measured as well as modeled within initial Polystar model– may either increase and decrease (Cormier and Cailletaud , 2010a), depending on the temperature rate history. It is indeed not possible to write $f_{\gamma'} = f_{\gamma' eq}(T)$ at any time of a thermo-mechanical loading since out of equilibrium states generating fine precipitates are possible in cases of fast heating and fast cooling rates. On heating, fine and coarse precipitates are dissolving, the dissolution kinetics being higher for a fine precipitate. On cooling, both fine and coarse precipitates volume fractions increase at different kinetics, depending on the cooling rate and on the temperature variation from the high temperature state (depending on the driving force for fine $\gamma'$ nucleation in the $\gamma$ channels) (Cormier and Cailletaud , 2010a, Giraud et al , 2013, le Graverend et al , 2014a). This fact makes impossible to satisfy separately, *i.e.* mechanism by mechanism / internal variable by internal variable, the positivity of each intrinsic dissipations $\mathbf{W} : \dot{\mathbf{w}}$ and $F_{\gamma'}\dot{f}_{\gamma'}$. This means that from a thermodynamics point of view, the evolution (rate) laws $\dot{\mathbf{w}} = ...$ and $\dot{f}_{\gamma'} = ...$ for internal variables $\mathbf{w}$, $f_{\gamma'}$ are coupled in a quite complex manner in order to always satisfy the positivity of the dissipation.

From the remarks

*i)* that the $\gamma$ width channel may increase and decrease in a reversible way by slow (at equilibrium) temperature variation,

*ii)* according to *i)*, that there is no evolution law of the form $\dot{\mathbf{w}} = ...$ in Polystar constitutive equations handling out of thermodynamics equilibrium states but rate independent equation (46),

*iii)* that the contribution of all rafting variables can be included in Helmholtz free energy density within single variable $\boldsymbol{\omega}$,

we propose in next section an alternative thermodynamics framework based on single tensorial mechanical rafting variable $\boldsymbol{\omega}$.

*4.5.2. Tensorial mechanical rafting variable $\boldsymbol{\omega}$ as state variable*

Helmholtz free energy density is assumed to be a function of total strain $\boldsymbol{\epsilon}$, of temperature $T$, of macroscopic plastic strain $\boldsymbol{\epsilon}^p$, of the two macroscopic isotropic hardening variables $p^{\text{d}}$ and $p^{\overline{\text{d}}}$ and of tensorial mechanical rafting variable $\boldsymbol{\omega}$,

$$\rho\psi = \frac{1}{2}(\boldsymbol{\epsilon} - \boldsymbol{\epsilon}^p) : \mathbb{E}\,(1 - \kappa_E\omega_{eq}) : (\boldsymbol{\epsilon} - \boldsymbol{\epsilon}^p) + \left(R_\infty + \frac{\kappa_{\text{ORO}}G}{\|\boldsymbol{\omega}\|}\right)p^{\text{d}} + \left(\overline{R}_\infty + \varpi\frac{\kappa_{\text{ORO}}G}{\|\boldsymbol{\omega}\|}\right)p^{\overline{\text{d}}} + \frac{1}{2}\left(\kappa_u - \kappa_\omega\,\omega_{eq}\right)\delta_u^2 \tag{54}$$

with $\mathbb{E}$ Hooke's tensor having cubic elasticity symmetry (material parameters $E$, $\nu$ and $G$) and where $\omega_{eq} = \sqrt{\frac{3}{2}}\|\boldsymbol{\omega}'\|$ is von Mises norm of symmetric second order tensor $\boldsymbol{\omega}$. The rafting-elasticity coupling parameter $\kappa_E$ is introduced but have in mind that the term $\kappa_E\omega_{eq}$ will ne neglected.

For the sake of –relative– simplicity the mechanical parts of isotropic hardenings are assumed saturated through material parameters $R_\infty$, $\overline{R}_\infty$ (if not, replace them by functions of $p^{\text{d}}$ and $p^{\overline{\text{d}}}$), the thermal expansion and heat capacity contributions have been omitted.

The state laws are

$$\boldsymbol{\sigma} = \rho\frac{\partial\psi}{\partial\boldsymbol{\epsilon}} = \mathbb{E}(1 - \kappa_E\omega_{eq}) : \boldsymbol{\epsilon}^e \qquad R = \rho\frac{\partial\psi}{\partial p^{\text{d}}} = R_\infty + \frac{\kappa_{\text{ORO}}G}{\|\boldsymbol{\omega}\|} \qquad \overline{R} = \rho\frac{\partial\psi}{\partial p^{\overline{\text{d}}}} = \overline{R}_\infty + \varpi\frac{\kappa_{\text{ORO}}G}{\|\boldsymbol{\omega}\|} \tag{55}$$

with elastic strain $\boldsymbol{\epsilon}^e = \boldsymbol{\epsilon} - \boldsymbol{\epsilon}^p = \boldsymbol{\epsilon} - \boldsymbol{\epsilon}^{p\text{d}} - \boldsymbol{\epsilon}^{p\overline{\text{d}}}$, and for rafting:

$$\boldsymbol{\Omega} = -\rho\frac{\partial\psi}{\partial\boldsymbol{\omega}} = \kappa_{\text{ORO}}\frac{G}{\|\boldsymbol{\omega}\|^2}\frac{\boldsymbol{\omega}}{\|\boldsymbol{\omega}\|}(p^{\text{d}} + \varpi p^{\overline{\text{d}}}) + \sqrt{\frac{3}{8}}\left[\kappa_E\,\boldsymbol{\epsilon}^e : \mathbb{E} : \boldsymbol{\epsilon}^e + \kappa_\omega\,\delta_u^2\right]\frac{\boldsymbol{\omega}'}{\|\boldsymbol{\omega}'\|} \tag{56}$$

$-\boldsymbol{\Omega}$ is the thermodynamics force associated with the internal variable $\boldsymbol{\omega}$.

The dissipation due to rafting, previous Eq. (52), becomes

$$\mathcal{D}_{\text{raft}} = \boldsymbol{\Omega} : \dot{\boldsymbol{\omega}} \tag{57}$$

a simple expression which includes $\gamma'$ precipitates contribution.

Dissipation $\mathcal{D}_{\text{raft}}$ has to be positive for any loading, isothermal or not, proportional or not.

## 5. Positive intrinsic dissipation from generic tensorial rafting evolution law

One aims at modeling rafting, coarsening and homothetic $\gamma$ channels width growth from a tensorial evolution law $\dot{\boldsymbol{\omega}} = ....$ The question is wether it is possible to propose a generic expression that always satisfies the second principle of thermodynamics. A first possibly is it to use the framework of standard generalized materials (Halphen and Neguyen , 1975, Lemaitre and Chaboche , 1991) and to write $\dot{\boldsymbol{\omega}} = \frac{\partial \mathcal{F}}{\partial \boldsymbol{\Omega}}$, with potential of dissipation $\mathcal{F}$ convex in $\boldsymbol{\Omega}$. This proves to be not general enough. For instance Tinga type evolution law (24) does not satisfy such a standard framework (see Appendix E).

A more general non standard evolution law is derived next, written in terms of dimensionless variable $\boldsymbol{\omega}$.

### *5.1. LSW homothetic growth (hg), loading independent*

The initial microstructure is represented by a spherical $\gamma$ channel width tensor $\mathbf{w} = w^0_{001}\,\mathbf{1}$ (*i.e.* $w_{ij} = w^0_{001}\delta_{ij}$ in terms of components) with $w^0_{001} \approx 50$ nm at room temperature for the considered CMSX-4. At zero load, the cuboidal morphology of the microstructure is kept but temperature enhanced diffusion controlled coarsening $\dot{w}_1 \approx \dot{w}_2 \approx \dot{w}_3 > 0$ takes place (standard LSW theory Lifshitz and Slyozov (1961), Wagner (1961), see Section 1): the channels width tensor evolves in a homothetic growth $\dot{\boldsymbol{\omega}} \propto \mathbf{1}$ (*i.e.* $w_{ij} \propto \delta_{ij}$).

After a first mechanical loading, having induced creep deformation, a continuation of anisotropic $\gamma$ channel widths growth has been observed at load removal (Matan et al , 1999): if rafting has taken place during an initial creep loading performed in direction $1 \equiv [001]$ and if a large enough plastic strain has been reached, the rafting phenomenon continues. This means in terms of widths evolutions rates that $\dot{w}_1 \geq 0$, $\dot{w}_2 \approx \dot{w}_3 < 0$ and $w_2 \approx w_3 \to 0$ at long times, evolutions that cannot be decribed from a law of the spherical type $\dot{\boldsymbol{\omega}} \propto \mathbf{1}$.

In order to properly model both standard LSW coarsening and Matan *et al* rafting continuation phenomenon at load removal, we prefer –instead of $\dot{\boldsymbol{\omega}} \propto \mathbf{1}$– to define homothetic growth as a $\gamma$ channel width growth proportional to second order $\gamma$ channel width tensor $\mathbf{w}$ as

$$\dot{\boldsymbol{\omega}}^{\rm hg} = \dot{\mathcal{G}}\,\frac{\mathbf{w}}{\|\mathbf{w}\|} = \dot{\mathcal{G}}\,\frac{\boldsymbol{\omega}}{\|\boldsymbol{\omega}\|} \qquad \dot{\mathcal{G}} \geq 0, \quad \frac{\partial \dot{\mathcal{G}}}{\partial \boldsymbol{\sigma}} = 0, \quad \frac{\partial \dot{\mathcal{G}}}{\partial \boldsymbol{\epsilon}^p} = 0, \quad \frac{\partial \dot{\mathcal{G}}}{\partial \dot{\boldsymbol{\epsilon}}^p} = 0 \tag{58}$$

where homothetic growth function $\dot{\mathcal{G}}$ is furthermore assumed to be independent from the intensity of the mechanical loading. Recall is made here that $\gamma$ channel width tensor $\mathbf{w}$ is itself proportional to dimensionless tensor $\boldsymbol{\omega}$. The positivity of $\dot{\mathcal{G}}$ will be justified next. Law (58) does not ensure negative $\dot{\omega}_2$ and $\dot{\omega}_3$ by itself but it has the sought asymptotic property $\dot{\omega}_i^{\rm hg} = 0$ when $w_i = 0$. Additional coarsening/rafting contributions (see Sections 5.2 and 5.3) are necessary to enforce the observed feature $\dot{w}_1 \geq 0$, $\dot{w}_2 \approx \dot{w}_3 < 0$, and $w_2 \approx w_3 \to 0$ at long times, both during tensile loading and at load removal.

### *5.2. Mechanical coarsening (mc)*

We define mechanical coarsening as the spherical growth of the $\gamma$ channel width due to mechanical loading,

$$\dot{\boldsymbol{\omega}}^{\rm mc} = \dot{C}\,\mathbf{1} \qquad \dot{C} \geq 0 \tag{59}$$

*i.e.* the loading enhanced contribution of the $\gamma$ channel width growth proportional to second order unit tensor $\mathbf{1}$, with $\dot{C}$ a function of loading intensity through the stress or/and the plastic strain. In a consistent manner with the observations made in Matan et al (1999), a plastic strain threshold for rafting will be introduced, enforcing $\dot{C} = 0$ as long as accumulated plastic strain remains below a threshold (as long as $\varepsilon^p < \overline{\varepsilon}^p_{\rm th}$ with $\overline{\varepsilon}^p_{\rm th}$ a material parameter, Heaviside term $\mathrm{H}(p^{\rm d}_2 - \overline{\varepsilon}^p_{\rm th})$ in Eq. (85).

### *5.3. Rafting (raft)*

When rafting is due to a tensile stress in direction $1 \equiv [001]$, one has in *Natural Anisotropy Basis (NAB)*

$$\mathbf{w} = \left[\begin{array}{ccc} w_1 & 0 & 0 \\ 0 & w_2 & 0 \\ 0 & 0 & w_3 \approx w_2 \end{array}\right]_{NAB} = g(f_{\gamma'})\, w^0_{001}\, \boldsymbol{\omega} \tag{60}$$

and the longitudinal $\gamma$ channel width $w_1$ grows, the transverse channels widths equally shrinks to zero ($\dot{w}_1 \geq 0$ and $w_2 \approx w_3 \to 0$). Rafting leads then to a non spherical tensorial rafting variable $\boldsymbol{\omega}$ (therefore $\mathbf{w}$) having a non zero deviatoric part $\boldsymbol{\omega}' = \boldsymbol{\omega} - \frac{1}{3}\,\mathrm{tr}\,\boldsymbol{\omega}\,\mathbf{1} \neq 0$ of the form (using equality $w_2 = w_3$)

$$\mathbf{w}' \propto \boldsymbol{\omega}' \propto \left[\begin{array}{ccc} 1 & 0 & 0 \\ 0 & -\frac{1}{2} & 0 \\ 0 & 0 & -\frac{1}{2} \end{array}\right]_{NAB} \propto \dot{\boldsymbol{\epsilon}}^{p\rm d} \tag{61}$$

*i.e.* proportional to plastic strain rate tensor $\dot{\boldsymbol{\epsilon}}^p = \dot{\boldsymbol{\epsilon}}^{p\rm d}$ as in present uniaxial tension case

$$\dot{\boldsymbol{\epsilon}}^p = \dot{p}\,\mathbf{n} = \dot{p}^{\rm d}\,\mathbf{n}^{\rm d} \qquad \mathbf{n} = \mathbf{n}^{\rm d} = \left[\begin{array}{ccc} 1 & 0 & 0 \\ 0 & -\frac{1}{2} & 0 \\ 0 & 0 & -\frac{1}{2} \end{array}\right]_{NAB} \tag{62}$$

One emphasizes in Eq. (62) that out of diagonal part in *Natural Anisotropy Basis* of strain rate tensor is zero, *i.e.* using the notations of Kelvin mode based plasticity (see Section 2) $\dot{\boldsymbol{\epsilon}}^p = \dot{\boldsymbol{\epsilon}}^{p\mathrm{d}} = \mathbb{P}^{\mathrm{d}} : \dot{\boldsymbol{\epsilon}}^p$, $\dot{\boldsymbol{\epsilon}}^{p\overline{\mathrm{d}}} = \mathbb{P}^{\overline{\mathrm{d}}} : \dot{\boldsymbol{\epsilon}}^p = 0$ , $\dot{p} = \dot{p}^{\mathrm{d}}$, $\dot{p}^{\overline{\mathrm{d}}} = 0$ as is present case yielding is due only to octahedral slip systems.

In a complementary manner, an uniaxial tensile stress is applied along $< 111 >$ direction gives

$$\boldsymbol{\sigma} \propto \frac{1}{3}\begin{bmatrix} 1 & 1 & 1 \\ 1 & 1 & 1 \\ 1 & 1 & 1 \end{bmatrix}_{NAB} \qquad \dot{\boldsymbol{\epsilon}}^p = \dot{\boldsymbol{\epsilon}}^{p\overline{\mathrm{d}}} \propto \frac{1}{2}\begin{bmatrix} 0 & 1 & 1 \\ 1 & 0 & 1 \\ 1 & 1 & 0 \end{bmatrix}_{NAB} = \mathbf{n}^{\overline{\mathrm{d}}} \qquad \dot{\boldsymbol{\epsilon}}^{p\mathrm{d}} = 0 \tag{63}$$

and experimentally only leads to coarsening (Golubovskii et al , 1987) at $\dot{\boldsymbol{\omega}}' = 0$. This means that cubic plasticity (through $\dot{\boldsymbol{\epsilon}}^{p\overline{\mathrm{d}}} = \dot{p}^{\overline{\mathrm{d}}}\,\mathbf{n}^{\overline{\mathrm{d}}}$) does not contribute to rafting.

A quite generic multiaxial evolution law for deviatoric part $\boldsymbol{\omega}'$ is then

$$\dot{\boldsymbol{\omega}}' \propto \dot{\boldsymbol{\epsilon}}^{p\mathrm{d}} = \mathbb{P}^{\mathrm{d}} : \dot{\boldsymbol{\epsilon}}^p \propto \mathbf{n}^{\mathrm{d}} \tag{64}$$

The question of the time dependency or independency of rafting evolution law is not addressed here so that at this stage one simply writes $\dot{\boldsymbol{\omega}}' = \dot{\mathcal{R}}\,\mathbf{n}^{\mathrm{d}}$. The question of the sign of the proportionality factor $\dot{\mathcal{R}}$ (for rafting) needs an answer. Two possibilities, addressed in more details in Section 8 are:

- in *modeling A* we enforce a positive dissipation due to rafting by itself ($\mathcal{D}_{\mathrm{raft}} \geq 0$, as $\mathcal{D}_{\mathrm{plast}} \geq 0$ this implies $\mathcal{D} \geq 0$),
- in *modeling B*, we allow the possibility to $\mathcal{D}_{\mathrm{raft}}$ to become negative but to enforce a positive global dissipation $\mathcal{D} \geq 0$.

Next proof (given in Section 5.5) of the positivity of intrinsic dissipation for *modeling A* will use a positive proportionality factor (*i.e.* $\dot{\boldsymbol{\omega}}' = \dot{\mathcal{R}}\mathbf{n}^{\mathrm{d}}, \dot{\mathcal{R}} \geq 0$) at positive scalar product $\mathbf{w} : \mathbf{n}^{\mathrm{d}} \geq 0$ equivalent to $\boldsymbol{\omega} : \mathbf{n}^{\mathrm{d}} = \omega_{ij} n^{\mathrm{d}}_{ij} \geq 0$; it will use a vanishing deviatoric rate $\dot{\boldsymbol{\omega}}' = 0$ (*i.e.* $\dot{\mathcal{R}} = 0$) at strictly negative $\boldsymbol{\omega} : \mathbf{n}^{\mathrm{d}} < 0$ so that we propose to write

$$\dot{\boldsymbol{\omega}}^{\mathrm{raft}} = (\dot{\boldsymbol{\omega}}^{\mathrm{raft}})' = \dot{\mathcal{R}}\,\mathcal{H}\,\mathbf{n}^{\mathrm{d}} \qquad \dot{\mathcal{R}} \geq 0 \tag{65}$$

where

- for *modeling A*

$$\mathcal{H} = \mathrm{H}(\boldsymbol{\omega} : \mathbf{n}^{\mathrm{d}}) \qquad \text{or} \qquad \begin{cases} \mathcal{H} = 1 \text{ if } \boldsymbol{\omega} : \mathbf{n}^{\mathrm{d}} \geq 0, \\ \mathcal{H} = 0 \text{ if } \boldsymbol{\omega} : \mathbf{n}^{\mathrm{d}} < 0 \end{cases} \tag{66}$$

- for *modeling B* the Heaviside function applies to intrinsic dissipation $\mathcal{D}$ itself,

$$\mathcal{H} = \mathrm{H}(\mathcal{D}) \qquad \text{or} \qquad \begin{cases} \mathcal{H} = 1 \text{ if } \mathcal{D} \geq 0, \\ \mathcal{H} = 0 \text{ if } \mathcal{D} < 0 \end{cases} \tag{67}$$

For compression in direction $1 \equiv [001]$

$$\mathbf{n} = \mathbf{n}^{\mathrm{d}} = \begin{bmatrix} -1 & 0 & 0 \\ 0 & \frac{1}{2} & 0 \\ 0 & 0 & \frac{1}{2} \end{bmatrix}_{NAB} \tag{68}$$

so that $\dot{\mathcal{R}} > 0$ implies $\dot{\omega}_1 < 0$, $\dot{\omega}_2 = \dot{\omega}_3 > 0$ as observed in the work of Fredholm and Strudel (1987) (Fig. 1, P-type coalescence in compressive loading).

Expression (65) is consistent with the observations: rafting during uniaxial compression creep tests (along $< 001 >$) is developing in the form of rods and/or plates almost aligned with the stress axis, the so-called P-type rafting (Giraud et al , 2012, Ott and Mughrabi , 1999, Tien and Copley , 1971) described in the Introduction. Once the uniaxial loading changes to a tensile stress, the former P-type is progressively broken to develop a $\gamma'$ rafting (Xingfu et al , 2009).

Note again that a threshold $\varepsilon^p_{\mathrm{th}}$ in term of accumulated plastic strain has been observed Matan et al (1999) so that one will later enforce $\dot{\mathcal{R}} = 0$ as long as $\varepsilon^p < \varepsilon^p_{\mathrm{th}}$ by means of multiplication by Heaviside term $\mathrm{H}(p_1^{\mathrm{Hill}} - \varepsilon^p_{\mathrm{th}})$ in Eq. (84).

### *5.4. Generic evolution law for tensorial internal variable $\boldsymbol{\omega}$*

To sum up a generic evolution law for rafting, coarsening and homothetic $\gamma$ channel width growth, is

$$\dot{\boldsymbol{\omega}} = \dot{\mathcal{R}}\,\mathcal{H}\,\mathbf{n}^{\mathrm{d}} + \dot{\mathcal{C}}\,\mathbf{1} + \dot{\mathcal{G}}\,\frac{\boldsymbol{\omega}}{\|\boldsymbol{\omega}\|} \qquad \mathbf{w} = g(f_{\gamma'})\,w^0_{001}\,\boldsymbol{\omega} \tag{69}$$

where normal $\mathbf{n}^{\mathrm{d}} = \mathbf{dir}(\dot{\boldsymbol{\epsilon}}^{p\mathrm{d}}) = \dot{\boldsymbol{\epsilon}}^{p\mathrm{d}}/\dot{p}^{\mathrm{d}}$ has to be seen in single crystal plasticity models as the macroscopic (mean) plastic strain direction due to active octahedral slip systems only (not the cubic ones). Evolution law (69) is consistent with Tinga et al (2009) evolution law (as shown in Appendix E). It applies to nickel-based single crystal superalloys having a negative misfit $\delta_u$.

*5.5. Dissipation due to rafting – Positivity of intrinsic dissipation*

Using state law (56), and generic evolution law (69) the intrinsic dissipation due to rafting becomes

$$\mathcal{D}_{\text{raft}} = \left( \kappa_{\text{ORO}} \frac{G}{\|\boldsymbol{\omega}\|^2} \frac{\boldsymbol{\omega}}{\|\boldsymbol{\omega}\|} (p^{\text{d}} + \varpi p^{\overline{\text{d}}}) + \sqrt{\frac{3}{8}} \left[ \kappa_E \boldsymbol{\epsilon}^e : \mathbb{E} : \boldsymbol{\epsilon}^e + \kappa_\omega \delta_u^2 \right] \frac{\boldsymbol{\omega}'}{\|\boldsymbol{\omega}'\|} \right) : \left( \dot{\mathcal{R}} \mathcal{H} \, \mathbf{n}^{\text{d}} + \dot{C} \, \mathbf{1} + \dot{\mathcal{G}} \frac{\boldsymbol{\omega}}{\|\boldsymbol{\omega}\|} \right) \tag{70}$$

so that, with the fact that normal $\mathbf{n}^{\text{d}} = (\mathbf{n}^{\text{d}})'$ is deviatoric and therefore that $\boldsymbol{\omega} : \mathbf{n}^{\text{d}} = \boldsymbol{\omega}' : \mathbf{n}^{\text{d}}$,

$$\begin{aligned} \mathcal{D}_{\text{raft}} =& \dot{\mathcal{R}} \left( \kappa_{\text{ORO}} \frac{G}{\|\boldsymbol{\omega}\|^3} (p^{\text{d}} + \varpi p^{\overline{\text{d}}}) + \sqrt{\frac{3}{8}} \frac{\kappa_E \boldsymbol{\epsilon}^e : \mathbb{E} : \boldsymbol{\epsilon}^e + \kappa_\omega \delta_u^2}{\|\boldsymbol{\omega}'\|} \right) \left( \boldsymbol{\omega} : \mathbf{n}^{\text{d}} \right) \mathcal{H} + \dot{C} \, \kappa_{\text{ORO}} \frac{G \, \text{tr} \, \boldsymbol{\omega}}{\|\boldsymbol{\omega}\|^3} (p^{\text{d}} + \varpi p^{\overline{\text{d}}}) \\ &+ \dot{\mathcal{G}} \left( \kappa_{\text{ORO}} \frac{G}{\|\boldsymbol{\omega}\|^2} (p^{\text{d}} + \varpi p^{\overline{\text{d}}}) + \sqrt{\frac{3}{8}} \left[ \kappa_E \boldsymbol{\epsilon}^e : \mathbb{E} : \boldsymbol{\epsilon}^e + \kappa_\omega \delta_u^2 \right] \frac{\|\boldsymbol{\omega}'\|}{\|\boldsymbol{\omega}\|} \right) \end{aligned} \tag{71}$$

with all terms always positive except scalar product $\boldsymbol{\omega} : \mathbf{n}^{\text{d}}$. Let us first check whether the dissipation due to rafting $\mathcal{D}_{\text{raft}} = \boldsymbol{\Omega} : \dot{\boldsymbol{\omega}}$ –which includes $\gamma'$ precipitates evolutions– remains positive or not.

When $\boldsymbol{\omega} : \mathbf{n}^{\text{d}} \geq 0$ in case of *modeling A –i.e.* when Heaviside function $\mathcal{H} = \text{H}(\boldsymbol{\omega} : \mathbf{n}^{\text{d}}) = 1$– one has $(\boldsymbol{\omega} : \mathbf{n}^{\text{d}})\mathcal{H} = \langle \boldsymbol{\omega} : \mathbf{n}^{\text{d}} \rangle_+ \geq 0$: the dissipation due to microstructure degradation $\mathcal{D}_{\text{raft}}$ is then positive for any rafting / mechanical coarsening / homothetic growth evolution law of generic form (69) under natural assumption $\dot{\mathcal{R}} \geq 0$, $\dot{C} \geq 0$ and $\dot{\mathcal{G}} \geq 0$. This includes any complex loading without rafting ($\mathbf{w}' = 0$) and any monotonic loading ($\mathbf{w}'$ coaxial with constant normal $\mathbf{n}^{\text{d}}$) such as creep loadings of Sections 7.3 and 7.4.

In the other loading cases, both dissipations $\mathcal{D}_{\text{raft}}$ and $\mathcal{D}$ may become negative if $\mathcal{H} = 1$ is set when $\boldsymbol{\omega} : \mathbf{n}^{\text{d}} < 0$. In order to avoid this in complex loading cases, we will consider *modeling B* which enforces $\mathcal{H} = 0$ to avoid negative dissipation by setting $\mathcal{H} = \text{H}(\mathcal{D})$ and by considering assumption $\dot{\mathcal{R}} \geq 0, \dot{C} \geq 0, \dot{\mathcal{G}} \geq 0$. In such a *modeling B*, the dissipation due to rafting may become negative, the positivity of intrinsic dissipation being then gained thanks to a large enough plastic dissipation $\mathcal{D}_{\text{plast}} > 0$.

To sum up, for both *modeling A* and *B*, the intrinsic dissipation $\mathcal{D}$ is shown to be always positive, for any loading, monotonic or not, proportional or not, isothermal or not. But this is not the case of the dissipation due to rafting $\mathcal{D}_{\text{raft}}$ only when *modeling B* is considered. Examples and consequences are detailed in Section 8.

*5.6. At thermodynamics equilibrium*

We have mentioned a few times some consequences of thermodynamics equilibrium. The first of them, implicit in this work, is the possibility to define temperature and more generally thermodynamics state variables at RVE scale. But a second consequence is encountered for CMSX-4 and MC2 superalloys at temperature rate below $10 - 20°\text{C/min}^{-1}$ and strain rates below $10^{-4}\text{s}^{-1}$ in case of strain controlled tests: at low thermomechanical loading rate, a microstructure chemical equilibrium is reached, especially in the matrix which is the phase mostly affected in terms of chemical composition by the dissolution/precipitation of $\gamma'$ particles. The constitutive phases are stabilized at an equilibrium volume fractions, only function of temperature for $\gamma'$ precipitates, $f_{\gamma'} = f_{\gamma' \text{eq}}(T)$ (Eq. (20) or (90), Fig. 4).

This second consequence allows for thermodynamics modeling (at equilibrium) at macroscopic scale without the explicit introduction of volume fractions of constitutive phases, as often done (Fan et al , 2015, Fedelich et al , 2009, 2012a, Tinga et al , 2009): these volume fractions are naturally replaced by corresponding temperature dependencies of the material parameters. In this case, generic evolution law (69) becomes (isothermal case, $\dot{\mathcal{R}} \geq 0$, $\dot{C} \geq 0, \dot{\mathcal{G}} \geq 0, \delta_u < 0$):

$$\dot{\mathbf{w}} \approx g(f_{\gamma' \text{eq}}(T)) w_{001}^0 \dot{\boldsymbol{\omega}} = w_0(T) \left[ \dot{\mathcal{R}} \mathcal{H} \, \mathbf{n}^{\text{d}} + \dot{C} \, \mathbf{1} + \dot{\mathcal{G}} \frac{\mathbf{w}}{\|\mathbf{w}\|} \right] \tag{72}$$

*i.e.* a rafting law directly expressed in terms of $\gamma$ channel width tensor rate $\dot{\mathbf{w}}$ with $w_0(T) = g(f_{\gamma' \text{eq}}(T)) w_{001}^0$ a function of temperature homogenenous to a length and at room temperature equal to initial $\gamma$ channel width $w_{001}^0$. For considered CMSX-4, $w_{001}^0 \approx 50$ nm, $w_0(1050°\text{C}) \approx 80$ nm.

## 6. Viscoplasticity coupled with tensorial rafting model

The thermodynamics framework and the ingredients for a constitutive modeling of viscoplasticity coupled to tensorial rafting have been developed in previous Sections. Let us summarize here the choices made to derive a multiaxial model for single crystal CMSX-4 superalloy at high temperature. Creep up to the secondary stage is the main domain of validity sought so that kinematic hardening and the coupling with damage are omitted in such a first model with tensorial rafting.

Concerning viscoplasticity, let us use the Kelvin modes based two criterion viscoplasticity framework of Section 2.4 for cubic single crystals. Let us recall the definitions $\boldsymbol{\sigma}^{\text{d}} \overset{\text{def}}{=} \mathbb{P}^{\text{d}} : \boldsymbol{\sigma}$ (also referred to as "diagonal deviatoric

stress", diagonal in *Natural Anisotropy Basis*), $\boldsymbol{\sigma}^{\overline{\mathrm{d}}} \overset{\text{def}}{=} \mathbb{P}^{\overline{\mathrm{d}}} : \boldsymbol{\sigma}$ (also referred to as "out of diagonal deviatoric stress" in *Natural Anisotropy Basis*), and partition $\boldsymbol{\sigma}' = \boldsymbol{\sigma}^{\mathrm{d}} + \boldsymbol{\sigma}^{\overline{\mathrm{d}}}$. One also has Kelvin partition of the plastic strain tensor

$$\boldsymbol{\epsilon}^p = \boldsymbol{\epsilon}_1^p + \boldsymbol{\epsilon}_2^p \qquad \begin{cases} \boldsymbol{\epsilon}_1^p = \boldsymbol{\epsilon}_1^{p\mathrm{d}} + \boldsymbol{\epsilon}_1^{p\overline{\mathrm{d}}} \\ \boldsymbol{\epsilon}_2^p = \boldsymbol{\epsilon}_2^{p\overline{\mathrm{d}}} \end{cases} \tag{73}$$

with $\boldsymbol{\epsilon}_1^{p\mathrm{d}} \overset{\text{def}}{=} \mathbb{P}^{\mathrm{d}} : \boldsymbol{\epsilon}_1^p$ (diagonal in *Natural Anisotropy Basis*), $\boldsymbol{\epsilon}_1^{p\overline{\mathrm{d}}} \overset{\text{def}}{=} \mathbb{P}^{\overline{\mathrm{d}}} : \boldsymbol{\epsilon}_1^p$ (out of diagonal in *Natural Anisotropy Basis*) and $\boldsymbol{\epsilon}_2^{p\mathrm{d}} = \mathbb{P}^{\mathrm{d}} : \boldsymbol{\epsilon}_2^p = 0$.

Concerning microstructure degradation, we use the formulation in terms of rafting variable $\boldsymbol{\omega}$ derived in Sections 4.5.2 and 5.

No damage is introduced in the present version of the model, this coupling and the description of tertiary creep being left to further work.

### *6.1. Proposed model (Part I Mechanics)*

The constitutive equation for cubic elasto-visco-plasticity coupled with tensorial rafting are:

- elasticity law coupled with rafting (with in practice the coupling of elasticity with rafting neglected, $\kappa_E \omega_{eq} << 1$)

$$\boldsymbol{\sigma} = \mathbb{E} : (\boldsymbol{\epsilon} - \boldsymbol{\epsilon}^p - \alpha\,(T - T_{\mathrm{ref}})\,\mathbf{1}) \tag{74}$$

  Hooke's tensor $\mathbb{E}$ has cubic material symmetry, $\alpha$ is the thermal expansion coefficient, $T_{\mathrm{ref}}$ is reference temperature.

- stress partition in cubic symmetry

$$\boldsymbol{\sigma} = \boldsymbol{\sigma}^{\mathrm{d}} + \boldsymbol{\sigma}^{\overline{\mathrm{d}}} + \frac{1}{3}\,\mathrm{tr}\,\boldsymbol{\sigma}\,\mathbf{1} \qquad \sigma_{eq}^{\mathrm{d}} = \sqrt{\frac{3}{2}\boldsymbol{\sigma}^{\mathrm{d}} : \boldsymbol{\sigma}^{\mathrm{d}}} \qquad \sigma_{eq}^{\overline{\mathrm{d}}} = \sqrt{\frac{3}{2}\boldsymbol{\sigma}^{\overline{\mathrm{d}}} : \boldsymbol{\sigma}^{\overline{\mathrm{d}}}} \tag{75}$$

  introducing equivalent von Mises norms $\sigma_{eq}^{\mathrm{d}}$ and $\sigma_{eq}^{\overline{\mathrm{d}}}$,

- criterion functions with saturated hardening and Orowan stress effect (Hill criterion for $f_1$, for the sake of simplicity quadratic norm $a = 2$ for $f_2$),

$$f_1 = \sigma_{\mathrm{Hill}} - R_\infty - \frac{\kappa_{\mathrm{ORO}} G}{\|\boldsymbol{\omega}\|} - \sigma_y \qquad f_2 = \sigma_{eq}^{\overline{\mathrm{d}}} - \overline{R}_\infty - \varpi\frac{\kappa_{\mathrm{ORO}} G}{\|\boldsymbol{\omega}\|} - \overline{\sigma}_y \tag{76}$$

  where

$$\sigma_{\mathrm{Hill}} = \sqrt{\frac{3}{2}\left(\boldsymbol{\sigma}^{\mathrm{d}} : \boldsymbol{\sigma}^{\mathrm{d}} + h^2 \boldsymbol{\sigma}^{\overline{\mathrm{d}}} : \boldsymbol{\sigma}^{\overline{\mathrm{d}}}\right)} \tag{77}$$

  with $h$ Hill material parameter for cubic (visco-)plasticity.

- plastic strain rate

$$\dot{\boldsymbol{\epsilon}}^p = \dot{p}_1^{\mathrm{Hill}} \frac{\partial f_1}{\partial \boldsymbol{\sigma}} + \dot{p}_2^{\overline{\mathrm{d}}} \frac{\partial f_2}{\partial \boldsymbol{\sigma}} \tag{78}$$

- accumulated plastic strain rates

$$\dot{p}_1^{\mathrm{Hill}} = \sqrt{\frac{2}{3}\left(\dot{\boldsymbol{\epsilon}}_1^{p\mathrm{d}} : \dot{\boldsymbol{\epsilon}}_1^{p\mathrm{d}} + \frac{1}{h^2}\dot{\boldsymbol{\epsilon}}_1^{p\overline{\mathrm{d}}} : \dot{\boldsymbol{\epsilon}}_1^{p\overline{\mathrm{d}}}\right)} \qquad \dot{p}_2^{\overline{\mathrm{d}}} = \sqrt{\frac{2}{3}\dot{\boldsymbol{\epsilon}}_2^{p\overline{\mathrm{d}}} : \dot{\boldsymbol{\epsilon}}_2^{p\overline{\mathrm{d}}}} \tag{79}$$

- viscosity laws

$$\dot{p}_1^{\mathrm{Hill}} = \left\langle -\frac{\sigma_{v\infty}}{K_N} \ln\left(1 - \frac{f_1}{\sigma_{v\infty}}\right)\right\rangle_+^N \qquad \dot{p}_2^{\overline{\mathrm{d}}} = \left\langle \frac{f_2}{\overline{K}_N}\right\rangle_+^{\overline{N}} \tag{80}$$

The material parameters are: $E$, $\nu$, $G$ for elasticity, thermal expansion coefficient $\alpha$, yield stresses $\sigma_y$ and $\overline{\sigma}_y$, Hill parameter $h$, saturated hardenings $R_\infty$ and $\overline{R}_\infty$, parameter $\kappa_{\mathrm{ORO}}$ for Orowan stress effect, viscosity parameters $K_N$, $N$, $\overline{K}_N$, $\overline{N}$ for orientations $< 001 >$ and $< 111 >$ viscoplasticity. A tendency to saturation of the viscous stress will be obtained for $< 001 >$ orientation so that viscosity law (19) is used, introducing the saturation value $\sigma_{v\infty}$ as material parameter.

*6.2. Particular uniaxial cases (Mechanics)*

For an uniaxial loading in direction $< 001 >$, $\sigma_{\text{Hill}} = |\sigma|$, $p_1^{\text{Hill}} = p = \int |\dot{\varepsilon}^p| \, \mathrm{d}t$ (with $\varepsilon^p$ the uniaxial plastic strain), $\boldsymbol{\sigma}^{\overline{\mathrm{d}}} = \mathbf{0}$, $\sigma_{eq}^{\overline{\mathrm{d}}} = 0$, $p_2^{\overline{\mathrm{d}}} = 0$ so that, at low strain rate,

$$|\dot{\varepsilon}^p| \approx \left\langle \frac{|\sigma| - R_\infty - \frac{\kappa_{\text{ORO}} G}{\|\boldsymbol{\omega}\|} - \sigma_y}{K_N} \right\rangle_+^N \qquad < 001 > \text{ orientation} \tag{81}$$

with then $\sigma_y = \sigma_{y001}$ the yield stress in direction $< 001 >$.

For an uniaxial loading in direction $< 111 >$, $\boldsymbol{\sigma}^{\mathrm{d}} = \mathbf{0}$, $\sigma_{eq}^{\mathrm{d}} = 0$, $p^{\mathrm{d}} = 0$, $\sigma_{eq}^{\overline{\mathrm{d}}} = |\sigma|$, $h p_1^{\text{Hill}} + p_2^{\overline{\mathrm{d}}} = p = \int |\dot{\varepsilon}^p| \, \mathrm{d}t$ (with $\varepsilon^p$ the uniaxial plastic strain), so that, at low strain rate,

$$|\dot{\varepsilon}^p| \approx \left\langle \frac{|\sigma| - \overline{R}_\infty - \varpi \frac{\kappa_{\text{ORO}} G}{\|\boldsymbol{\omega}\|} - \overline{\sigma}_y}{\overline{K}_N} \right\rangle_+^{\overline{N}} + h \left\langle \frac{h|\sigma| - R_\infty - \frac{\kappa_{\text{ORO}} G}{\|\boldsymbol{\omega}\|} - \sigma_y}{K_N} \right\rangle_+^N \qquad < 111 > \text{ orientation} \tag{82}$$

For small enough values of $h$, the right hand inside term can be neglected and Eq. (82) then come back to Norton law (with then $\overline{\sigma}_y = \sigma_{y111}$ the yield stress in direction $< 111 >$). The value $h \approx 0.5$ will be obtained in section Appendix F by cross identification with a Schmid law based single crystal visc-plasticity model.

*6.3. Proposed model (Part II Tensorial evolution law for rafting)*

General evolution law (69) satisfying second principle of thermodynamics is rewritten, taking care to ensure $\dot{\mathcal{R}} \geq 0$, $\dot{C} = \dot{\omega}_{\text{mc}} \geq 0$, $\dot{\mathcal{G}} = \sqrt{3}\, \dot{\omega}_{\text{LSW}} \geq 0$,

$$\dot{\boldsymbol{\omega}} = \dot{\boldsymbol{\omega}}^{\text{raft}} + \dot{\omega}_{\text{mc}} \mathbf{1} + \sqrt{3}\, \dot{\omega}_{\text{LSW}} \frac{\boldsymbol{\omega}}{\|\boldsymbol{\omega}\|} \qquad \text{or} \qquad \dot{\omega}_{ij} = \dot{\omega}_{ij}^{\text{raft}} + \dot{\omega}_{\text{mc}} \delta_{ij} + \sqrt{3}\, \dot{\omega}_{\text{LSW}} \frac{\omega_{ij}}{\|\boldsymbol{\omega}\|} \tag{83}$$

Pre-factor $\sqrt{3} = \|\mathbf{1}\|$ is such as if $\mathbf{w} \propto \mathbf{1}$, $\boldsymbol{\omega}^{\text{hg}} = \omega_{\text{LSW}} \mathbf{1}$ with initial values $\omega_{\text{LSW}}(t=0) = 1$, $\boldsymbol{\omega}^{\text{raft}} = \mathbf{0}$, $\omega_{\text{mc}} = 0$ and $\omega(t=0) = \mathbf{1}$. Recall that $\dot{\boldsymbol{\omega}}^{\text{raft}} = (\dot{\boldsymbol{\omega}}^{\text{raft}})'$ is a deviatoric second order tensor.

To account for $\gamma'$ rafting and mechanical coarsening using a unified expression from the previous models Cormier and Cailletaud (2010a), Tinga et al (2009), we propose:

$$\dot{\boldsymbol{\omega}}^{\text{raft}} = K_{\text{raft}} \exp\left( -\frac{Q - \min(\sigma_{eq}^{\mathrm{d}}, \sigma_{lim}^{\mu}) U_{\text{raft}}}{k_{\mathrm{B}} T} \right) \mathrm{H}(p_1^{\text{Hill}} - \varepsilon_{\text{th}}^p)\, \mathcal{H}\, \mathbf{n}^{\mathrm{d}} \tag{84}$$

$$\dot{\omega}_{\text{mc}} = K_{\text{mc}} \exp\left( -\frac{Q - \sigma_{eq} U_{\text{mc}}}{k_{\mathrm{B}} T} \right) \mathrm{H}(p_2^{\overline{\mathrm{d}}} - \overline{\varepsilon}_{\text{th}}^p) \tag{85}$$

with either $\mathcal{H} = \mathrm{H}(\boldsymbol{\omega} : \mathbf{n}^{\mathrm{d}})$ in *modeling A* or $\mathcal{H} = \mathrm{H}(\mathcal{D})$ in *modeling B*.

In equation 84 the stress affection on rafting has been bounded replacing $\sigma_{eq}^{\mathrm{d}}$ by $\min(\sigma_{eq}^{\mathrm{d}}, \sigma_{lim}^{\mu})$ in the Arrhenius-Tinga exponent (equation 24) in order to correctly model monotonic tension (higher magnitude of stress than creep).

As already discussed, a rafting threshold $\varepsilon_{\text{th}}^p$ and a mechanical coarsening threshold $\overline{\varepsilon}_{\text{th}}^p$ are introduced according to Matan et al (1999). In the next section, one will obtain $\varepsilon_{\text{th}}^p = 10^{-4}$ and $\overline{\varepsilon}_{\text{th}}^p \approx 0^+$ from mechanical measurements. As rafting does not occur for tension in direction $< 111 >$, the contribution $\dot{\boldsymbol{\omega}}^{\text{raft}}$ is made dependent on $\sigma_{eq}^{\mathrm{d}}$ (vanishing for tension along $< 111 >$, see Eq. (75)). Full von Mises stress $\sigma_{eq}$, non zero for both $< 001 >$ and $< 111 >$ orientations, is assumed to drive the mechanical coarsening contribution $\dot{\omega}_{\text{mc}}$.

In the initial Polystar model $K_{\text{raft}}$ and $K_{\text{mc}}$ are functions of both the accumulated plastic strain and the loading rate. One considers next them as material parameters, temperature dependent only. Thermal/stress activation constants $Q$ and $U$ are assumed not to depend on temperature, $k_{\mathrm{B}}$ is Boltzmann constant.

Matan *et al* plastic strain threshold (Matan et al , 1999) is introduced through Heaviside functions H. It corresponds to the density of dislocations on octahedral slip systems necessary to relax the misfit stresses (so that $\varepsilon_{\text{th}}^p >> \overline{\varepsilon}_{\text{th}}^p$). Once the $\gamma/\gamma'$ lattice mismatch is relaxed with a given dislocation density, rafting can proceed, even in the absence of any applied stress. This phenomenon is not represented in Tinga approach.

For homothetic growth no threshold has been observed so that the evolution law (Cormier and Cailletaud , 2010a)

$$\dot{\omega}_{\text{LSW}} = \frac{K_{\text{LSW}}}{3\omega_{\text{LSW}}^2} \exp\left( -\frac{Q}{k_{\mathrm{B}} T} \right) \tag{86}$$

consistent with both Eq. (1) and Eq. (22) is considered.

*6.4. Particular uniaxial cases (Tensorial evolution law for rafting)*

For an uniaxial loading in direction $< 001 >$, $\sigma^{\mathrm{d}}_{eq} = \sigma_{eq} = |\sigma|$, $\mathbf{n}^{\mathrm{d}} = \frac{3}{2}\frac{\boldsymbol{\sigma}'}{\sigma_{eq}}$, $p = p_1^{\mathrm{Hill}}$, so that

$$\dot{\boldsymbol{\omega}} = K_{\mathrm{raft}} \exp\left(-\frac{Q - \min(|\sigma|, \sigma^{\mu}_{lim})U_{\mathrm{raft}}}{k_{\mathrm{B}}T}\right) \mathrm{H}(p - \varepsilon^{p}_{\mathrm{th}})\, \mathcal{H}\, \mathbf{n}^{\mathrm{d}} \tag{87}$$

For an uniaxial loading in direction $< 111 >$, $\sigma^{\mathrm{d}}_{eq} = 0$, and $\sigma_{eq} = |\sigma|$ so that, at $\overline{\varepsilon}^{p}_{\mathrm{th}} = 0^{+}$,

$$\dot{\boldsymbol{\omega}} = K_{\mathrm{mc}} \exp\left(-\frac{Q - |\sigma|U_{\mathrm{mc}}}{k_{\mathrm{B}}T}\right) \mathbf{1} \tag{88}$$

*6.5. Proposed model (Part III $\gamma'$ precipitates evolution / $\gamma$ channel width)*

For the $\gamma'$ precipitates volume fraction $f_{\gamma'}$, the evolution law retained is the one of anisothermal Polystar model in Giraud et al (2013), previously identified le Graverend et al (2014a),

$$\dot{f}_{\gamma'} = \left(1 - \delta_{\gamma'} e^{-\frac{p_1^{\mathrm{Hill}}}{e_{\gamma'}}}\right) \frac{f_{\gamma'\mathrm{eq}}(T) - f_{\gamma'}}{\tau_{\gamma'}} \tag{89}$$

Parameter $\delta_{\gamma'} = 0.8$ is such as $0 < \delta_{\gamma'} < 1$ in order to ensure $f_{\gamma'} = f_{\gamma'\mathrm{eq}}(T)$ at thermodynamics equilibrium, at rate controlled by characteristic time $\tau_{\gamma'} = 200\ \mathrm{s}^{-1}$ and by parameter $e_{\gamma'} = 5\,10^{-3}$; $f_{\gamma'\mathrm{eq}}(T)$ is equilibrium volume fraction, function of the absolute temperature $T$ only. Instead of Eq. (20), we use for considered CMSX-4 superalloy a modified expression (plotted in Fig. 4):

$$f_{\gamma'\mathrm{eq}}(T) = \left(f^0_{\gamma'} - (f^0_{\gamma'} - f^1_{\gamma'})\left\langle\frac{T - T_0}{T_1 - T_0}\right\rangle_{+}\right)\left(1 - \left\langle\frac{T - T_1}{T_2 - T_1}\right\rangle^2_{+}\right) \tag{90}$$

with $f^0_{\gamma'} = 0.7$, $f^1_{\gamma'} = 0.48$, $T_0 = 1073$ K, $T_1 = 1418$ K, $T_2 = 1543$ K for the considered CMSX-4. All these parameters have been identified based on our own experiments. These experiments consists in stereological analyzes of SEM pictures taken from different specimens first submitted to a creep deformation at 1050°C and 140 MPa for 100 hours whose aim is to develop a regular gamma-prime rafted structure. They were then held for 1 hour at different temperatures ranging from 850° C to 1300° C, then water quenched to be able to extract the gamma-prime volume fraction from area-fraction measurements. Note that stereological analyzes were performed in both the primary dendrite arms and in the interdendritic spacings, as shown in Fig. 4. The $\gamma'$ volume fraction is constant from ambient temperature to around 800° C (Link et al , 2011).

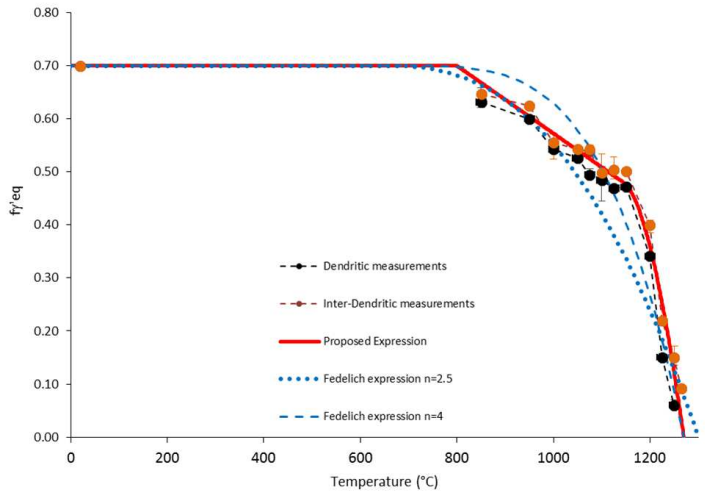


Figure 4: Equilibrium volume fraction $f_{\gamma'\mathrm{eq}}$ of $\gamma'$ precipitates as a function of temperature (here in °C). Measurements: marks, Proposed expression: Eq. (90), Fedelich expression: Eq. (20).

As a matter of fact, once yielding has taken place, a $\gamma'$ dissolution kinetics is observed, enhanced by the level of plasticity (Ghighi et al , 2013, Giraud et al , 2013, le Graverend et al , 2014a). The coupling with plasticity is written in terms of accumulated plastic strain $p_1^{\mathrm{Hill}}$ (representative of octahedral slips, with $e_{\gamma'}$ a material parameter) since $\gamma'$ microstructure evolutions are mainly driven by the slip activity in the $\gamma$ matrix, *i.e.* on the octahedral slip systems (Giraud et al (2013)).

The $\gamma$ channel width tensor is then, using mixture law (40):

$$\mathbf{w} = g(f_{\gamma'})\, w^0_{001}\, \boldsymbol{\omega} \qquad g(f_{\gamma'}) = \frac{1 - f_{\gamma'}}{1 - f^0_{\gamma'}} \tag{91}$$

with $w^0_{001} \approx 50$ nm, $f^0_{\gamma'} = 0.7$ respectively the channel width and $\gamma'$ volume fraction at room temperature.

## 7. Creep and rafting along different orientations of CMSX-4 superalloy under isothermal condition at 1050°C

The time integration of the constitutive equations –by means of simple Euler explicit scheme for presented results– allows to calculate the model responses to any loading case. Note that, in 1D as well as in 3D, the proposed elasto-viscoplastic model with tensorial rafting only needs the coupled computation of the strain, stress, plastic strain and of dimensionless tensorial variable $\boldsymbol{\omega}$ (constitutive equations of Sections 6.1 and 6.3). The determination of both the $\gamma'$ volume fraction $f_{\gamma'}$ and the physical $\gamma$ channel width tensor $\mathbf{w}$ at any time can be computed in a post-processing manner (constitutive equations of Section 6.5, the coupling with mechanics being made through dimensionless tensor $\boldsymbol{\omega}$ instead of width tensor $\mathbf{w}$).

### *7.1. $\gamma'$ precipitates volume fraction*

For an isothermal loading, the thermodynamics equilibrium is quickly reached (small characteristic time $\tau_{\gamma'}$) and $f'_\gamma \approx f_{\gamma' \mathrm{eq}}(T)$. At 1050°C, it is a $\gamma'$ precipitates volume fraction $f'_\gamma = 0.54$. For the next calculations the initial $\gamma$ channel width is $w_0(1050°C) = w_{001}(t = 0) = w_i(t = 0) = 80$ nm (measured). Using Eq. (91), one has at this temperature $g(f'_\gamma) = 1.533$. One gets then a 20°C $\gamma$ channel width $w^0_{001} = 52$ nm, value very close to the standard 50 nm for CMSX-4 and MC2 superalloys. We consider this as a validation of mixture law (91) for $g(f'_\gamma)$ function.

### *7.2. LSW homothetic growth*

At 1050°C, only few experimental datas are available for load free LSW homothetic growth of the cuboidal microstructure (marks in Fig. 5 from reference Fedelich et al (2012a)). The fitting curves due to different authors for similar nickel based single crystal superalloys are also plotted

- by means of Eq. (86) for MC2 superalloy (curve from le Graverend (2013), $w_0(1050°C) = w(t = 0) = 80$ nm).
- by means of Eq. (21) with CMSX-4 material parameters from Fedelich et al (2012a) with here also $w_0(1050°C) = 80$ nm ($w = 80\,[1 + 0.198\,t]^{0.0745}$ nm with $t$ in hours),

The retained choice corresponds to Eq. (86)-(91) with $K_{\mathrm{LSW}} \exp\left(-\frac{Q}{k_B T}\right) = 1.1\ 10^{-6}\ \mathrm{s}^{-1}$.

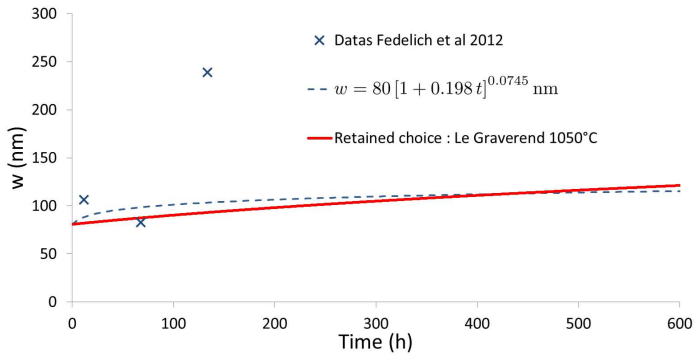


Figure 5: Channel width evolution as a function of time $t$ in hours (1050°C)

### *7.3. < 001 > creep*

During tensile creep along the < 001 > direction, there is $\gamma'$ rafting perpendicular to the applied stress (Fig. 6c, $\gamma$ width channel $w_1$ increases, $w_2 = w_3$ decrease to zero). In the present model the evolution is gouverned by a $K_{\mathrm{raft}} = 1.7\ 10^{-7}\mathrm{s}^{-1}$ and it is stress enhanced according to non zero Tinga *et al* material parameter $u = \frac{U_{\mathrm{raft}}}{k_B T} = 0.025$ within Arrhenius exponential. The mechanical responses are given in Fig. 6a-b for three creep stresses: 140 MPa, 180 MPa, 200 MPa. The black thin lines of the figures corresponds to experiments performed on CMSX-4 specimens oriented close to a < 001 > orientation with less than 5 degrees misorientation. One sees in Fig. 6a and 6b that the experimental curves are well reproduced by the model up to the 5% of strain, meaning that the creep rate increase only results from the microstructure degradation and not from a damage mechanism in the form

of, e.g., cavitation. It is also seen from Fig. 6c that the evolutions of the gamma channel widths, using Matan *et al* threshold $\varepsilon^p_{\text{th}} = 10^{-4}$, reproduce quite well the experimental observations at the end of the tests. For coupling viscoplasticity and microstructural degradation an Orowan parameter $\kappa_{\text{ORO}} = 2.1$ MPa$^{-1}$ has been identified. The shear modulus of the material is $G = 96$ MPa. The index of rafting $x_{\text{raft}}$ (see Section 3.4) is plotted in Fig. 6d, it shows the completion of rafting phenomenon during the initial nonlinear creep regime ($x_{\text{raft}}$=1 for fully rafted microstructure). The further nonlinearity of $\dot{p}$ *versus* $p$ curves (Fig. 6b) is due to LSW diffusion term. At each stress level tested, the widths of the $\gamma'$ channels (corresponding to the experimental points on Fig.6c) have been calculated as the average of the Gaussian distribution of the values mesured on SEM micrographs, showed in Fig.7a. The error bars correspond to the standard deviation of the distributions.

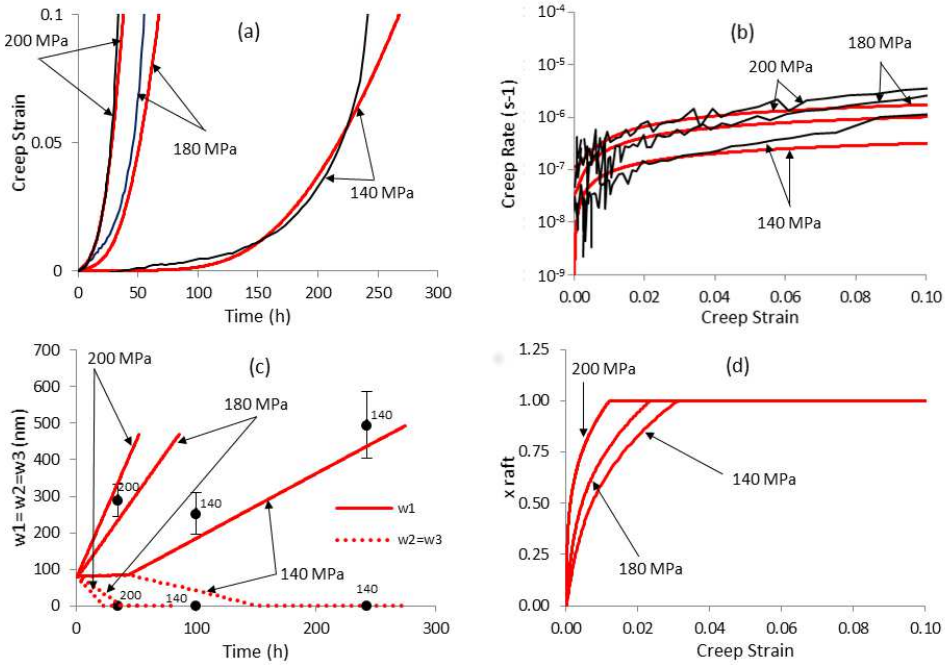


Figure 6: [001] creep responses of CMSX-4 alloy at 1050°C: a) Creep curves $\varepsilon(t)$, b) $\dot{p}$ *vs* $p$ curves, c) $\gamma$ channel width curves (upper lines: model $w_1(t) > w_0$, lower lines: model $w_2(t) = w_3(t) < w_0$, marks: measurements at 140 MPa and 200 MPa), d) Index of rafting $x_{\text{raft}} = w_{eq}/\,\text{tr}\,\mathbf{w}$ as a function of accumulated plastic strain $p$.

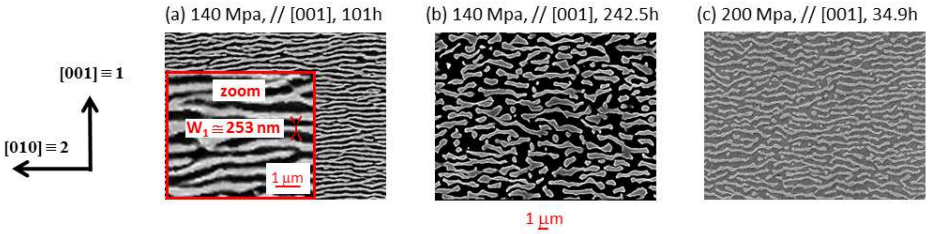


Figure 7: $\gamma/\gamma'$ rafted microstructure at 1050°C along [001]: a) at 140 MPa after 101 h, b) at 140 MPa after 242.5 h c) at 200 MPa after 34.9 h. Note that the gamma-prime phase appears in dark while the gamma matrix is in light gray.

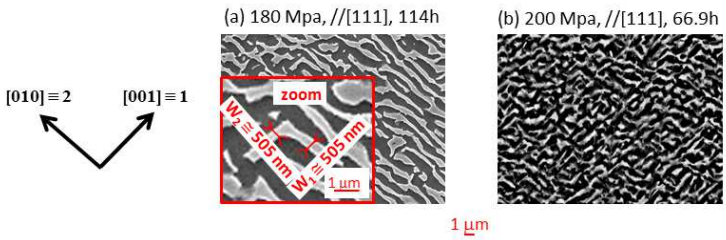


Figure 8: $\gamma/\gamma'$ rafted microstructure at 1050°C along [111]: a) at 180 MPa after 114 h, b) at 200 MPa after 66.9 h. Note that the gamma-prime phase appears in dark while the gamma matrix is in light gray

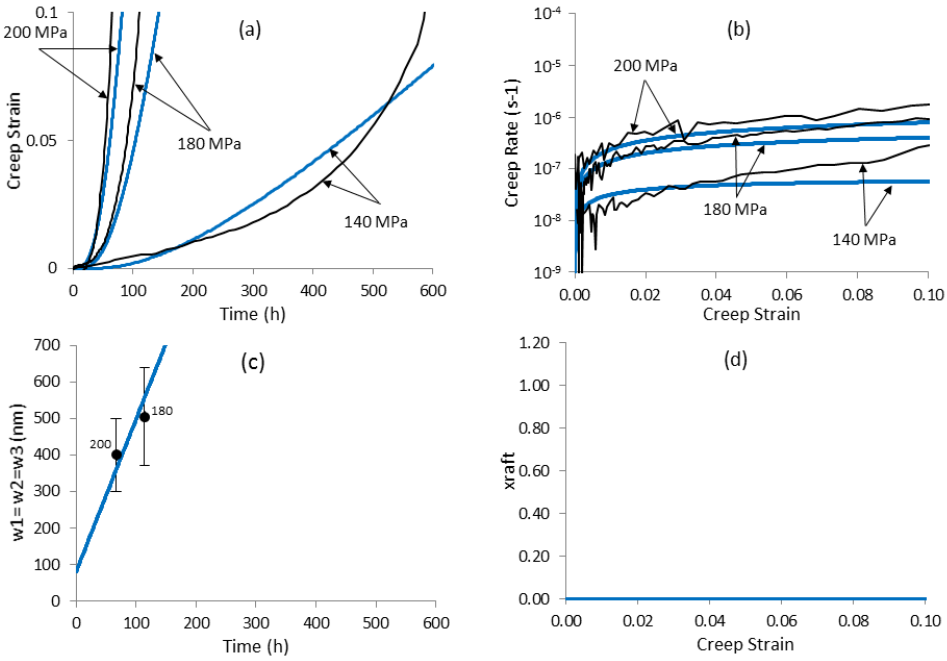


Figure 9: < 111 > creep responses of CMSX-4 alloy at 1050°C (Thick lines: model at $h = 0$, $\varpi = 1$): a) Creep curves $\varepsilon(t)$, b) $\dot{p}$ *vs* $p$ curves, c) $\gamma$ channel width curves (lines: model $w_1(t) = w_2(t) = w_3(t) > w_0$, marks: measurements at 180 MPa and 200 MPa), d) Index of rafting $x_{\text{raft}} = w_{eq}/\operatorname{tr}\mathbf{w} = 0$ as a function of accumulated plastic strain $p$.

### *7.4. < 111 > creep*

For creep in direction < 111 > there is $\gamma'$ coarsening but no $\gamma'$ rafting, neither in experiments (as it can be seen in Fig.8 and which corresponds to black thin lines in 9 and 10) nor in the model ($\text{H}(p_1^{\text{Hill}} - \varepsilon_{\text{th}}^p) = 0$ so that the $K_{\text{raft}}$ term vanishes in evolution law for $\boldsymbol{\omega}$, thick lines in the Figures). The three $\gamma$ channel widths $w_i$ are equal in the 3 crystallographic directions [001] ≡ 1, [100] ≡ 2 and [010] ≡ 3, with a zero index of rafting ($x_{\text{raft}} = 0$, Fig. 9c-d). A zero threshold $\overline{\varepsilon}_{\text{th}}^p = 0^+$ allows to properly model the microstructure change. The evolution of the channel width has been modeled with a $K_{\text{mc}} = 1.4\,10^{-5}\text{s}^{-1}$ and it has found to be independent on the stress level so that $U_{\text{mc}} = 0$. The coupling with the microstructure degradation is due to a non zero value of parameter $\varpi$ ($\varpi = 1$ in Fig. (9), $\varpi = 0.8$ in Fig. (10)).

A first identification is presented in Fig. (9) with $h = 0$ (and $\varpi = 1$), with the same remarks than for direction [001]: the nonlinearities, pronounced concerning the creep rate, are due to the microstructure change with no need to introduce damage up to $\varepsilon^p = 0.05$ of plastic strain. Let us point out a key point in the success of the modeling: a zero plastic strain rate $\dot{p} = 0$ is obtained by the model during the first hours of the creep test, up to ≈2.5h for $\sigma = 180$ MPa creep test and up to ≈15h for $\sigma = 140$ MPa creep test. There is no creep elongation as long as the Orowan stress contribution – parametrized by $\varpi$– is large ($f_2 < 0$). When coarsening takes place, the term $\varpi\frac{\kappa_{\text{ORO}}G}{\|\boldsymbol{\omega}\|}$ decreases so that apparent yield stress $\overline{\sigma}_y + \overline{R}_\infty + \varpi\frac{\kappa_{\text{ORO}}G}{\|\boldsymbol{\omega}\|}$ diminishes up to allow for creep (at $f_2 > 0$).

A second identification is presented in Fig. 10 with a non zero Hill parameter $h$, better than first identification at low strain (up to a few percents) and low stress (here $\sigma = 140$ MPa). The value $h = 0.5$ is considered (value theoretically justified in Appendix F) with $\varpi = 0.8$ for the coupling with microstructure change. Exactly the same microstructure evolution is obtained than for first identification. Let us last point out that damage has not been introduced, it will be needed for a better modeling of creep at $\varepsilon^p > 0.03$ for this second identification.

### *7.5. Responses in monotonic tension*

The tension curves are given in Fig. 11 for the two orientations < 001 >, < 111 > and the two identifications. Tensile test data along the < 111 > orientation are extracted from (Fedelich et al , 2012b) The proper modeling of < 001 > tension at strain rate $10^{-3}\text{s}^{-1}$ is gained thanks to a saturation value of viscous stress for criterion function $f_1$ ($\sigma_{v\infty} = 600$ MPa). Compared to first identification (with $h = 0$, $\varpi = 1$), the second identification (with $h = 0.5$, $\varpi = 0.8$) underestimates a little the ultimate stress for orientation < 111 >.

It is observed in Fig.11a a stress softening for the slowest tensile tests (at $10^{-5}s^{-1}$) whereas a plateau is observed for tensile tests at $10^{-4}$ and $10^{-3}s^{-1}$. This decrease in flow stress for the solwest tension test results from the progressive degradation of the the gamma/gamma-prime microstructure since this test is long enough to develop gamma-prime rafting (not shown here). Such a microstructure degradation is well-captured by the model since a decrease of the Orowan stress is observed under this strain rate conditions, while the Orowan stress is almost constant for the tests performed at 10-4 and 10-3s-1. One also has to note that the stress peak observed just after yielding is not reproduced by our model since this peak results from the micromechanisms of dislocation deposition in vertical and then horizontal gamma-channel before recovery processes (e.g. dislocation climb) occur

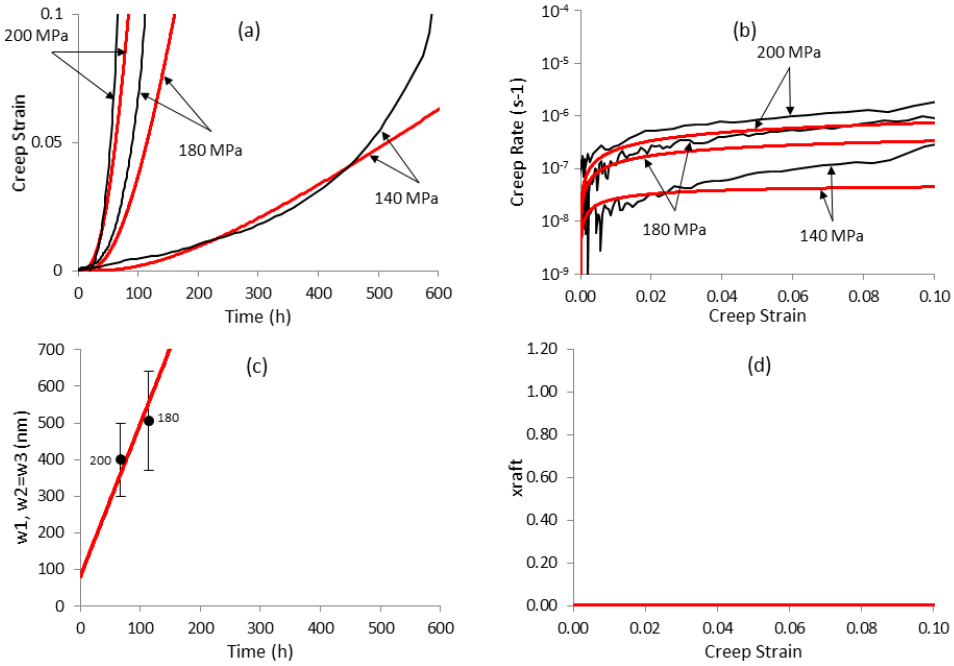


Figure 10: $< 111 >$ creep responses of CMSX-4 at 1050°C ($h = 0.5$, $\varpi = 0.8$): a) Creep curves $\varepsilon(t)$, b) $\dot{p}$ *vs* $p$ curves, c) $\gamma$ channel width curves $w_1(t) = w_2(t) = w_3(t)$, d) Index of rafting $x_{\text{raft}} = w_{eq}/\operatorname{tr}\mathbf{w}$ as a function of accumulated plastic strain $p$.

(Mughrabi , 2009). Due to parameter $\varpi \approx 1$, the softening phenomenon also occurs in the model for tension in direction $< 111 >$, but unseen! The softening rate in $< 001 >$ is related to the value of material parameters $U_{\text{raft}} \neq 0$ representing a stress enhanced rafting phenomenon (therefore a quicker softening of Orowan stress when $U_{\text{raft}}$ is taken larger). In $< 111 >$ there is no rafting and the material parameter acting in mechanical coarsening is $U_{\text{mc}} = 0$ (stress independency). The softening obtained for Orowan stress (and of the stress) is so slow for tension in $< 111 >$ that it is barely seen in Fig. 11b.

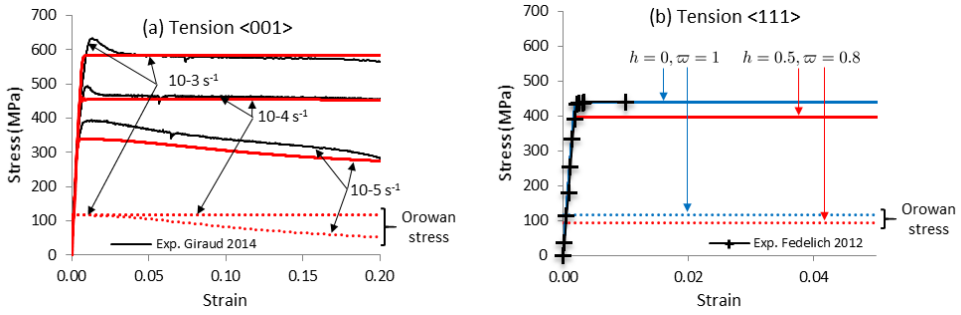


Figure 11: a) $< 001 >$ uniaxial tension curve at $10^{-5}\text{s}^{-1}$, $10^{-3}\text{s}^{-1}$ and $10^{-3}\text{s}^{-1}$ (Orowan stress also reported), b) $< 111 >$ uniaxial tension curve at $10^{-3}\text{s}^{-1}$ (Orowan stress also reported) for the two identification $h = 0$, $\varpi = 1$ and $h = 0.5$, $\varpi = 0.8$: . CMSX-4 at 1050°C (stress (model): thick lines, Orowan stress (model): dotted lines).

## 8. Thermodynamics of rafting under complex loading

In the aim of both checking the ability of the model to reproduce complex microstructure evolutions and the positivity of intrinsic dissipation, we have simulated a complex experiment starting first by a compression creep test at 1050°C for 100 hours and then, a stress reversal. Experimental data for such experiments can be found in Tetzlaff and Mughrabi (2000). In Section 5.3, we have proposed two possibilities to ensure the positivity of intrinsic dissipation: *modeling A* with as argument of Heaviside function $\mathcal{H}$ the scalar product $\boldsymbol{\omega} : \mathbf{n}^{\text{d}}$ (Eq. (66), this strong assumption enforces the positivity of the dissipation due to rafting itself, as illustrated in Fig. 12d) and *modeling B* with as argument of $\mathcal{H}$ the total dissipation $\mathcal{D}$ (Eq. (67), $\mathcal{D} \geq 0$ but negative values of the dissipation due to rafting are accepted, see Fig. 12d).

Recall first that these two possibilities of modeling give exactly the same responses in creep and in monotonic tension: the responses of Section 7 are those of both *modeling A* and *B*. Within these cases both $\mathcal{D}_{\text{raft}} \geq 0$ and $\mathcal{D} \geq 0$.

Differences only occur for complex loading cases, for instance with load reversal, when rafting takes place. In order to emphasize them and to retain one modeling (it will hereafter be *modeling B*) we study here an academic

loading made of a first creep stage in compression, 100 hours at $\sigma = -140$ MPa, followed by a 10 hours long load reversal at stress rate $\dot{\sigma} = 7.78\,10^{-3}$ MPa s$^{-1}$ up to a second creep stage, this time at positive stress $\sigma = 140$ MPa (other positive $\sigma$ and $\dot{\sigma}$ give similar results with different phenomenon rates). The loading direction is [001] $\equiv$ 1.

During the initial stage in compression a P-type rafting is well obtained (see Fig. 1, compressive case and Fig. 2), $w_1 = 0$ and $w_2 = w_3 > w_0$ with an index of rafting $x_{\text{raft}} = 0.5$. This situation is otained up to time $t = 100$ h of the start of the load reversal (the microstructure evolution is given in Fig. 12a). The microstructure evolution rate, stress enhanced, is much lower in the load reversal stage: the crossing of the elasticity domain and the corresponding low stress level decrease quite much the rate of rafting, rate which even vanishes when $\mathcal{H} = 0$ for thermodynamics considerations (as then $\dot{\omega}^{\text{raft}} = 0$). For both *modeling A* and *B* the intrinsic dissipation $\mathcal{D}$ remains positive (as proven in Section 5.5) but not the dissipation due to rafting $\mathcal{D}_{\text{raft}}$ for *modeling B* at $\mathcal{H} = \text{H}(\mathcal{D})$ (see Fig. 12d).

The main difference between both modeling approaches is obtained in the second creep stage at positive stress:

- for *modeling A*, the (slow) microstructure evolution is due to LSW homothetic growth only as then $\boldsymbol{\omega} : \mathbf{n}^{\text{d}} < 0$ and $\mathcal{H} = 0$ from $t = 105$ h up to the end: the microstructure remains P-type rafted at $x_{\text{raft}} = 0.5$, feature which is not consistent with the experimental results of Tetzlaff and Mughrabi (2000).
- for *modeling B*, the stage at $\mathcal{H} = 0$ is short (between $t = 107$ h and $t = 108.7$ h) and rafting takes place again for $t > 108.7$ h, up to fully N-type rafted microstructure at $x_{\text{raft}} = 1$: this is in full agreement with the experimental results of Tetzlaff and Mughrabi (2000) on similar nickel based single crystal superalloys with a negative misfit.

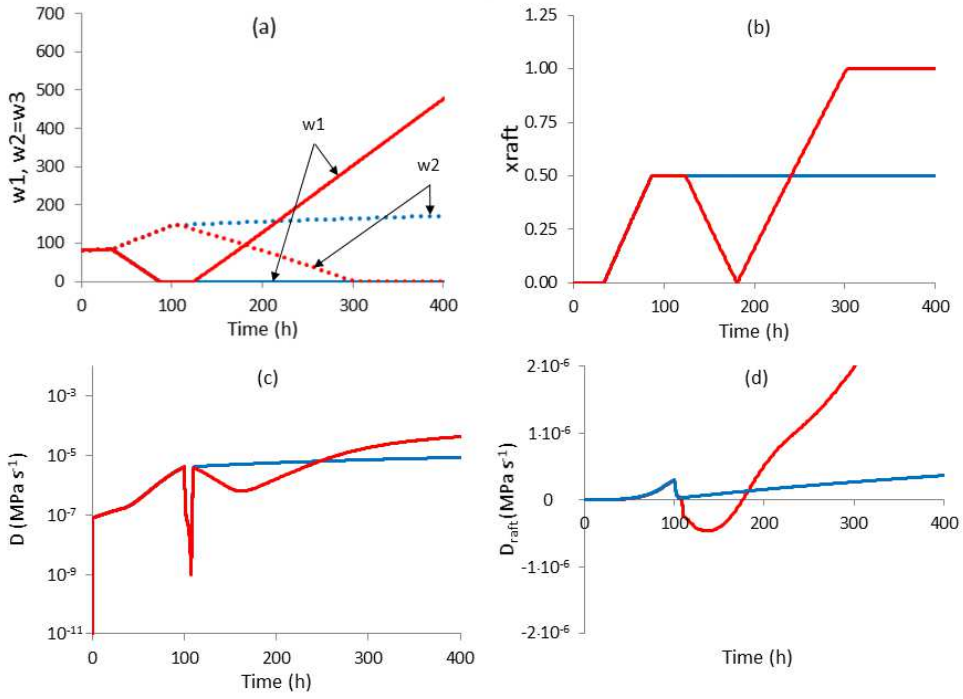


Figure 12: —— and ····· : *modeling A* with $\mathcal{H} = \text{H}(\boldsymbol{\omega} : \mathbf{n}^{\text{d}})$, —— and ····· : *modeling B* with $\mathcal{H} = \text{H}(\mathcal{D})$.
a) Evolution of $\gamma$ channel widths $w_1$ (solid lines), $w_2 = w_3$ (dotted lines), b) Evolution of index of rafting $x_{\text{raft}} = w_{eq}/\,\text{tr}\,\mathbf{w}$, c) Evolution of intrinsic dissipation $\mathcal{D}$ (logarithmic scale to underline the positivity of $\mathcal{D}$), d) Evolution of dissipation due to rafting $\mathcal{D}_{\text{raft}}$.

Let us conclude on the thermodynamics features. Both modeling approaches are fully equivalent in standard (constant) creep and in monotonic loading cases, either tensile or compressive. Both modeling always satisfy the second principle of thermodynamics but, the most stricking result is that *modeling B* allows for a negative dissipation due to rafting (compensated by positive plastic dissipation $\mathcal{D}_{\text{plast}}$ to ensure $\mathcal{D} \geq 0$). The expression for Heaviside term $\mathcal{H}$ chosen to ensure a positive intrinsic dissipation has a major role on the rafting evolution: *modeling A* with $\mathcal{H} = \text{H}(\boldsymbol{\omega} : \mathbf{n}^{\text{d}})$ spuriously blocks the tensile evolution after a pre-compression stage of rafting (of P-type), when *modeling B* with $\mathcal{H} = \text{H}(\mathcal{D})$ allows to properly model the change from P-type rafting in compression to N-type rafting in tension. This is the modeling to retain.

## 9. Isotropization at very high temperature

Let us last point out an interesting feature due to the consideration of Hill (cubic) criterion for yielding function $f_1$ and of material parameter $h$: the possibility to model the observed visco-plastic isotropization at very high

temperature (> 1100°C, Caron et al (1988), Hana et al (2010), Mataveli et alal (2010)). In proposed model an isotropization is simply gained by a temperature dependency of Hill parameter $h$ made such as

$$h = h(T) \underset{\text{high T}}{\longrightarrow} 1 \tag{92}$$

if in the same time the temperature dependent sum yield stress + hardening $\overline{\sigma}_y(T) + \overline{R}_\infty(T)$ for criterion function $f_2$ is made larger than $\sigma_y(T) + R_\infty(T)$ for criterion function $f_1$, *i.e.* material parameters such as $\dot{\boldsymbol{\epsilon}}_2^p << \dot{\boldsymbol{\epsilon}}_1^p$. Such an isotropisation of the viscoplastic properties is generally obtained under conditions of fast development of the gamma-prime rafting, without any degradation of the stability of the rafted structure (i.e. no $\gamma - \gamma'$ topological inversion (Epishin et al (2000, 2001)). Under such conditions, a creep life anisotropy factor of 2 at maximum is experimentaly obtained.

## Conclusion

Starting from literature models / sets of constitutive equations (Cormier and Cailletaud (2010b), Tinga et al (2009), Fedelich et al (2009, 2012a)) for the physical and mechanical descriptions of the $\gamma - \gamma'$ rafting – including coarsening – process, we propose an original phenomenological model for nickel based single crystal superalloys having a negative $\gamma - \gamma'$ negative misfit (mostly Ni-base superalloys like CMSX-4 and SR99). Our work main originality is to give a thermodynamics (state) status to the tensorial rafting variable $\boldsymbol{\omega}$ representative of $\gamma$ channel widths in the three < 001 > directions. This is made possible thanks to a Kelvin mode based description of cubic visco-plasticity but a Schmid criterion based can neverthless be recovered. The originality is also to derive the full thermodynamics framework of elasto-visco-plasticity coupled with anisotropic rafting phenomenon, including novel coupling of macroscopic Orowan stress with the norm of second order tensor $\boldsymbol{\omega}$. The rafting / mechanical coarsening / LSW homothetic growth is represented by a tensorial rate evolution law $\dot{\boldsymbol{\omega}} = ....$

CMSX-4 observed N-type rafting, normal to loading direction, and P-type rafting, parallel to loading direction, are well reproduced during tension/compression creep testing along the < 001 > orientation. CMSX-4 observed coarsening (microstructure growth) with no rafting is represented for < 111 > orientation. The increase of creep plastic strain rate and corresponding convexity of creep curves are obtained, at least up to a few percents of strain, without damage (thanks to to microstructure degradation). Matan et al (1999) plastic strain threshold is introduced within the proposed model. Mechanical rafting of CMSX-4 is shown to be stress enhanced (material parameter $U_{\text{raft}} \neq 0$), this stress dependency being responsible of the progressive softening observed during slow rate tension tests along the < 001 > orientation. Mechanical coarsening of CMSX-4 is found stress independent (material parameter $U_{\text{mc}} = 0$) so that there is no apparent softening in tension curve for < 111 > orientation.

The second principle of thermodynamics is satisfied by the proposed constitutive equations (intrinsic dissipation proven to be positive). An interesting point is that in the model retained for complex loading, only the total dissipation, sum of (visco-)plastic and rafting dissipations, remains positive. The dissipation due to $\gamma'$ rafting may take –thermodynamics admissible– negative values. This is shown to be a key feature of the proper description of rafting in case of alternated / cyclic loading.

Note last that the present work gives also the possibility to model the mechanical/rafting behavior of single crystals superalloys at positive misfit $\delta_u$ (mostly Co-based superalloys (Pyczak et al , 2013, Tanaka et al , 2012)). For those, the N-type rafting occurs in compression while the P-type rafting occurs in tension (Mughrabi (2014)). The evolution law for tensorial $\gamma$ channel width variable has to be changed into

$$\dot{\boldsymbol{\omega}} = -\text{sgn}(\delta_u)\dot{\mathcal{R}}\,\text{H}(\mathcal{D})\,\mathbf{n}^{\text{d}} + \dot{C}\,\mathbf{1} + \dot{\mathcal{G}}\,\frac{\boldsymbol{\omega}}{||\boldsymbol{\omega}||}, \qquad \dot{\mathcal{R}} \geq 0, \quad \dot{C} \geq 0, \quad \dot{\mathcal{G}} \geq 0$$

With $\text{sgn}(\delta_u) = \frac{\delta_u}{|\delta_u|}$ and where the Heaviside function $\mathcal{H} = \text{H}(\mathcal{D})$ ensures the positivity of the dissipation.


## Acknowledgements

The authors are grateful to Safran Helicopter Engines for funding this work. Dr. C. Moriconi, R. Eng. A. Burteau and Dr. Z. Hervier (both at SAFRAN Helicopter Engines) are especially thanked for their continuous interest in this study. Dr. D. Bertheau (Institut Pprime/ISAE-ENSMA) is acknowledged for technical assistance during tensile tests.


## Appendix A. Kelvin decomposition of elasticity tensor

The elasticity fourth rank tensor $\mathbb{E}$ (resp. its Voigt matricial representation $[E]$) has eigenvalues $\Lambda^{(I)}$ and corresponding second rank symmetric eigentensors $\mathbf{e}^{(I)}$ (resp. eigenvectors $\hat{e}^{(I)}$) are solutions of the eigenproblem

$$\mathbb{E} : \mathbf{e}^{(I)} = \Lambda^{(I)}\mathbf{e}^{(I)}\,, \qquad \mathbf{e}^{(I)} : \mathbf{e}^{(J)} = \delta_{IJ} \tag{A.1}$$

with $\delta_{IJ}$ the Kronecker symbol. The couples ($\Lambda^{(I)}$, $\mathbf{e}^{(I)}$ or $\hat{e}^{(I)}$) are the Kelvin modes (or strains here), the eigenvalues $\Lambda^{(I)}$ are the Kelvin moduli (Rychlewski , 1984). These moduli are at most six (Cowin et al , 1991), they are only two in case of isotropic elasticity ($3K$ and $2G$ if $K$ and $G$ are the bulk and shear moduli).

Kelvin decomposition of Hooke tensor is then simply the following re-writing

$$\mathbb{E} = \sum_{I=1}^{6} \Lambda^{(I)} \mathbf{e}^{(I)} \otimes \mathbf{e}^{(I)} \qquad \mathbb{E} = \sum_{k=1}^{N\leq 6} \Lambda^k \mathbb{P}^k \qquad \mathbb{S} = \mathbb{E}^{-1} = \sum_{k=1}^{N\leq 6} \frac{1}{\Lambda^k}\, \mathbb{P}^k \qquad \mathbb{P}^k = \sum_{I/\Lambda^{(I)}=\Lambda^k} \mathbf{e}^{(I)} \otimes \mathbf{e}^{(I)} \tag{A.2}$$

There is always a family of six orthogonal eigentensors $\mathbf{e}^{(I)}$ but some eigenvalues can be multiple, depending on the material symmetry. The terms of identical moduli $\Lambda^{(I)} = \Lambda^k$ are grouped to form Kelvin projectors (François , 1995), if $\mathbb{S}$ is compliance tensor, with $N$ the number of different Kelvin moduli. The projectors $\mathbb{P}^k$ are unique for a given elasticity tensor $\mathbb{E}$.

The elastic energy density reads

$$w_e = \frac{1}{2}\boldsymbol{\epsilon} : \mathbb{E} : \boldsymbol{\epsilon} = \frac{1}{2}\boldsymbol{\sigma} : \mathbb{S} : \boldsymbol{\sigma} = \frac{1}{2}\sum_{k=1}^{N} \Lambda^k\, \boldsymbol{\epsilon}^k : \boldsymbol{\epsilon}^k = \frac{1}{2}\sum_{k=1}^{N} \frac{1}{\Lambda^k}\, \boldsymbol{\sigma}^k : \boldsymbol{\sigma}^k \tag{A.3}$$

with $\boldsymbol{\epsilon}$ and $\boldsymbol{\sigma}$ the strain and stress tensors and where $\boldsymbol{\sigma}^k = \mathbb{P}^k : \boldsymbol{\sigma}$. For a given material symmetry, this equation defines in a unique and objective manner the Kelvin stress $\boldsymbol{\sigma}^k$ as the projection of the stress tensor on the $k^{th}$ Kelvin mode. If the same projection is made for the strain, *i.e.* $\boldsymbol{\epsilon}^k = \mathbb{P}^k : \boldsymbol{\epsilon}$, the elasticity law $\boldsymbol{\sigma} = \mathbb{E} : \boldsymbol{\epsilon}$ is equivalent to $\boldsymbol{\sigma}^k = \Lambda^k \boldsymbol{\epsilon}^k\ \forall k$ (no sum).

*In case of cubic material symmetry* the Kelvin eigentensors are (in the material (cubic) Natural Anisotropy Basis)

$$\mathbf{e}^{(1)} = \begin{bmatrix} \frac{1}{\sqrt{3}} & 0 & 0 \\ 0 & \frac{1}{\sqrt{3}} & 0 \\ 0 & 0 & \frac{1}{\sqrt{3}} \end{bmatrix}_{NAB}, \quad \mathbf{e}^{(2)} = \begin{bmatrix} \frac{1}{\sqrt{2}} & 0 & 0 \\ 0 & -\frac{1}{\sqrt{2}} & 0 \\ 0 & 0 & 0 \end{bmatrix}_{NAB}, \quad \mathbf{e}^{(3)} = \begin{bmatrix} \frac{1}{\sqrt{6}} & 0 & 0 \\ 0 & \frac{1}{\sqrt{6}} & 0 \\ 0 & 0 & -\frac{2}{\sqrt{6}} \end{bmatrix}_{NAB}$$
$$\mathbf{e}^{(4)} = \begin{bmatrix} 0 & \frac{1}{\sqrt{2}} & 0 \\ \frac{1}{\sqrt{2}} & 0 & 0 \\ 0 & 0 & 0 \end{bmatrix}_{NAB}, \quad \mathbf{e}^{(5)} = \begin{bmatrix} 0 & 0 & 0 \\ 0 & 0 & \frac{1}{\sqrt{2}} \\ 0 & \frac{1}{\sqrt{2}} & 0 \end{bmatrix}_{NAB}, \quad \mathbf{e}^{(6)} = \begin{bmatrix} 0 & 0 & \frac{1}{\sqrt{2}} \\ 0 & 0 & 0 \\ \frac{1}{\sqrt{2}} & 0 & 0 \end{bmatrix}_{NAB} \tag{A.4}$$

They defines the three the projectors $\mathbb{P}^k$ – renammed $\mathbb{P}^{\mathrm{H}}$, $\mathbb{P}^{\mathrm{d}}$, $\mathbb{P}^{\overline{\mathrm{d}}}$ – in an objective and unique manner,

$$\begin{cases} \mathbb{P}^{k=1} = \mathbb{P}^{\mathrm{H}} = \mathbf{e}^{(1)} \otimes \mathbf{e}^{(1)} \\ \mathbb{P}^{k=2} = \mathbb{P}^{\mathrm{d}} = \mathbf{e}^{(2)} \otimes \mathbf{e}^{(2)} + \mathbf{e}^{(3)} \otimes \mathbf{e}^{(3)} \\ \mathbb{P}^{k=3} = \mathbb{P}^{\overline{\mathrm{d}}} = \mathbf{e}^{(4)} \otimes \mathbf{e}^{(4)} + \mathbf{e}^{(5)} \otimes \mathbf{e}^{(5)} + \mathbf{e}^{(6)} \otimes \mathbf{e}^{(6)} \end{cases} \tag{A.5}$$

so that one has the strain partition $\boldsymbol{\sigma} = \boldsymbol{\sigma}^{\mathrm{H}} + \boldsymbol{\sigma}^{\mathrm{d}} + \boldsymbol{\sigma}^{\overline{\mathrm{d}}}$ with Kelvin stresses

$$\boldsymbol{\sigma}^{\mathrm{H}} = \mathbb{P}^{\mathrm{H}} : \boldsymbol{\sigma} = \frac{1}{3}\,\mathrm{tr}\,\boldsymbol{\sigma}\,\mathbf{1} \qquad \boldsymbol{\sigma}^{\mathrm{d}} = \mathbb{P}^{\mathrm{d}} : \boldsymbol{\sigma} \qquad \boldsymbol{\sigma}^{\overline{\mathrm{d}}} = \mathbb{P}^{\overline{\mathrm{d}}} : \boldsymbol{\sigma} \tag{A.6}$$

also defined in an objective and unique manner. In cubic Natural Anisotropy Basis, $\boldsymbol{\sigma}^{\mathrm{d}} = (\boldsymbol{\sigma}^{\mathrm{d}})'$ is diagonal deviatoric part of $\boldsymbol{\sigma}$ and $\boldsymbol{\sigma}^{\overline{\mathrm{d}}} = (\boldsymbol{\sigma}^{\overline{\mathrm{d}}})'$ is out of diagonal deviatoric part of $\boldsymbol{\sigma}$.

## Appendix B. Heteregenous field in torsion

Consider here the thin tube of longitudinal axis in [001] (= $\mathrm{e}_z = \mathrm{e}_3$) orientation tested in torsion in Nouailhas and Cailletaud (1995). Unit vectors $\mathrm{e}_k$ of cartesian basis are set parallel to each < 001 > directions, defining Natural Anisotropy Basis of present cubic material. Radial and tangential unit vectors are $\mathrm{e}_r = \cos\theta\,\mathrm{e}_1 + \sin\theta\,\mathrm{e}_2$, $\mathrm{e}_\theta = -\sin\theta\,\mathrm{e}_1 + \cos\theta\,\mathrm{e}_2$.

At homogeneous shear strain $\gamma = 2\varepsilon_{\theta z}$ applied in torsion on the tube the non zero stress components are $\sigma_{13} = G\gamma\cos\theta$, $\sigma_{12} = -G\gamma\sin\theta$ so that diagonal deviatoric stress tensor $\boldsymbol{\sigma}^{\mathrm{d}} = 0$ and out of diagonal deviatoric stress tensor $\boldsymbol{\sigma}^{\overline{\mathrm{d}}} = \boldsymbol{\sigma}$. Non quadratic norm $\|\boldsymbol{\sigma}^{\overline{\mathrm{d}}}\|_a$ introduced in section 2.3 is at the elasticity limit

$$\|\boldsymbol{\sigma}^{\overline{\mathrm{d}}}\|_a = G\gamma\,(|\cos\theta|^a + |\sin\theta|^a)^{\frac{1}{a}} \qquad a \geq 1 \tag{B.1}$$

It is constant for $a = 2$ (homogeneous von Mises stress field in torsion at $\sigma^{\overline{\mathrm{d}}}_{eq} = 3^{-1/a} G\gamma = const$, it is heterogeneous for $a \neq 2$ with

- *for $a > 2$:* the maximum value of the yield criterion $\bar{f}$ is reached when radial basis vector $\mathrm{e}_r$ is aligned with < 100 > orientation (at angle $\theta = k\frac{\pi}{2}$, $k$ integer), the minimum value of $\bar{f}$ is reached when radial basis vector $\mathrm{e}_r$ is in direction < 110 > (at angle $\theta = \frac{\pi}{4} + k\frac{\pi}{2}$ from < 100 > orientation).

- *for* $1 \leq a < 2$*:* the location of minima and maxima of $\bar{f}$ are inverted, the minimum value being reached at $\theta = k\frac{\pi}{2}$, the maximum value at angle $\theta = \frac{\pi}{4} + k\frac{\pi}{2}$ from $< 001 >$: yielding will initiate for the $< 110 >$ orientations, at $\frac{\pi}{4}$ from $< 100 >$ orientations.

The second case is the one observed in experiments (Nouailhas and Cailletaud , 1995) so that a value of material parameter $a \in [1, 2[$ has to be considered (a simple choice being $a = 1$).

## Appendix C. Thermo-elastic terms

Additional thermo-mechanical terms have to be considered. If the thermo-elastic effect of misfit is derived from simple mixture law (Lemaitre et al , 2009), potential $\rho\psi_{TM}$ is added to isothermal potential defined in Eq. (54), with $T_{\text{ref}}$ the thermo-elastic reference temperature,

$$\rho\psi_{TM} = -3f_\gamma K_\gamma \alpha_\gamma (T - T_{\text{ref}}) \operatorname{tr}\boldsymbol{\epsilon} - 3f_{\gamma'} K_{\gamma'} (\alpha_{\gamma'} (T - T_{\text{ref}}) + \delta_u) \operatorname{tr}\boldsymbol{\epsilon} - \rho C_\varepsilon (T \ln \frac{T}{T_{\text{ref}}} - T + T_{\text{ref}}) \tag{C.1}$$

or, introducing $K$ and $\alpha$ the homogenized bulk modulus and thermal expansion coefficient,

$$\rho\psi_{TM} = -3K\alpha (T - T_{\text{ref}}) \operatorname{tr}\boldsymbol{\epsilon} - 3f_{\gamma'} K_{\gamma'} \delta_u \operatorname{tr}\boldsymbol{\epsilon} - \rho C_\varepsilon (T \ln \frac{T}{T_{\text{ref}}} - T + T_{\text{ref}}) \tag{C.2}$$

so that $f_{\gamma'}$ the $\gamma'$ precipitates volume fraction, $K_{\gamma'}$ the elastic bulk modulus of such a $\gamma'$ phase, $\delta_u$ the unconstrained misfit (homogeneous to a strain); $C_\varepsilon$ is the material specific heat capacity assumed constant over a large temperature range. Latent heat due to phase change has been neglected.

From state law $\boldsymbol{\sigma} = \rho\frac{\partial\psi}{\partial\boldsymbol{\epsilon}}$ one gets

$$\boldsymbol{\epsilon} = \mathbb{E}^{-1} : \boldsymbol{\sigma} + \alpha(T - T_{\text{ref}})\mathbf{1} + \boldsymbol{\epsilon}^p + f_{\gamma'}\frac{K_{\gamma'}}{K}\delta_u \mathbf{1}$$

## Appendix D. Link with index of rafting $\xi$

For an uniaxial loading performed in direction $1 \equiv [001]$ (the most important one from a technological point of view), the transverse channel widths remain equals, $w_2 = w_3 = cw_1$ with $c$ a scalar, pure coarsening being $c = 1$ and complete rafting $c = 0$. In cubic Natural Anisotropy Basis,

$$\mathbf{w} = \begin{bmatrix} w_1 & 0 & 0 \\ 0 & cw_1 & 0 \\ 0 & 0 & cw_1 \end{bmatrix}_{NAB} \qquad \mathbf{w}' = \begin{bmatrix} \frac{2}{3}(1-c)w_1 & 0 & 0 \\ 0 & -\frac{1}{3}(1-c)w_1 & 0 \\ 0 & 0 & -\frac{1}{3}(1-c)w_1 \end{bmatrix}_{NAB} \tag{D.1}$$

and $\operatorname{tr}\mathbf{w} = (1 + 2c)w_1$, $w_{eq} = \sqrt{\frac{3}{2}}\|\mathbf{w}'\| = (1 - c)w_1$ so that the 3D index of rafting $x_{\text{raft}}$ is simply related to $c$ (and reciprocally) as $x_{\text{raft}} = \frac{w_{eq}}{\operatorname{tr}\mathbf{w}} = \frac{1-c}{1+2c}$ or $c = \frac{1-x_{\text{raft}}}{1+2x_{\text{raft}}}$ Note that this relationship between $c$ and $x_{\text{raft}}$ applies to any more complex rafting / coarsening / homothetic growth process ensuring $w_2 \approx w_3$.

In order to make a link with Fedelich rafting index $\xi$, let us place ourselves in the same state of comparison than for definition (23) and use the fact that both definitions of coarsening expression $w_{\text{cube}}$ and of complete rafting expression $w_{\text{raft}}$ are made at given volume fraction $f_{\gamma'}$ and at given periodicity $\lambda$. Isotropic periodicity $\lambda_i = \lambda$ is assumed so that, from Eq. (29),

$$f_{\gamma'} = \left(1 - \frac{w_1}{\lambda}\right)\left(1 - \frac{w_2}{\lambda}\right)\left(1 - \frac{w_3}{\lambda}\right) = \left(1 - \frac{w_1}{\lambda}\right)\left(1 - c\frac{w_1}{\lambda}\right)^2 \tag{D.2}$$

The definition (23) is valid for tensile loading. From the assumption $w_1 = w = w_{\text{cube}} + \xi(w_{\text{raft}} - w_{\text{cube}})$ it is possible to write $\frac{w}{\lambda} = 1 - f_{\gamma'}^{1/3} + \xi(f_{\gamma'}^{1/3} - f_{\gamma'})$, so that we get explicitly $c = c(f_{\gamma'}, \xi)$ as a function of $f_{\gamma'}$ and $\xi$.

Finally inverting $c = \frac{1-x_{\text{raft}}}{1+2x_{\text{raft}}}$, the index of rafting $x_{\text{raft}} = w_{eq}/\operatorname{tr}\mathbf{w}$ is related to both the $\gamma'$ precipitates volume fraction and index of rafting $\xi$ as

$$x_{\text{raft}} = \frac{1 - c(f_{\gamma'}, \xi)}{1 + 2c(f_{\gamma'}, \xi)} = x_{\text{raft}}(f_{\gamma'}, \xi) \tag{D.3}$$

Eq. (D.3) applies to tensile loading in $< 001 >$ direction. Recall that it is an approximate expression obtained thanks to the assumption of equal periocities in the three directions of space $\lambda_1 = \lambda_2 = \lambda_3 = \lambda$. It gives back $x_{\text{raft}} = 0$ when $\xi = 0$ (coarsening) and $x_{\text{raft}} = 1$ when $\xi = 1$ (rafting).

## Appendix E. From Tinga *et al* evolution law to $\dot{\mathbf{w}} = ...$

Let us consider uniaxial tension or compression along orientation 1 ≡ [001]. Diagonal deviatoric part of stress tensor $\boldsymbol{\sigma}^{\mathrm{d}}$ (in cubic Natural Anisotropy Basis) is equal to stress deviator $\boldsymbol{\sigma}'$ and defines normal $\mathbf{n}^{\mathrm{d}}$, as

$$\boldsymbol{\sigma}' = \boldsymbol{\sigma}^{\mathrm{d}} = \frac{2}{3}\sigma \left[\begin{array}{ccc} 1 & 0 & 0 \\ 0 & -\frac{1}{2} & 0 \\ 0 & 0 & -\frac{1}{2} \end{array}\right]_{NAB} = \frac{2}{3}\sigma^{\mathrm{d}}_{eq}\,\mathbf{n}^{d} \qquad \sigma^{\mathrm{d}}_{eq} = \sigma_{eq} = |\sigma| \tag{E.1}$$

Evolution law (24) gives a diagonal second order tensor $\boldsymbol{\ell}$ which commutes with normal $\mathbf{n}^{\mathrm{d}}$. Altogether with the assumption of constant volume of precipitates $V_{\gamma'} = \ell_1\ell_2\ell_3 = \ell_L\ell_T^2 = \ell_0^3$ inherent to Eq. (24) this defines

$$\boldsymbol{\ell} = \left[\begin{array}{ccc} \ell_L & 0 & 0 \\ 0 & \frac{\ell_0^{3/2}}{\sqrt{\ell_L}} & 0 \\ 0 & 0 & \frac{\ell_0^{3/2}}{\sqrt{\ell_L}} \end{array}\right]_{NAB} \qquad \mathbf{L} = \boldsymbol{\ell}\cdot\mathbf{n}^{\mathrm{d}} = \mathbf{n}^{\mathrm{d}}\cdot\boldsymbol{\ell} = \mathrm{sgn}(\sigma)\left[\begin{array}{ccc} \ell_L & 0 & 0 \\ 0 & -\frac{\ell_0^{3/2}}{2\sqrt{\ell_L}} & 0 \\ 0 & 0 & -\frac{\ell_0^{3/2}}{2\sqrt{\ell_L}} \end{array}\right]_{NAB} \tag{E.2}$$

where we set $\ell_1 = \ell_L$ and $\ell_2 = \ell_3 = \ell_T = \ell_0^{3/2}/\sqrt{\ell_L}$ respectively the longitudinal and the transverse sizes of large $\gamma'$ precipitates. Evolution law (24) becomes

$$\dot{\boldsymbol{\ell}} = -\frac{1}{\tau_\ell}\,\frac{\sigma_{eq}}{\sigma_{eq}+\sigma_\varepsilon}\exp\left(-\frac{Q_\ell - \sigma_{eq}U}{k_{\mathrm{B}}T}\right)\mathbf{L} = -\frac{1}{\tau_\ell}\,\frac{\sigma^{\mathrm{d}}_{eq}}{\sigma^{\mathrm{d}}_{eq}+\sigma_\varepsilon}\exp\left(-\frac{Q_\ell - \sigma^{\mathrm{d}}_{eq}U}{k_{\mathrm{B}}T}\right)\mathbf{L} \tag{E.3}$$

Using in present uniaxial case the fact that in tension $\mathrm{sgn}(\sigma) = 1$, $\ell_L < \ell_0$ due to $\dot{\ell}_1 < 0$ (from Eq. (24)), and in compression $\mathrm{sgn}(\sigma) = -1$, $\ell_L > \ell_0$ (from Eq. (24)), one gets

$$\mathbf{L} = \frac{2\ell_L^{3/2}+\ell_0^{3/2}}{3\sqrt{\ell_L}}\,\mathbf{n}^{\mathrm{d}} + \mathrm{sgn}(\sigma)\frac{\ell_L^{3/2}-\ell_0^{3/2}}{3\sqrt{\ell_L}}\,\mathbf{1} = \frac{2\ell_L^{3/2}+\ell_0^{3/2}}{3\sqrt{\ell_L}}\,\mathbf{n}^{\mathrm{d}} - \frac{\left|\ell_L^{3/2}-\ell_0^{3/2}\right|}{3\sqrt{\ell_L}}\,\mathbf{1} \tag{E.4}$$

Eq. (24) can be rewritten in a tensorial form valid for tensile of compressive loading in any < 001 > directions,

$$\dot{\boldsymbol{\ell}} = \frac{1}{\tau_\ell}\,\frac{\sigma^{\mathrm{d}}_{eq}}{\sigma^{\mathrm{d}}_{eq}+\sigma_\varepsilon}\exp\left(-\frac{Q_\ell - \sigma^{\mathrm{d}}_{eq}U}{k_{\mathrm{B}}T}\right)\left[\frac{\left|\ell_L^{3/2}-\ell_0^{3/2}\right|}{3\sqrt{\ell_L}}\,\mathbf{1} - \frac{2\ell_L^{3/2}+\ell_0^{3/2}}{3\sqrt{\ell_L}}\,\mathbf{n}^{\mathrm{d}}\right] \tag{E.5}$$

Combined with an anisotropic periodicity growth $\dot{\boldsymbol{\lambda}} = \dot{\boldsymbol{\lambda}}' + \frac{1}{3}\mathrm{tr}\,\dot{\boldsymbol{\lambda}}\,\mathbf{1} \geq 0$ (growth meaning that $\dot{\boldsymbol{\lambda}}$ is a definite positive second order tensor), one obtains an evolution law for $\gamma$ channel width $\dot{\mathbf{w}} = \dot{\boldsymbol{\lambda}} - \dot{\boldsymbol{\ell}}$ as the sum of a deviatoric part (interpreted as rafting contribution, including homothetic growth) and of a spherical or isotropic part (coarsening, including homothetic growth). As furthermore second order periodicity tensor $\boldsymbol{\lambda}$ also has equal transverse elongations $\lambda_2 = \lambda_3 = \lambda_T$, it is of the form

$$\dot{\boldsymbol{\lambda}} = \dot{\mathcal{L}}\,\mathbf{n}^{\mathrm{d}} + \dot{\lambda}_{\mathrm{iso}}\mathbf{1} \qquad \dot{\lambda}_{\mathrm{iso}} = \frac{1}{3}\,\mathrm{tr}\,\dot{\boldsymbol{\lambda}} \tag{E.6}$$

so that evolution law (24) combined with anisotropic periodicity growth ends up in to

$$\begin{aligned} \dot{\mathbf{w}} &= \dot{\mathbf{w}}'_{\mathrm{raft+hom}} + \dot{w}_{\mathrm{coars+hom}}\,\mathbf{1} \\ \dot{\mathbf{w}}'_{\mathrm{raft+hom}} &= \left[\frac{1}{\tau_\ell}\,\frac{2\ell_L^{3/2}+\ell_0^{3/2}}{3\sqrt{\ell_L}}\,\frac{\sigma^{\mathrm{d}}_{eq}}{\sigma^{\mathrm{d}}_{eq}+\sigma_\varepsilon}\exp\left(-\frac{Q_\ell - \sigma^{\mathrm{d}}_{eq}U}{k_{\mathrm{B}}T}\right) + \dot{\mathcal{L}}\right]\mathbf{n}^{\mathrm{d}} \\ \dot{w}_{\mathrm{coars+hom}} &= \dot{\lambda}_{\mathrm{iso}} - \frac{1}{\tau_\ell}\,\frac{\left|\ell_L^{3/2}-\ell_0^{3/2}\right|}{3\sqrt{\ell_L}}\,\frac{\sigma_{eq}}{\sigma_{eq}+\sigma_\varepsilon}\exp\left(-\frac{Q_\ell - \sigma_{eq}U}{k_{\mathrm{B}}T}\right) \end{aligned} \tag{E.7}$$

The $\gamma'$ rafting contribution is therefore proportional to the normal $\mathbf{n}^{\mathrm{d}}$ to yield surface $f = \sigma^{\mathrm{d}}_{eq} - \sigma_y$. A periodicity growth term $\dot{\lambda}_{\mathrm{iso}} \geq 0$ large enough is needed to ensure coarsening.

It is important to point out that, even if only < 001 > loading are considered here, one has anticipated the fact that misoriented $\gamma'$ rafting is also governed by the diagonal deviatoric part of stress tensor $\boldsymbol{\sigma}^{\mathrm{d}}$ in Natural Anisotropy Basis: even if one has the equality $\sigma_{eq} = \sigma^{\mathrm{d}}_{eq}$ in < 001 > uniaxial loading cases, rafting contribution in Eq. (E.7) is written in terms of invariant $\sigma^{\mathrm{d}}_{eq}$. For coarsening the whole stress components may act so the full von Mises stress $\sigma_{eq}$ is kept.

**Remark.** *If parameter $\sigma_\varepsilon$ is not small, the term $\frac{\sigma^{\rm d}_{eq}}{\sigma^{\rm d}_{eq}+\sigma_\varepsilon}$ (resp. $\frac{\sigma_{eq}}{\sigma_{eq}+\sigma_\varepsilon}$) introduces, through hardening, a dependency to accumulated plastic strain $p^{\rm d}$ (resp. $p$) that tends to saturate.*

## Appendix F. Model rewritten in crystal plasticity framework

We give here the reformulation of proposed model in crystral plasticity framework (Asaro , 1983, Asaro and Lubarda , 2006, Hill and Rice , 1972, Peirce et al , 1983, Rice , 1975, Schmid and Boas , 1935), framework often used for the description of constitutive equations of Ni-based single crystal superalloys (Fedelich , 2002, Méric et al , 1991). For the sake of simplicity, isotropic hardening is assumed saturated, no kinematic hardening is introduced.

### *Appendix F.1. Constitutive equations*

In standard crystal plasticity framework, the constitutive equation for elasto-visco-plasticity coupled with tensorial rafting are:

- *elasticity law coupled with rafting*

$$\boldsymbol{\sigma} = \mathbb{E}(1-\kappa_E\omega_{eq}) : (\boldsymbol{\epsilon} - \boldsymbol{\epsilon}^p - \alpha\,(T-T_{\rm ref})\,\mathbf{1}) \approx \mathbb{E} : (\boldsymbol{\epsilon} - \boldsymbol{\epsilon}^p - \alpha\,(T-T_{\rm ref})\,\mathbf{1}) \tag{F.1}$$

  with in practice the coupling of elasticity and of thermal expansion with rafting neglected.

- *resolved shear stresses* on octahedral and cubic slip systems $g$ (Schmid and Boas , 1935)

$$\tau^o_g = \mathrm{m}^{\rm o}_{\rm g}\cdot\boldsymbol{\sigma}\cdot\mathrm{n}^{\rm o}_{\rm g} \qquad \tau^{\rm c}_{\rm g} = \mathrm{m}^{\rm c}_{\rm g}\cdot\boldsymbol{\sigma}\cdot\mathrm{n}^{\rm c}_{\rm g} \tag{F.2}$$

  with $\mathrm{m}^{\rm o}_{\rm g}$, $\mathrm{m}^{\rm c}_{\rm g}$ the unit vectors of the slip directions and $\mathrm{n}^{\rm o}_{\rm g}$, $\mathrm{n}^{\rm c}_{\rm g}$ the normals to the slip planes, $\dot\gamma_g$ the slip rates. In general multiaxial case a maximum of 12 octahedral slip systems (with for each $\tau^o_g = m^o_g\sigma$) and of 6 cubic systems (with for each $\tau^c_g = m^c_g\sigma$) can be activated. $m^o_g$ and $m^c_g$ are the Schmid factor on octahedral and cubic slip systems (Ghosh et al , 1990).

  - *In tension along* $< 001 >$ there are 8 active octahedral slip systems at $\tau^o = m^o_{001}\sigma$ with $m^o_{001} = \frac{1}{\sqrt{6}}$, no active cubic slip systems.
  - *In tension along* $< 111 >$ there are 6 active octahedral slip systems at $\tau^o_g = m^o_{111}\sigma$ with $m^o_{111} = \frac{2}{3}$ and 3 active cubic slip systems at $\tau^c_g = m^c_{111}\sigma$ with $m^c_{111} = \frac{\sqrt{2}}{3}$.

- *plastic strain rate*

$$\dot{\boldsymbol{\epsilon}}^p = \dot{\boldsymbol{\epsilon}}^{po} + \dot{\boldsymbol{\epsilon}}^{pc} = \frac{1}{2}\sum_{g=1}^{12}\left(\mathrm{n}^{\rm o}_{\rm g}\otimes\mathrm{m}^{\rm o}_{\rm g} + \mathrm{m}^{\rm o}_{\rm g}\otimes\mathrm{n}^{\rm o}_{\rm g}\right)\dot\gamma^o_g + \frac{1}{2}\sum_{g=1}^{6}\left(\mathrm{n}^{\rm c}_{\rm g}\otimes\mathrm{m}^{\rm c}_{\rm g} + \mathrm{m}^{\rm c}_{\rm g}\otimes\mathrm{n}^{\rm c}_{\rm g}\right)\dot\gamma^c_g \tag{F.3}$$

  allowing to define the total, octahedral and cubic macroscopic accumulated plastic strains as

$$p = \int\sqrt{\frac{2}{3}\dot{\boldsymbol{\epsilon}}^p : \dot{\boldsymbol{\epsilon}}^p}\,\mathrm{d}t \qquad p^o = \int\sqrt{\frac{2}{3}\dot{\boldsymbol{\epsilon}}^{po} : \dot{\boldsymbol{\epsilon}}^{po}}\,\mathrm{d}t \qquad p^c = \int\sqrt{\frac{2}{3}\dot{\boldsymbol{\epsilon}}^{pc} : \dot{\boldsymbol{\epsilon}}^{pc}}\,\mathrm{d}t \tag{F.4}$$

- *viscosity laws* for octahedral and cubic slip systems (saturated hardening, coupling with Orowan stress),

$$\dot\gamma^o_g = \left\langle -\frac{\tau_{v\infty}}{k^o}\ln\left(1 - \frac{|\tau^o_g| - m^o_g\frac{\kappa_{\rm ORO}G}{\|\boldsymbol{\omega}\|} - \rho^o}{\tau_{v\infty}}\right)\right\rangle_+^{n^o} \qquad \dot\gamma^c_g = \left\langle\frac{|\tau^c_g| - \varpi\, m^c_g\frac{\kappa_{\rm ORO}G}{\|\boldsymbol{\omega}\|} - \rho^c}{k^c}\right\rangle_+^{n^c} \tag{F.5}$$

  with, from macroscopic parameters of section 6.1, identified for orientations $< 001 >$ and $< 111 >$

$$n^o = N \qquad \rho^o = m^o_{001}(\sigma_y + R_\infty), \qquad k^o = m^o_{001}(8m^o_{001})^{1/N}K_N, \qquad \tau_{v\infty} = m^o_{001}\sigma_{v\infty} \tag{F.6}$$

$$n^c = \overline{N} \qquad \rho^c = m^c_{111}(\overline{\sigma}_y + \overline{R}_\infty), \qquad k^c = m^c_{111}(3m^c_{111})^{1/N}\overline{K}_N, \tag{F.7}$$

- *microstructure degradation*, written at RVE macroscopic scale using "diagonal" Kelvin stress $\boldsymbol{\sigma}^{\rm d} = \mathbb{P}^{\rm d} : \boldsymbol{\sigma}$ (projector $\mathbb{P}^{\rm d}$ defined in Eq. (A.5)), and its von Mises norm $\sigma^{\rm d}_{eq} = \sqrt{\frac{3}{2}\boldsymbol{\sigma}^{\rm d} : \boldsymbol{\sigma}^{\rm d}}$,

$$\dot{\boldsymbol{\omega}} = \dot{\boldsymbol{\omega}}^{\rm raft} + \dot\omega_{\rm mc}\,\mathbf{1} + \sqrt{3}\,\dot\omega_{\rm LSW}\frac{\boldsymbol{\omega}}{\|\boldsymbol{\omega}\|} \qquad \begin{cases}\dot{\boldsymbol{\omega}}^{\rm raft} = K_{\rm raft}\exp\left(-\dfrac{Q - \min(\sigma^{\rm d}_{eq},\sigma^\mu_{lim})U_{\rm raft}}{k_{\rm B}T}\right)\mathrm{H}(p^o - \varepsilon^p_{\rm th})\,\mathcal{H}\,\mathbf{n}^{\rm d}\\ \dot\omega_{\rm mc} = K_{\rm mc}\exp\left(-\dfrac{Q - \sigma_{eq}U_{\rm mc}}{k_{\rm B}T}\right)\mathrm{H}(p^c - \overline{\varepsilon}^p_{\rm th})\\ \dot\omega_{\rm LSW} = \dfrac{K_{\rm LSW}}{3\omega^2_{\rm LSW}}\exp\left(-\dfrac{Q}{k_{\rm B}T}\right)\end{cases} \tag{F.8}$$

- *volume fractions of $\gamma'$ precipitates,* using crystal plasticity octahedral accumulated plastic strain $p^o$,

$$\dot{f}_{\gamma'} = \left(1 - \delta_{\gamma'} e^{-\frac{p^o}{\epsilon_{\gamma'}}}\right) \frac{f_{\gamma' \text{eq}}(T) - f_{\gamma'}}{\tau_{\gamma'}} \qquad f_{\gamma' \text{eq}}(T) \text{ from Eq. (90)} \tag{F.9}$$

- *$\gamma'$ channel width tensor*

$$\mathbf{w} = g(f_{\gamma'})\, w^0_{001}\, \boldsymbol{\omega} \qquad g(f_{\gamma'}) = \frac{1 - f_{\gamma'}}{1 - f^0_{\gamma'}} \tag{F.10}$$

*Appendix F.2. Tension along* $< 001 >$

For an uniaxial loading in direction $< 001 >$, there are 8 active octahedral slip systems and no active cubic slip systems so that one exactly recovers Eq. (81)

$$|\dot{\varepsilon}^p| = 8 m^o_{001} \left\langle \frac{m^o_{001}|\sigma| - \frac{\kappa_{\text{ORO}} G}{\|\boldsymbol{\omega}\|} - \rho^o}{k^o} \right\rangle_+^{n^o} = \left\langle \frac{|\sigma| - R_\infty - \frac{\kappa_{\text{ORO}} G}{\|\boldsymbol{\omega}\|} - \sigma_y}{K_N} \right\rangle_+^{N} \qquad < 001 > \text{ orientation} \tag{F.11}$$

*Appendix F.3. Tension along* $< 111 >$

For an uniaxial loading in direction $< 111 >$, the accumulated plastic rate is the sum of the contributions of 6 octahedral slip systems and of 6 cubic slip systems,

$$|\dot{\varepsilon}^p| = 3 m^c_{111} \left\langle \frac{m^c_{111}|\sigma| - \rho^c - \varpi \frac{\kappa_{\text{ORO}} G}{\|\boldsymbol{\omega}\|}}{k^c} \right\rangle_+^{n^c} + 6 m^o_{111} \left\langle \frac{m^o_{111}|\sigma| - \frac{\kappa_{\text{ORO}} G}{\|\boldsymbol{\omega}\|} - \rho^o}{k^o} \right\rangle_+^{n^o} \qquad < 111 > \text{ orientation} \tag{F.12}$$

or, using Schmid factor $m^o_{111} = \frac{2}{3} m^o_{001}$ and parameters definition (F.7),

$$|\dot{\varepsilon}^p| = \left\langle \frac{|\sigma| - \overline{R}_\infty - \overline{\sigma}_y - \varpi \sigma_{\text{ORO}}}{\overline{K}_N} \right\rangle_+^{\overline{N}} + \frac{1}{2} \left\langle \frac{\frac{2}{3}|\sigma| - R_\infty - \sigma_{\text{ORO}} - \sigma_y}{K_N} \right\rangle_+^{N} \qquad < 111 > \text{ orientation} \tag{F.13}$$

which, making the approximation $\frac{1}{2} \approx \frac{2}{3} \approx h$, is found close to be Eq. (82) obtained from macroscopic Klevin modes based model of section 6.1.

## References


Ardakani, M. G., Ghosh, R. N., Brien, V., Shollock, B. A., McLean, M., 1998. Implication of dislocation micromechanisms for changes in orientation and shape of single crystal superalloys. Scripta Mater., 39, 465–472.

Arramon, Y. P., Mehrabadi, M. M., Martin, D. W., Cowin, S. C., 2000. A multidimensional anisotropic strength criterion based on kelvin modes. Int. J. Solids Struct., 37, 2915–2935.

Arrell, D., Hasselqvist, M., Sommer, C., Moverare, J., 2004. On TMF damage, degradation effects, and the associated TMin influence on TMF test results in $\gamma/\gamma'$ alloys. Superalloys 2004-Tenth International Symposium on Superalloys; 19-23 September, Champion, PA, USA, TMS, 291–294.

Asaro, R., 1983. Crystal Plasticity. J. Appl. Mech.-T. ASME, 50, 921–934.

Asaro, R., Lubarda, V., 2006. Mechanics of Solids and Materials. Cambridge University Press.

Asaro, R J., Rice J .R., 1977. Strain localization in ductile single crystals. J. Mech. Phys. Solids, 25, 309–338 .

Barlat, F., Aretz, H., Yoon, J. W., Karabin, M. E., Brem, J. C., Dick, R. E., 2005. Linear transformation-based anisotropic yield functions. Int. J. Plasticity, 21, 1009–1039.

Benyoucef, M.; Clement, N., Coujou, A., 1993. Transmission electron microscopy in situ deformation of MC2 superalloy at room temperature. Mater. Sci. Eng., A164, 401–406.

Bertram, A., Olschewski, J., 1996. Anisotropic creep modelling of the single crystal superalloy SRR99. Comp. Mater. Sci., 5, 12–16.

Biegler, M. W., Mehrabadi, M. M., 1995. An energy-based constitutive model for anisotropic solids subject to damage. Mech. Mater., 19, 151–164.

Biermann, H., Grossman, B. V., Schneider, T., Feng, H., Mughrabi, H, 1996. Investigation of the $\gamma/\gamma'$ morphology and internal stresses in a monocrystalline turbine blade after service: determination of the local thermal and mechanical loads. R.D. Kissinger, D.J. Deye, D.L. Anton, A.D. Cetel, M.V. Nathal, T.M. Pollock, D.A. Wooford (Eds.) Superalloys 1996, TMS, Seven Springs, Champion, PA, USA, 201–210.

de Bussac, A., 1993. Loi de comportement avec double viscosité: application to AM1 $< 001 >$ entre 20 °et 1150 °C. Technical Report YKOM1/YLEV 60.318, Snecma, Villaroche, France.

Cailletaud G., 1992. A micromechanical approach to inelastic behaviour of metals. Int. J. Plasticity, 8, 55–73.

Caron, P., Khan, T., 1983. Improvement of creep strenght in a nickel-base single crystal superalloy by heat treatment. Mater. Sci. Eng., 61, 173–194.

Caron, P., Ohta, Y., Nakagawa, Y. G., Khan, T., 1988. Creep deformation anisotropy in single crystal superalloys. Superalloys 1988, PA, USA, 215 224.

Caron, P., Ramusat, C., Diologent, F., 2008. Influence of the $\gamma'$ fraction on the topological inversion during high temperature creep of single crystal superalloys. R. Reed, K. Green, P. Caron, T. Gabb, M. Fahrmann, E. Huron, S. Woodard (Eds.) Superalloys, TMS, Warrendale, PA, Seven Springs, Champion, PA, USA, 159–167.

Chen, W., Immarigeon, J. P., 1998. Thickening behaviour of $\gamma'$ precipitates in nickel base superalloys during rafting. Scripta Mater., 39, 167–174.

Cormier, J., 2016. Thermal cycling creep resistance of Ni-based single crystal superalloys, Superalloys 2016, Seven Springs, PA, USA, 385-394

Cormier, J., Cailletaud, G., 2010. Constitutive modeling of the creep behavior of single crystal superalloys under non-isothermal conditions inducing phase transformations. Mater. Sci. Eng., A527, 6300–6312.

Cormier, J., Cailletaud, G., 2010. Constitutive modelling of the creep behaviour of single crystal superalloys under non-isothermal conditions inducing phase transformations. Technische Mechanik, 30, 56–73.
Cormier, J. , Mauget, F., Graverend, J. B., Moriconi, C., Mendez, J., 2015. Issues Related to the Constitutive Modeling of Ni-based Single Crystal Superalloys under Aeroengine Certification Conditions. Aerospace Lab Journal, 9, 1–13.
Cormier, J., Milhet, X., Mendez, J., 2007. Non-isothermal creep at very high temperature of the Nickel based single crystal superalloy MC2. Acta Mater., 55, 6250–6259.
Cowin, S., Mehrabadi, M., Sadegh, A., 1991. Kelvin's Formulation of the Anisotropic Hooke's Law. SIAM Journal, J. Wu, T. Ting, and D. Barnett, Soc. Ind. and Applied Math, 340–356.
Desmorat, B., Duvaut, G., 2003. Compliance optimization with nonlinear elastic materials : Application to constitutive laws dissymmetric in tension/compression. Eur. J. Mech.- A/Solids 22, 179–192.
Desmorat, R., 2000. Dissymétrie de comportement élastique anisotrope couplé ou non à l'endommagement. C.R.A.S., Série IIb 328, 445–450.
Desmorat, R., 2009. Kelvin decomposition and multiple effective stresses concept in anisotropic materials. C.R. Mécanique., 337, 733–738.
Desmorat, R., Marull, R., 2011. Non-quadratic Kelvin modes based plasticity criteria for anisotropic materials. Int. J. Plasticity, 27, 328–351.
Diologent, F., Caron, P., d'Almeida, T., Jacques, A., Bastie, P., 2003. The $\gamma/\gamma'$ mismatch in Ni based superalloys : in situ measurements during a creep test. Nucl. Instrum. and Methods, B 200, 346–351.
Dirand, L., Cormier, J., Jacques, A., Chateau-Cornu, J. P., Schenk, T., Ferry, O., Bastie, P., 2013. Measurement of the effective $\gamma/\gamma'$ lattice mismatch during high temperature creep of Ni-based single crystal superalloy. Mater. Charact., 77, 32–46.
Draper, S., Hull, D., Dreshfield, R., 1989. Observations of directional gamma prime coarsening during engine operation. Met. Trans., 20A , 683–688.
Epishin, A., Link, T., Bruckner, U., Klingelhoffer, H., Portella, P., 2005. Influence of High temperature creep damage on low cycle fatigue of CMSX-4. R.S. Mishrs, J.C. Earthman, S.V. Raj, R. Viswanathan (Eds.) Materials Science and Technology, 231–239.
Epishin, A., Link, T., Bruckner, U., Portella, P., 2001. Kinetics of the topological inversion of the $\gamma/\gamma'$ microstructure during creep of a nickel-based superalloy. Acta Mater., 49, 4017–4023.
Epishin, A., Link, T., Klingelhoffer, H., Fedelich, B., Bruckner, U., Portella, P., 2009. New technique for characterization of microstructural degradation under creep: Application to the nickel-base superalloy CMSX-4. Mater. Sci. Eng., A510–511, 262–265.
Epishin, A., Link, T., Klingelhoffer, H., Portella, P., Fedelich, B., 2010. Creep damage of single-crystal superalloys: mechanisms and effect on low cyle fatigue. Mater. High Temp., 23, 53–59.
Epishin, A., Link, T., Nazmy, M., Staubli, M., Klingelhoffer, H., Nolze, G., 2008. Microstructural degradation of CMSX-4: kinetics and effect on mechanical properties. R. Reed, K. Green, P. Caron, T. Gabb M. Fahrmann, E. Huron, S. Woodard (Eds.) Superalloys 2008, TMS, Seven Springs, PA, USA, 725–731.
Epishin, A. , Link, T., Portella, P., 2000. Bruckner, U., Evolution of the $\gamma/\gamma'$ microstructure during high-temperature creep of a nickel-base superalloy. Acta Mater., 48, 4169–4177.
Fan, Y. N., Shi, H. J., Qiu W. H., 2015. Constitutive modeling of creep behavior in single crystal superalloys: Effects of rafting at high temperatures. Mater. Sci. Eng., A 644, 225–233.
Fedelich, B., 2002. A microstructural model for the monotonic and the cyclic mechanical behavior of single crystals of superalloys at high temperatures. Int. J. Plasticity, 18, 1–49.
Fedelich, B., Künecke, G., and Epishin, A. 2006. Modelling of rafting and its influence in Ni-base superalloys, Proc. of the 8th Liege Conference Materials for Advanced Power Engineering, ed. J. Lecomte-Beckers et al (Forschungszentrum JŸlich, 475–484.
Fedelich, B., Künecke, G., Epishin, A., Link, T., Portella, P., 2009. Constitutive modelling of creep degradation due to rafting in single crystals Ni-base superalloys. Mat. Sci. Eng., A510–511, 273–277.
Fedelich, B., Epishin, A., Link, T., Klingelöhffer, H., Künecke, G., Portella P., 2012. Experimental characterization and mechanical modeling of creep induced rafting in superalloys. Comp. Mater. Sci., 64, 2–6.
Fedelich, B., Epishin, A., Link, T., Klingelhöffer, H., Künecke G., Portella, P., 2012. Rafting during high temperature deformation in single crystal superalloy : experimental and modeling, Proceeding of the 12*th* international symposium on superalloys, Seven Spring, Pennsylvania, 491.
Fährmann, M., Fährmann, E., Paris, O., Fratzl, P., Pollock, T.M., 1996. An experimental study of the role of plasticity in the rafting kinetick of a single crystal Ni-base superalloy. R.D. Kissinger, D.J. Deye, D.L. Anton, A.D. Cetel, M.V. Nathal, T.M. Pollock, D.A. Woodford (Eds.) Superalloys 1996, TMS, Seven Springs, PA, USA, 191–200.
François, M., 1995. Identification des symétries matérielles de matériaux anisotropes. Université Paris VI Ph.D, Cachan.
Fredholm, A., Strudel, J. L., 1987. High temperature creep mechanisms in single crystals of some high performance nickel base superalloys, in: e.a. J. B. Mariott (Ed.) Petten International Conference, Elsevier Applied science, London, U.K., 9–18.
Gaubert, A., Jouiad, M., Cormier, J., Bouar, Y. L., Ghighi, J., 2015. Three-dimensional imaging and phase-field simulations of the microstructure evolution during creep tests of < 011 >-oriented Ni-based superalloys, Acta Mater., 84, 237–255.
Ghighi, J., 2013. Modélisation du fluage des superalliages monocristallins : effets d'anisotropie et de microstructure. ENSMA, Ph. D. thesis.
Ghighi, J. , Cormier, J., 2013. Ostoja-Kuczynski, E., Mendez, J., Cailletaud, G. , Azzouz, F., A Microstructure Sensitive Approach for the Prediction of the Creep Behaviour and Life under Complex Loading Paths. Technische Mechanik, 32, 205–220.
Ghosh, R.N., Curtis, R.V., McLean, M., 1990. Creep deformation of single crystal superalloys-modelling the crystallographic anisotropy. Acta Metall. Mater., Vol. 38, No. 10, 1977-1992.
Giraud, R., Cormier, J., Hervier, Z., Berheau, Z., Harris, K., Wahl, J., Milhet, X., Mendez, J., Organista, A., 2012. Effect of the prior microstructure degradation on the high temperature/low stress non-isothermal creep behavior of CMSX-4 Ni-based single crystal superalloy. R.C. Reed, E. Huron, M.C. Hardy, M.J. Mills, R. Montero, P.D. Portella, J. Telesman (Eds.) Superalloys 2012, TMS, Seven Springs, PA, USA, 265–274.
Giraud, R., Hervier, Z., Cormier, J., St Martin, G., Hamon, F., Milhet, X., Mendez, J., 2013. Strain effect on the $\gamma'$ dissolution at high temperature of a Nickelbased single crystal superalloy, Metal. Mater. Trans. A, 44 (1), 131–146.
le Graverend, J. B., 2013. Etude et modélisation des effets d'incursion à très haute température sur le comportement mécanique d'un superalliage monocristallin pour aubes de turbine. ENSMA, Ph. D. thesis.
le Graverend, J. B., Cormier, J., Gallerneau, F., Villechaise, P., Kruch, S., Mendez, J., 2014. in Int. J. Plasticity, 59, 55–83.
le Graverend J.-B., Cormier J., Gallerneau F., Kruch S., Mendez J., 2014. Highly non-linear creep life induced by a short close $\gamma'$-solvus overheating and a prior microstructure degradation on a nickel-based single crystal superalloy. Mater. Design, 56, 990–997.
Golubovskii, E. R. , Toloraiya, V. N., Svetlov, I. L. , Khvatskii, K. K., Pod'yaehev, A. P., 1987. Question of the influence of crystallographic orientation on the stress-rupture strenght and creep of a nickel alloy. REPORT 1, Problemy Prochnosti, 9, 11–17.
Heckl, A., Neumeier, S., Göken, M., Singer, R. F., 2011. The effect of Re and Ru on $\gamma/\gamma'$ microstructure, g-solid solution strengthening and creep strength in nickel-base superalloys. Mater. Sci. Eng., A528, 3435–3444.
Helphen, B., Neguyen, Q., 1975. Sur les matériaux standard généralisés. J. de Mécanique, 14, 39–63.
Hana,G. M., Yua,J. J., Suna,Y. L., Suna,X. F., Hua, Z. Q., 2010. Anisotropic stress rupture properties of the nickel-base single crystal superalloy SRR99. Mat Sci Eng, A527, 5383–5390.
Harada, H., Yokokawa, T., Ohno, K., Yamagata, T. and Yamazaki, M., 1990. High Temperature Materials for Power Engineering. Ed. E. Bachelet et al Kluwer, Dordrecht, 1387.
Hill, R., 1950. The mathematical theory of plasticity. At the Clarendon press.
Hill, R., 1979. Theoretical plasticity of textured aggregates. Math Proc. Cambridge Phil. Soc., 85(1), 179–191.
Hill, R. J., Rice, J. R., 1972. Constitutive Analysis of Elastic/Plastic Crystals at Arbitrary Strain. J. Mec.Phy. Solids, 20, 401–413.
Ichitsubo, T., Koumoto, D., Hirao, M., Tanaka, K., Osawa, M., Yokokawa, T., Harad, H., 2003. Rafting mechanism for Ni-base superalloy under external stress : elastic or elastic-plastic phenomena. Acta Mater., 51, 4033–4044.

Johnson, G. R., Cook, W. H., 1983. A constitutive model and data for metals subjected to large strains, high strain rates and high temperatures, Proceedings of the 7th International Symposiumon Ballistics The Hague, The Netherlands, pp. 541–547.
Kamaraj M., 2003. Rafting in single crystal nickel-base superalloys: An overview, Sadhanna, 28, 115–128.
Kirka, M., Brindley, K., Neu, R., Antolovich, S., Shinde, S., Gravett, P., 2015. Influence of coarsened and rafted microstructures on the thermomechanical fatigue of a Ni-base superalloy. Int. J. Fatigue, 81, 191–201.
Thomson (Lord Kelvin), W. K., 1856. Elements of a mathematical theory of elasticity. Phil. Trans. R. Soc. 166, 481.
Thomson (Lord Kelvin), W. K., 1878. Elasticity, Encyclopaedia Britannica. Adam and Charles Black, Edinburgh.
Leidermark, D., Moverare, J. J., Johansson, S., Simonsson, K., Sjostrom, S., 2010. Tension/compression asymmetry of a single-crystal superalloy in virgin and degraded condition. Acta Mater., 58, 4986–4997.
Lemaitre, J., 1971. Sur la détermination des lois de comportement des matériaux eléasto-visco-plastiques. Thèse d'état, Université Paris XI (Orsay).
Lemaitre, J., Chaboche, J. L., Mécanique des matériaux solides, Dunod Paris, 1985, *Engl. Transl.*: Mech. Solids Mater., Cambridge Univ. Press, 1991.
Lemaitre, J., Chaboche, J. L., Benallal, A. and Desmorat R., 2009. Mécanique des matériaux solides, 3rd Edition, Dunod Paris.
Lemaitre, J., Desmorat, R., 2005. *Engineering Damage Mechanics: Ductile, Creep, Fatigue and Brittle Failures*, Springer.
Li, S., Tao, J., Sugui, T., Zhuangoli, H., 2007. Influence of precipitate morphology on tensile creep of a single crystal nickel-base superalloy. Mater. Sci. Eng., A 454–455, 461–466.
Lifshitz, I. M., Slyozov, V. V., 1961. J. Phys. Chem. Solids, 19, 35–50.
Link, T. , Epishin, A., Paulisch, M., May, T., 2011. Topography of semicoherent $\gamma/\gamma'$-interfaces in superalloys: Investigation of the formation mechanism.Mater. Sci. Eng., A 528, 6225–6234.
Louchet, F., Hazotte, A., 1997. A model for low stress cross-diffusional creep and directional coarsening of superalloys. Scripta Mater., 37, 589–597.
Ma, A., Dye, D., Reed, R.C., 2008. A model for the creep deformation behaviour of single-crystal superalloy CMSX-4. Acta Mater., 56 (8), 1657–1670.
MacKay, R. A., Ebert, L. J., 1985. The development of $\gamma/\gamma'$ lamellar structures in a nickel-base superalloy during elevated temperature mechanical testing. Met. Trans. A, 16A, 1969–1982.
MacKay R. A., and Maier R. D., 1982. Metall. Mater. Trans. A, 13A, 1747–1754.
MacLachlan, D., W., Wright, L., W., Gunturi, S., Knowles, D. M., 2001. Int. J. Plasticity, 17, 441–467.
Mahnken, R., 2002. Anisotropic creep modeling based on elastic projection operators with applications to CMSX-4 superalloy. Comput. Method App. M., 191, 1611–1637.
Matan, N., Cox, D., Rae, C. M. F. and Reed, R. C., 1999. On the kinetics of rafting in CMSX-4 superalloy single crystals, Acta Mater., 47, 2031–2045.
Mataveli Suave, L., Cormier, J., Villechaise, P., Bertheau, D., Mauget, F., Cailletaud, G., Marcin, L., 2016. High temperature creep damage mechanisms in a directionally solidified alloy: impact of crystallography and environment. Superalloys 2016, PA, USA, 747–756.
Mauget, F. , Hamon, F. , Morisset, M., Cormier, J., Riallant, F., Mendez, J., 2016. Damage mechanisms in an EB-PVD Thermal Barrier Coating System during TMF and TGMF testing conditions under combustion environment, Int. J. Fatigue, In press.
Méric, L., Poubanne, P., Cailletaud, G., 1991. Single crystal modeling for structural calculations : part 1 – model presentation. J. Eng. Mater. Tech. 113, 162–170.
Milhet, X. , Arnoux, M. , Cormier, J. , Mendez, J., Tromas, C., 2012. On the influence of the dendritic structure on the creep behavior of a Re-containing superalloy at high temperature/low stress. Mater. Sci. Eng., A546, 139–145.
Mughrabi, H., 2009. Microstructural aspects of high temperature deformation of monocrystalline nickel base superalloys: some open problems. Mater. Sci. Tech., 25, 191–204.
Mughrabi H., 2014. The importance of sign and magnitude of $\gamma/\gamma'$ lattice misfit in superalloys – with special reference to the new $\gamma'$-hardened cobalt-base superalloys. Acta Mater., 25, 191–204.
Mughrabi, H., Tetzlaff, U. , 2000. Microstructure and high-temperature strength of monocrystalline nickel-base superalloys. Adva. Eng. Mater., 2, 319–326.
Nabarro, F. R. N., Cress, C.M., Kotschy ,P., 1995. The thermodynamic driving force for rafting in superalloys. Acta Mater. 44, 3189–3198.
Nabarro, F. R. N., 1996. Rafting in superalloys, Metall. Mater. Trans., A27, 513–530.
Nouailhas, D., Cailletaud, G., 1995. Tension-torsion behavior of single crystal superalloys : experiment and finite element analysis. Int. J. Plast., 11, 451–470.
Ott, M., Mughrabi, H., 1999. Dependence of the high-temperature low-cycle fatigue behaviour of the monocrystalline nickel-base superalloys CMSX-4 and CMSX-6 on the $\gamma/\gamma'$-morphology. Mater. Sci. Eng., A 27, 24–30.
Peirce, D., Asaro, R. J., Needleman A., 1983. Material rate dependence and localized deformation in crystalline solids. Acta Metall., 31, 1951–76.
Pineau, A., 1976. Influence of uniaxial stress on the morphology of coherent precipitates during coarsening-elastic energy considerations, Acta Metall., 24, 559–564.
Pollock, T. M., Argon, A. S., 1994. Directional coarsening in nickel-base single crystals with high volume fractions of coherent precipitates, Acta Metall. Mater., 42, 1859–1874.
Pyczak, F., Bauer, A., Göken, M.,Neumier, S., Lorenz, U., Oehring, M., et al, 2013. Plastic deformation mechanisms in a crept L12 hardened Co-base superalloy, Mater. Sci. Eng., A571, 13–18.
Reed, R. C., 2006. The Superalloys - Fundamentals and Applications, Cambridge University Press, Cambridge, UK.
Reed, R. C., Cox, D. C., Rae, C. M. F., 2007. Damage accumulation during creep deformation of a single crystal superalloy at $1150°C$, Mater. Sci. Eng., A 448, 88–96.
Reed R.C., Cox D.C., Rae C.M.F., 2007. Kinetics of rafting in a single crystal superalloy: effects of residual microsegregation, Mater. Sci. Tech., 23, 893–902.
Reed, R. C., Matan, N., Cox, D. C., Rist, M. A., Rae, C. M. F., 1999. Creep of CMSX-4 superalloy single crystals: effects of rafting at high temperature, Acta Mater., 47. 3367–3381.
Rice, J. R., 1975. Continuum Mechanics and Thermodynamics of Plasticity in Relation to Microscale Deformation Mechanisms. Constitutive Equations in Plasticity (ed. A. S. Argon), M.I.T. Press, 23–79.
Rice, J. R., Tracey, D. M., 1969. On the ductile enlargment of voids in triaxial stress fields,J. Mech. Phys. Solids,17, 201–217.
Roebuck, B., Cox, D., and Reed, R., 2001. The temperature dependence of $\gamma'$ volume fraction in a Ni-based single crystal superalloy from resisitivity measurements, Scr. Mater., 44, 917–921.
Royer, A., Bastie, P., Véron, M., 1998. In situ determination of $\gamma'$ phase volume fraction and of rlations between lattice parameters and precipitate morphology in Ni-based single crystal superalloy. Acta Mater., 46, 5357–5368.
Rychlewski, J., 1984. On hooke's law. Prikl. Matem. Mekhan. 48, 303–314.
Sass, V., Glatzel, U., Feller-Kniepmeier, M., 1996. Anisotropic creep properties of nickel-base superalloy CMSX-4, Acta Mater., 44, 1967–1977.
Schmid, E., Boas, W., 1935. Kristallplastizitaet mit besonderer Beruecksichtigung der Metalle.
Shi, Z. , Li, J., Liu, S., 2012. Effect of long term aging on microstructure and stress rupture properties of a nickel based single crystal superalloy. Progress in Natural Science: Materials International, 22, 426–432.
Staroselsky, A., Cassenti, B. N., 2010. Combined rate-independent plasticity and creep model for single crystal. Mech. Mater., 42, 945–959.
Steuer, S. , Hervier, Z., Thabart, S., Castaing, C., Pollock, T. M., Cormier J., 2014. Creep behavior under isothermal and non-isothermal conditions of AM3 single crystal superalloy for different solutioning cooling rates, Mater. Sci. Eng., A601, 145–152.

Stinville, J., Cormier, J., Templier, C. and Villechaise P., 2015. Modeling of the lattice rotations induced by plasma nitriding of 316L polycrystalline stainless steel. Acta Mater., 83,10–16.
Svoboda, J., Lukas, P., 1996. Modelling of kinetics of directional coarsening in Ni-superalloys. Acta Mater., 44, 2557–2565.
Svoboda, J., and Lukas, P., 1997. Modelling of recovery controlled creep in nickel-base superalloys single crystals. Acta Mater., 45, 125–135.
Svoboda J., Lukas P.,1998. Model of creep in < 001 >-oriented superalloys single crystals. Acta Mater., 46, 3421–3431.
Svoboda, J., Lukas, P., 2000. Creep deformation modelling of superalloy single crystals. Acta Mater., 48, 2519–2528.
Tetzlaff, U., Mughrabi, H., 2000. Enhancement of Thermomechanical Fatigue Resistance of a Monocrystalline Nickel-base Superalloy by Prerafting. Superalloys 2000, edited by T. Pollock., R.D. Kissinger, R.R. Bowman, K.A. Green, M. McLean, S. Olson, and J.J. Schirra, TMS, Seven Springs, PA, USA, T.M, 274–282.
Tanaka, K, Ooshima, M., Tsuno, N., Sato, A., Inui, H.,2012. Creep deformation of single crystals of new Co?Al?W−based alloys with fcc/L12 two-phase microstructures. Philos. Mag., 92, 4011–4027.
Tian, S., Zhang, S., Li, C., Yu, H., Su, Y., Yu, X., Yu, L., 2012. Microstructure Evolution and Analysis of a [011] Orientation, Single-Crystal, Nickel-Based Superalloy During Tensile Creep, Met. Mat. Trans., 43A, 3880–3889.
Tien, J., K., and Copley, S., M., 1971. The effect of orientation and sense of applied uniaxial stress on the morphology of coherent gamma prime precipitates in stress annealed nickel-base superalloy crystals, Met. Trans., 2, 543–553.
Tien, J. K., Gamble, R. P., 1971. Effects of stress coarsening on coherent particle strengthening. Met. Trans., 3, 2157–2162.
Tinga, T, Brekelmans, W. A. M., Geers, M. G. D., 2009. Time-incremental creep-fatigue damage rule for single crystal Ni-base superalloys. Mat. Sci. Eng., A508,200–208.
Tinga, T., Brekelmans, W. A. M., Geers, M. G. D., 2009. Directional coarsening in nickel-base superalloys and its effect on the mechanical properties. Computational Mater. Sci., 47, 471–481.
Xingfu, Y., Sugui, T., Hongqiang, D., Huichen, Y., Minggang, W., Lijuan, S., Shusen, C., 2009. Microstructure evolution of a pre-compression nickel-base single crystal superalloy during tensile creep, Mater. Sci. and Eng., A506, 80–86.
Véron, M., Bastie, P., 1997. Strain induced directional coarsening in nickel based superalloys: Investigation on kinetics using the small angle neutron scattering (SANS) technique, Acta Mater., 45, 3277–3282.
Véron, M., Brechet, Y., Louchet, F., 1996. Strain induced directional coarsening in Ni-based superalloys, Scripta Mater., 34, 1883–1886.
Wagner C. , 1961. Theorie der alterung von niederschlägen durch umlösen. Zeitschrift für Elektrochemie, 65, 581–591.
Zhang, J. X. , Wang, J. C., Harada, H. , Koizumi, Y., 2005. The effect of lattice mismatch on the dislocation motion in superalloys during high-temperature low-stress creep, Acta Mater., 53, 4623–4633.
Zhou N., Shen C., Mills M.J., Wang Y., 2007. Phase field modeling of channel dislocation activity and $\gamma'$ rafting in single crystal Ni-Al, Acta Mater., 55, 5369–5381.